RSC Advances

REVIEW

View Article Online
View Journal | View Issue

Cite this: *RSC Adv.*, 2020, **10**, 40745

The oxazolomycin family: a review of current knowledge

Patrik Oleksak, [ab] Jozef Gonda, [b] Eugenie Nepovimova, [a] Kamil Kuca [a] and Kamil Musilek *[a]

Oxazolomycin A and neooxazolomycin were firstly isolated in 1985 by the group of Uemura *et al.* from the *Streptomyces* sp. bacteria. To date, there have been reported 15 different natural compounds commonly classified as part of the oxazolomycin family. All oxazolomycin compounds possess extraordinary structures and they represent a synthetic challenge. Such molecules are additionally known for their wide range of biological activity including antibacterial, antiviral and cytotoxic effects. The present review summarizes the structural elucidation and classification of oxazolomycin compounds, their biosynthesis and biological activity. It is further focused on the total syntheses of oxazolomycins and one formal synthesis reported to date.

Received 1st October 2020
Accepted 25th October 2020

DOI: 10.1039/d0ra08396h

rsc.li/rsc-advances

1 Introduction

1.1 Discovery of oxazolomycins

The oxazolomycin family is a commonly used term for a group of molecules which includes 15 derivatives isolated from natural sources to date. As the first members of this group oxazolomycin A (**1**; Fig. 1) and neooxazolomycin (**2**) were isolated and recognized in 1985 by Uemura *et al.* from *Streptomyces* sp.[1,2] In the same year (1985), curromycin A (**6**) and curromycin B (**7**) were described as the products of a genetically modified strain of *Streptomyces hygroscopicus*.[3] Curromycin A and curromycin B were formerly termed as triedimycin A and triedimycin B.[4] In 1997 16-methyloxazolomycin (**5**) was isolated as a product from *Streptomyces* sp. as another member of the oxazolomycin family.[5] Two novel oxazolomycins, specifically oxazolomycin B (**3**) and oxazolomycin C (**4**) were reported in 1998 by Kanzaki *et al.* as the products of *Streptomyces albus* JA3453.[6] Otani *et al.* in 2000 reported isolation of KSM-2690 B (**8**) and KSM-2690 C (**9**) from the broth filtrate of *Streptomyces* strain KSM-2690 and they were classified as novel oxazolomycins.[7] In 2005 Potts *et al.* reported discovery of lajollamycin (**10**) as the product of the strain *Streptomyces nodosus* (NPS007994) and was named for the area of collection in Scripps Canyon, La Jolla in California, USA.[8] Other lajollamycins were isolated in 2014 by Oh *et al.* from *Streptomyces* strain SMC72 and they were identified as lajollamycin B (**11**), lajollamycin C (**12**) and lajollamycin D (**13**).[9] The latest two oxazolomycins reported in 2017 by Koomsiri *et al.* were identified from a culture broth of *Streptomyces subflavus* subsp. *irumaensis* AM-3603 and called oxazolomycin A2 (**14**) and bisoxazolomycin (**15**).[10]

1.2 Structural elucidation of oxazolomycins

Uemura *et al.* reported as the first structure of oxazolomycin A (**1**), involving spiro-β-lactone-γ-lactam moiety.[1] They also identified presence of 5-substituted oxazole ring in the structure as well as (*Z*)-configurated trisubstituted double bond considering nuclear Overhauser effect (NOE) enhancements between methyl (C4′) and H5′. Uemura *et al.* also reported a structure of neooxazolomycin (**2**), which in contrast to **1** contains bicyclic γ-lactone-γ-lactam moiety.[2] Neooxazolomycin is the only member of oxazolomycin family which contains bicyclic core. Structural elucidation of both **1** and **2** was achieved by application of a combination of X-ray crystallography and chemical correlation of the degradation products.[11] A completely geometric and stereochemical alignment of **1** and **2** was reported still in 1985.[1,2] Moreover, the structure of **1** was unambiguously provided in 2011 in the first total synthesis reported by Hatakeyama *et al.*[12] The first total synthesis of **2** was reported earlier in 1990 by Kende *et al.* and confirmed the assigned configuration.[13]

Further in 1985, structures of curromycin A (**6**) and curromycin B (**7**) were reported with double bond geometries, however without the stereochemical alignment.[3] Structure of both curromycins is similar to **1**, but these curromycins involve 2-methyl substituted oxazole ring. Additionally, compound **6** contains $-CH_2OMe$ residue at C16-position and compound **7** possesses the methyl group at the same position C16.[3] Kim *et al.* reported in 1997 isolation, structural elucidation and biological properties of 16-methyloxazolomycin (**5**), with partial stereochemical determination.[5] Structural recognition of **5** revealed considerable similarities with the structure of **1**. Geometry of

[a]*University of Hradec Kralove, Faculty of Science, Department of Chemistry, Rokitanskeho 62, 500 03, Hradec Kralove, Czech Republic. E-mail: kamil.musilek@uhk.cz*
[b]*Pavol Jozef Safarik University, Faculty of Science, Department of Organic Chemistry, Moyzesova 11, 040 01, Kosice, Slovak Republic*

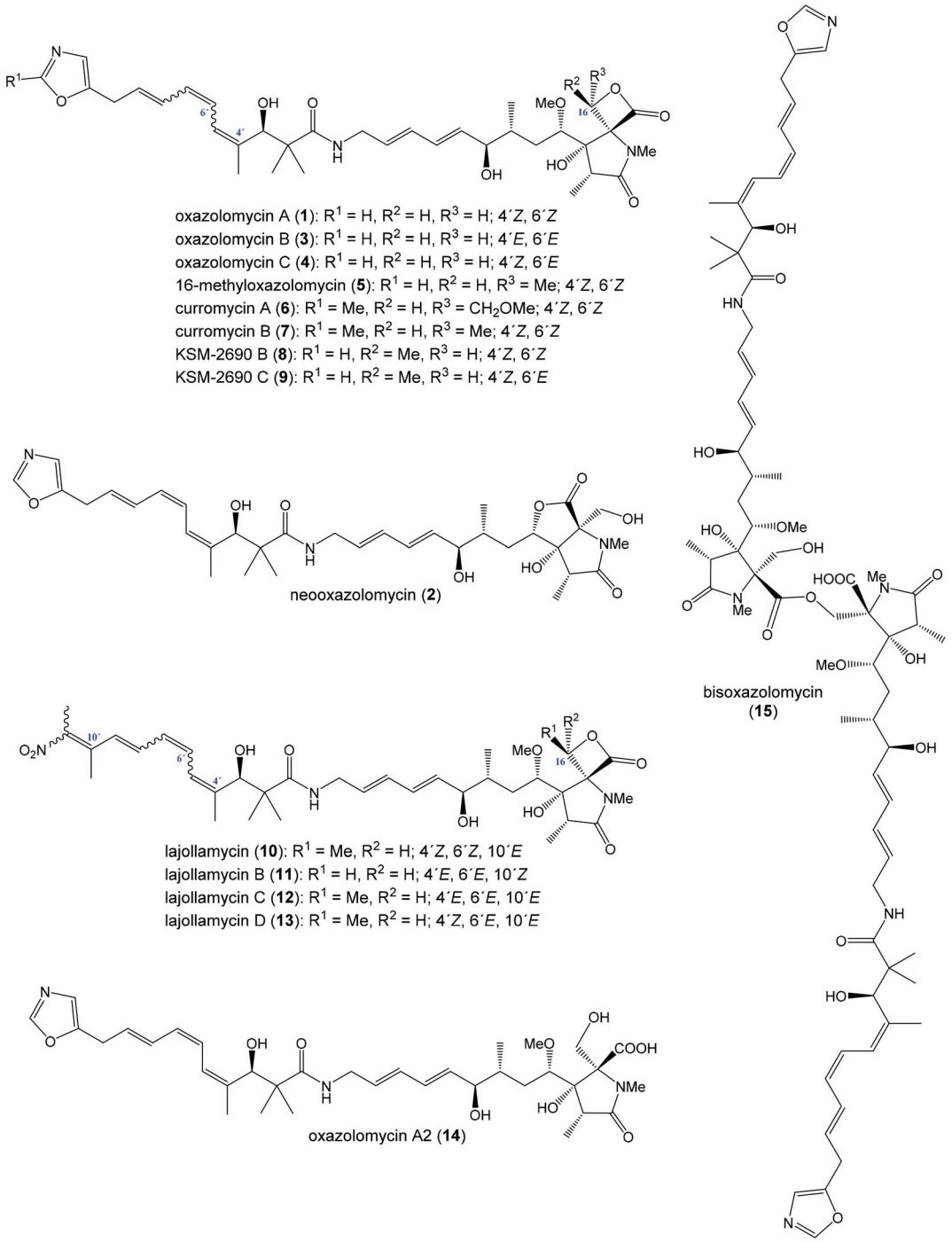

Fig. 1 Oxazolomycin family members.

diene and triene system as well as presence of 5-substituted oxazole moiety are identical to **1**. In contrast to oxazolomycin A, spiro-β-lactone-γ-lactam core of 16-methyloxazolomycin incorporates methyl group at C16-position, alike in the structure of curromycin B. The stereochemistry of β-lactone-γ-lactam moiety of **5** was deduced to be identical to **1** by NMR (NOESY) experiments, which also proved (*S*)-configuration of C16. Moreover, a stereochemical determination of β-lactone-γ-lactam core of **5** was determined as (2*R*,3*S*,15*S*)-configuration using NOESY experiments.[5] Completely stereochemical determination of **5** was reported in 1999 by Kim *et al.*, which confirmed identical configurations at all common, backbone stereocenters with **1**.[14]

Kanzaki *et al.* reported in 1998 structures of two novel oxazolomycins: oxazolomycin B (**3**) and oxazolomycin C (**4**), both are geometrical isomers of oxazolomycin A.[6] Olefinic proton signals were assigned by ^{1}H–^{1}H COSY and the coupling constants values of ^{1}H NMR, the geometry was assigned by an

analysis of NOE difference spectra and NOESY. The obtained data showed that the geometries of diene system in **3** and **4** are identical to **1**, but configuration of triene system is (4′*E*,6′*E*,8′*E*)- for **3** and (4′*Z*,6′*E*,8′*E*)- for **4** in contrast to (4′*Z*,6′*Z*,8′*E*)-configurated triene system of **1**. Kanzaki *et al.* reported also biological activities of **3** and **4**, but stereochemical aspects were not determined.[6]

Otani *et al.* reported in 2000 isolation and structures of KSM-2690 B (**8**) and KSM-2690 C (**9**), the two novel members of oxazolomycin family.[7] Structure of both **8** and **9** were elucidated using FAB-MS, UV and IR spectra, 1D and 2D NMR methods. Acquired spectral data of **8** were compared with those for 16-methyloxazolomycin (**5**) reported by Kim *et al.*, which suggested that **8** is a stereochemical isomer of **5**.[14] To clarify stereochemical differences Otani *et al.* analyzed ROESY and NOE correlations of **8**, when β-lactone-γ-lactam moiety of **8** was assigned with (2*R*,3*S*,15*S*,16*R*)-configurations in contrast to that of 16-methyloxazolomycin (**5**) with (2*R*,3*S*,15*S*,16*S*)-configurated stereocenters.[7] But some stereocenters (C4, C6, C7 and C3′) were not examined, ^{1}H NMR data indicated close similarities of both compounds except for the C16 center and consequently compound **8** was determined as a novel stereoisomer of **5**.

The spectral data indicated that **9** is an isomer of **8** but differences were observed in the chemical shifts for the triene moiety of **9**. And the chemical shifts of triene moiety in **9** were closely similar to that reported by Kanzaki *et al.* for oxazolomycin C.[6] Otani *et al.* determined (4′*Z*,6′*E*,8′*E*)-configurations of triene moiety in **9** when NOE correlations of β-lactone-γ-lactam core were identical to these of **8**.[7] In addition, KSM-2690 C (**9**) was determined as geometric isomer of **8**, however configuration of four stereocenters (C4, C6, C7 and C3′) were not examined.[7]

Isolation and structural characterization of lajollamycin (**10**) was reported by Potts *et al.* in 2005.[8] NMR data of **10** exhibited similarities with other oxazolomycins such as presence of spiro-β-lactone-γ-lactam core, amide linkage and conjugated olefinic system. Surprisingly, structure of **10** exhibited absence of oxazole ring system and further analysis revealed presence of nitro group in the structure. Analysis of NOESY and HMBC correlations indicated elongation of the triene system typical for oxazolomycins by an additional double bond that was substituted with two methyl moieties. The double bond geometries of the tetraene system were determined by NOESY and NOEDS analysis, which revealed (4′*Z*,6′*Z*,8′*E*,10′*E*)-configurated tetraene in the structure of **10**. Absolute configuration of **10** was determined by Oh *et al.* in 2014 by analysis of the ROESY NMR correlations, applied a *J*-based configuration analysis and the modified Mosher's method.[9]

In the same work Oh *et al.* reported isolation and structural elucidation of another lajollamycins as the members of the oxazolomycin family.[9] Structures of lajollamycin B (**11**), lajollamycin C (**12**) and lajollamycin D (**13**) were determined by FAB-HRMS, 1D and 2D NMR analysis. The double bond geometries of these lajollamycins were determined by analysis of coupling constants and ROESY correlations. The configurations of tetraene moiety were elucidated as (4′*E*,6′*E*,8′*E*,10′*E*)-configurations for **11** and **12** and as (4′*Z*,6′*E*,8′*E*,10′*E*)-configurations for **13**. Oh *et al.* reported proposition of the absolute configurations for **11**, **12** and **13** that were identical to those determined for **10** based on the similarities in acquired data and a shared biogenesis.[9] However, in 2019 Hatakeyama *et al.* reported first total synthesis of lajollamycin B and its C10′ geometric isomer.[15] Surprisingly, a spectroscopic comparison with data for **11** reported by Oh *et al.*[9] found to be identical with unexpected isomer. Thus, Hatakeyama *et al.* carefully reinvestigated Oh's 2D NMR spectroscopic data of **11** and unambiguously assigned NOESY spectra to both prepared isomers. ^{1}H and ^{13}C NMR spectra of both isomers exhibited close similarities with (*E*)- and (*Z*)-configurated terminal nitrotetraene derivatives prepared by Hatakeyama and co-workers. According to these findings Hatakeyama *et al.* revised the initially assigned geometry of lajollamycin B from (10′*E*)- to (10′*Z*)-configurated double bond.[15]

The last two members of oxazolomycin family were isolated, characterized and reported in 2017 by Koomsiri *et al.*[10] Both structures were elucidated using HR-ESI-MS, UV and IR spectra, optical rotation, 1D and 2D NMR spectroscopy. Structure of oxazolomycin A2 (**14**) indicated close similarity to oxazolomycin A (**1**), but difference in chemical shifts of the oxymethylene H_2-16 was observed. These observations suggested, that **14** is the analog of **1** with hydrolyzed β-lactone. Indeed, **14** could be prepared by basic hydrolysis of **1**.[10] Moreover, oxazolomycin A2 has been synthetized as an intermediate in total synthesis of **1** reported by Hatakeyama *et al.* in 2011, however crude **14** was directly used to further reaction without isolation.[12] Spectral data of bisoxazolomycin (**15**) suggested that structure is an asymmetric dimer of **1** consisting of *N*-methyl-γ-lactam segments I and II.[10] Both segments were confirmed by the ^{1}H–^{13}C long-range correlations. The chemical shifts of the oxymethylene of H_2-16 in segment I were similar to those of **14**, but the chemical shifts of the oxymethylene of H_2-16″ in segment II were moved to more shaded area (higher ppm). Moreover, **15** could be transformed by basic hydrolysis to **14**. Thus, bisoxazolomycin was revealed to be a new dimer of **14**, with an ester bond between C17 and C16″.

1.3 Structural classification of oxazolomycins

Relatively complicated structures of oxazolomycins can be divided into three fragments, usually termed as left-hand, middle and right-hand fragment. The structure of dimeric bisoxazolomycin (**15**) consist of two segments, named as segment I and segment II by Koomsiri *et al.* (Fig. 2).[10] The both segments can be divided into three fragments. These fragments and their analogues are crucial intermediates for total syntheses of all members of oxazolomycin family reported to date.[12,13,15–17]

The left-hand fragment represents one of two different structural arrangements. The most common framework is the oxazole-triene-amide[18] also known as inthomycin derivative.[19] Inthomycin A (**16**; Fig. 2) with (4*Z*,6*Z*,8*E*)-configurated triene is present in the structures of oxazolomycin A, oxazolomycin A2, neooxazolomycin, 16-methyloxazolomycin, curromycin A, curromycin B, KSM-2690 B and in the both segments of bisoxazolomycin. Inthomycin B (**17**) which possesses (4*Z*,6*E*,8*E*)-configurated triene is present in the structures of oxazolomycin

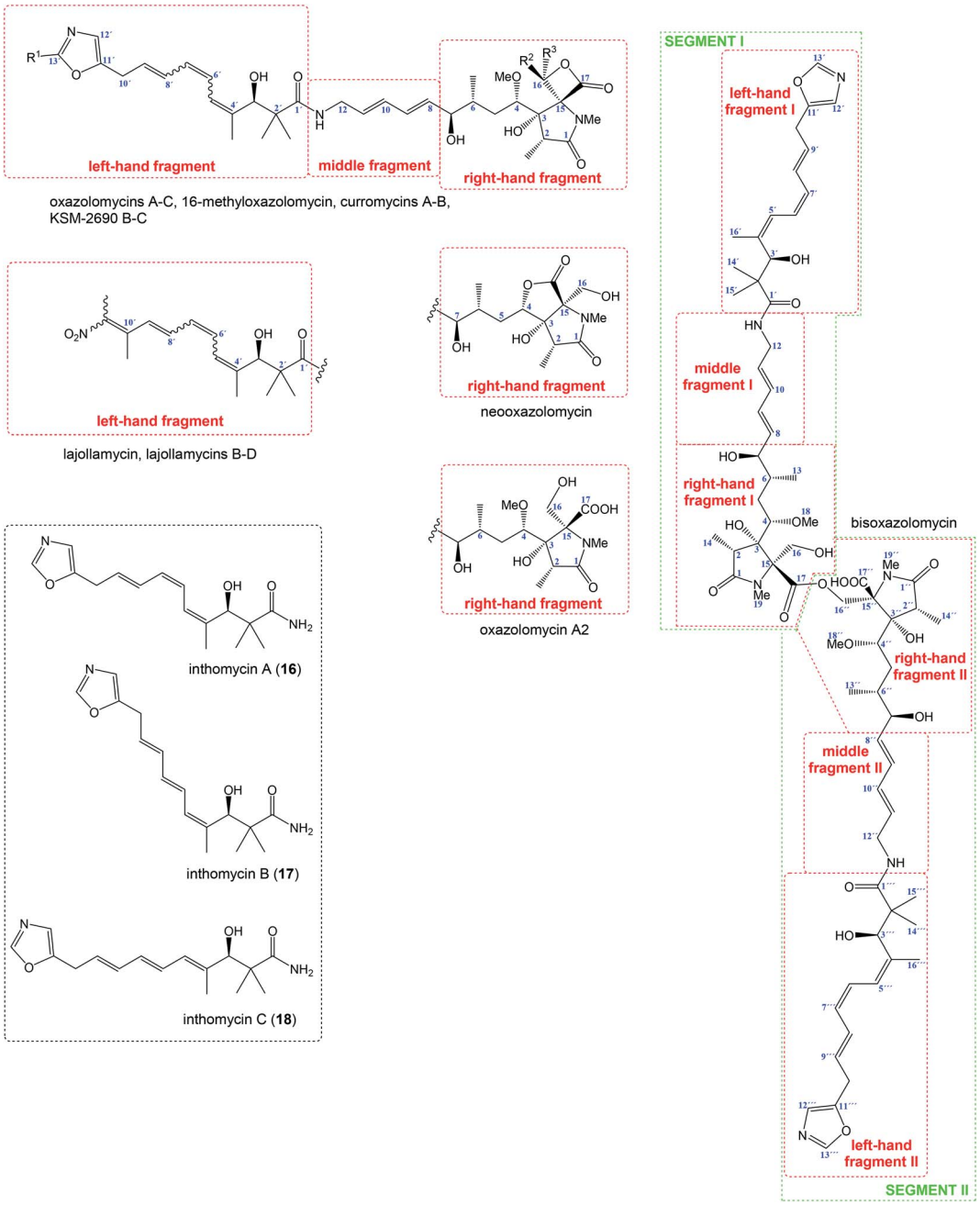

Fig. 2 Structural division of oxazolomycin family members and structure of inthomycins.

C and KSM-2690 C. Finally, inthomycin C (**18**) with (4*E*,6*E*,8*E*)-configurated triene moiety represents left-hand fragment of oxazolomycin B. The second structural framework for left-hand fragment is tetraene-nitro-hydroxy-amide which is typical for all lajollamycins including lajollamycin, lajollamycin B, lajollamycin C and lajollamcin D.

The middle fragment represents pentadienylamine,[18] which contains (*E*,*E*)-configurated diene moiety. This fragment is present in the structures of all members of oxazolomycin family. Indeed, middle fragment is a subunit of larger chain bounded at C5 and C4′ positions and it is absolutely same including stereochemistry for all oxazolomycins.

The right-hand fragment is structurally different for some members, however in general it can be designated as a pyroglutamate core. For almost all members of the oxazolomycin family right-hand fragment represents spiro-β-lactone-γ-lactam core, which can be further substituted with methyl or methoxymethyl group at the C16 position. Oxazolomycin A2 is the only natural member of oxazolomycins, which right-hand fragment contains monocyclic γ-lactam core. The unusual pyroglutamate core is incorporated in the structure of neooxazolomycin, which is the only natural oxazolomycin with bicyclic γ-lactone-γ-lactam moiety.

2 Biosynthesis of oxazolomycins

2.1 Feeding experiments

Thiericke *et al.* reported in 1992 feeding experiments on *Streptomyces albus* (strain JA3453) to investigate skeletal origin of oxazolomycin A (**1**) by using following [^{13}C]-labelled precursors: sodium [1,2-$^{13}C_2$]acetate, sodium [1-^{13}C]propionate, L-[*methyl*-^{13}C]methionine, L-[1-^{13}C]alanine and [1-^{13}C]glycine.[20] Single dose of labelled precursor was added to shake-cultures of *Streptomyces albus* (strain JA3453) 24 h after inoculation. Culture broth was harvested 72 h, isolated and purified samples were determined by ^{13}C NMR spectroscopy. Thiericke *et al.* observed intact incorporation of acetate into the positions C1′/C2′, C3′/C4′, C5′/C6′, C7′/C8′, C9′/C10′ of left-hand fragment, C5/C6, C7/C8, C9/C10 positions near by middle fragment and C1/C2 positions of γ-lactam core.[20] Methylation mediated by L-[*methyl*-^{13}C]methionine proved the origin of all *C*-linked methyl groups, attached at positions C4′, 2×(C2′), C6 and at C2, as well as *O*-linked and *N*-linked methyl groups. Feeding experiments with [1-^{13}C]glycine revealed incorporation into the positions C11 and C11′ of **1**. Application of sodium [1-^{13}C]propionate and L-[1-^{13}C]alanine in feeding experiments had not confirmed incorporation of marked atoms into the structure of **1**.[20]

In the same work Thiericke *et al.* examined hypothetical incorporation of inthomycins into the structure of **1**.[20] Thus, [^{14}C]-labelled inthomycins were prepared by feeding of [1,2-$^{14}C_2$]acetate to the inthomycin producing organism *Streptomyces* strain Gö2. However, feeding experiments of purified [^{14}C]-labelled inthomycins to the oxazolomycin producing strain proved that only 0.4% of labelled intermediate was incorporated into the structure of **1**. Moreover, amount of inthomycins during fermentation drastically decreased to 1%. Therefore, inthomycins themselves seem not to be intermediates involved in the biosynthesis of oxazolomycin A.[20]

2.2 Investigation of the oxazolomycin A gene cluster

Despite of significant results from labeling data,[20] the origins of some carbons (C3, C4, C16 and C13′) remained unclear. However, chemical,[21] biochemical[22,23] and genetic investigations[24] of some other natural products with similar moieties to the C3–C4 unit of oxazolomycins suggested that two-carbon moiety is probably derived from a metabolic intermediate of the glycolytic pathway, which serves as a precursor for the unusual methoxymalonyl-acyl carrier protein (methoxymalonyl-ACP) extender unit.[25] These information enabled Zhao *et al.* to isolate the oxazolomycin A gene (*ozm*) cluster from *Streptomyces albus* JA3453 by cloning the methoxymalonyl-ACP biosynthetic locus and localizing the *ozm* cluster.[7] The *ozm* cluster was confirmed by gene inactivation, affording mutant strains that had lost oxazolomycin production.[26] The boundaries of the *ozm* cluster were evaluated by Zhao *et al.* and delimitated by gene inactivation of *orf(−1)*, *orf(−2)* and *orf(−3)–orf(−5)* for the upstream boundary[26] and *orf(+1)*, *orf(+2)* and *orf(+3)–orf(+5)* for the downstream boundary.[25] These experiments and bioinformatics analysis established that the *ozm* cluster spans at most 79.5 kb of DNA consisting of 20 open read frames (ORFs) designated *ozmA* to *ozmU* (Fig. 3).[25–27] The functions of ORFs (Table 1) were predicted by comparing the deduced gene products with proteins of known function in the databases.

The *ozmA* to *ozmU* genes encode corresponding proteins (OzmA to OzmU):[25]

- Nonribosomal peptide synthetases (NRPSs): OzmL, OzmO.
- Hybrid polyketide synthase-nonribosomal peptide synthetase (PKS-NRPS): OzmH.
- *trans*-Acyltransferase (*trans*-AT) type I modular polyketide synthases (PKSs): OzmJ, OzmK, OzmN and OzmQ.
- Enzymes for methoxymalonyl-ACP biosynthesis: OzmB, OzmD, OzmE, OzmF and OzmG.

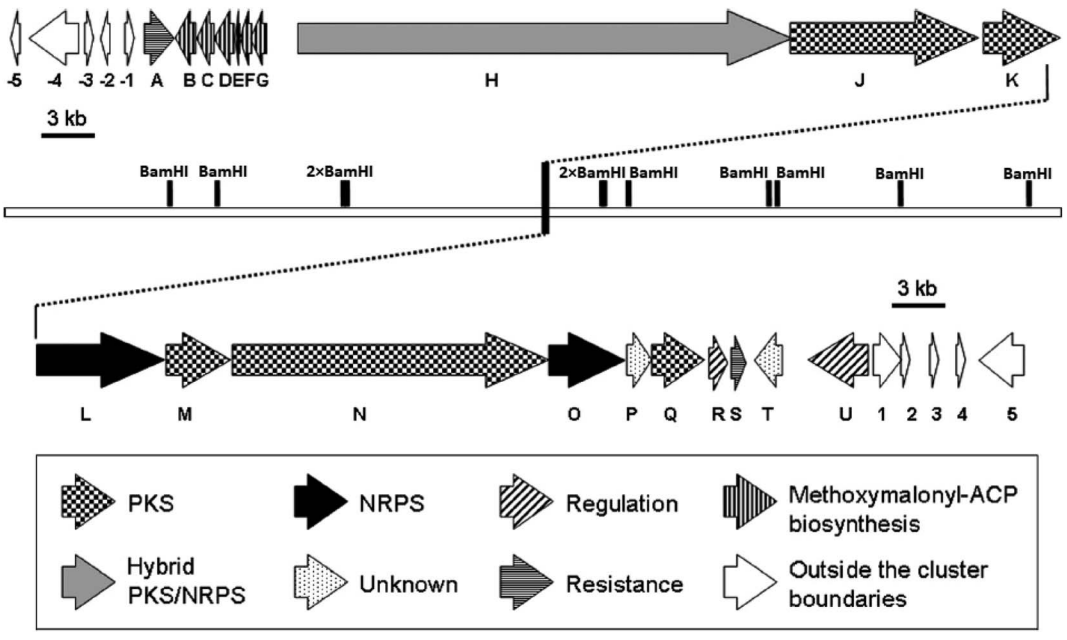

Fig. 3 Genetic organization in the *ozm* cluster. Numbers refer to genes outside *ozm* cluster, letters refer to genes inside *ozm* cluster.[25]

Table 1 Deduced open read frames (ORF) functions in the *ozm* cluster[25]

	Gene	Size[a]	Protein homolog[b]	Proposed function
Upstream region of *ozm* cluster	*orf(−5)*	335	Franean1_1604(ABW11043, 52/39)	Transcriptional regulator
	orf(−4)	775	SAV_1033(NP_822208 83/71)	Integral membrane protein
	orf(−3)	158	SAV_1074(NP_822249, 83/79)	Bacterioferritin comigratory protein
	orf(−2)	339	SACE_5658(CAM04844, 59/47)	Transcriptional regulator
	orf(−1)	315	CMS_2856(YP_001711489, 84/71)	Nucleoside hydrolase
ozm cluster	*ozmA*	482	SgcB(AAF13999, 28/43)	Antibiotic efflux protein
	ozmB	366	GdmH(ABI93783, 65/76)	Glyceryltransferase/phosphatase
	ozmC	325	DpsC(AAA65208, 25/39)	Acyltransferase
	ozmD	366	GdmI(ABI93784, 64/75)	Acyl-dehydrogenase
	ozmE	93	GdmJ(ABI93785, 63/78)	ACP
	ozmF	221	TtmC(AAZ08058, 60/77)	*O*-Methyltransferase
	ozmG	287	TtmB(AAZ08059, 63/72)	3-Hydroxyacyl-CoA-dehydrogenase
	ozmH	7737	PksP(E69679, 35/51)	Hybrid NRPS/PKS
	ozmJ	2926	ObsC(AAS00421, 52/64)	PKS
	ozmK	1202	BryB(ABK51300, 34/50)	PKS
	ozmL	1993	McyA(AAF00960, 37/55)	NRPS
	ozmM	1039	MmpIII(AAM12912, 47/59)	Acyltransferase/oxidoreductase
	ozmN	4971	LnmJ(AF484556, 38/48)	PKS
	ozmO	1196	PedF(AAS47564, 42/56)	NRPS
	ozmP	382	—	Unknown
	ozmQ	842	NosB(AAF15892, 55/69)	PKS
	ozmR	308	Orf5(BAA32133, 53/64)	Transcriptional regulator
	ozmS	214	SC5F8.18(CAB93746, 71/78)	Transporter
	ozmT	439	SCH63.25(CAC10316, 77/83)	Thr-tRNA synthetase
	ozmU	929	AfsR(BAA14186, 33/45)	Transcriptional activator
Downstream region of *ozm* cluster	*orf(+1)*	445	CypC(ABS73471, 42/59)	Cytochrome P450
	orf(+2)	221	—	Unknown
	orf(+3)	282	SC5F8.24(CAB93752, 70/81)	RNA polymerase sigma factor
	orf(+4)	344	—	Unknown
	orf(+5)	700	—	Unknown

[a] Size represents the number of amino acids. [b] Given in parentheses are accession numbers and percentage identity/percentage similarity.

- Discrete AT enzymes: OzmM and OzmC.
- Hypothetical proteins as candidates for resistance: OzmA and OzmS.
- Proteins as candidates for regulation or postmodification: OzmR, OzmU and OzmT.
- Proteins with uncertain functions: OzmP.

2.2.1 Genes encoding NRPSs. The *ozmO* and *ozmL* genes encode modular multidomain NRPSs with unusual architecture. The *ozmO* gene encodes the OzmO protein (1196 amino acids) that may serve as the loading module. The OzmO protein consists of a hypothetical formylation (F) domain, an adenylation (A) domain and a peptide carrier protein (PCP) domain. Isotope-labelling feeding experiments[20] and studies on the specificity-conferring codes of the A domains[28] suggest that glycine is activated by the A domain of OzmO and then loaded onto the PCP domain. Further studies[29,30] suggest that F domain of OzmO protein causes formylation of glycyl-S-PCP to generate *N*-formylglycyl-S-PCP. The *ozmL* gene encodes OzmL (1993 amino acids) a modular NRPS which probably representing the last module of the oxazolomycin's hybrid NRPS-PKS multienzyme. The OzmL involves following five domains: condensation (C) domain, A domain, methyltransferase (MT) domain, PCP domain and other C domain. Predicted amino acid specificity for the A domain of OzmL is serine,[28] consistent with the results of isotope-labeling experiments.[20] Mutational analysis[31] and crystallographic studies[32] have indicated that the second histidine in N-terminal C domain of OzmL acts as a crucial catalytic active size for condensation of two aminoacyl substrates or an aminoacyl and peptide substrate.[25]

2.2.2 Genes encoding a hybrid NRPS-PKS. The *ozmH* gene encodes a giant hybrid NRPS-PKS protein OzmH (7737 amino acids). The OzmH protein consists of one NRPS module with predicted specificity for glycine and four PKS modules. The protein together contains: five ketosynthetases (KSs), four ketoreductases (KRs), two dehydratases (DHs), two methyltransferases (MTs) and five acyl carrier proteins (ACPs). The unusual tandem KS domains were identified in module 10 of OzmH. The first KS domain contains a mutated catalytic triad of Cys–Asn–His, whereas the second KS possesses a full catalytic triad of Cys–His–His.[33,34] The His–His residues are essential for malonyl-ACP decarboxylation to generate a carbon anion and the Cys residue catalyzes condensation between acyl-S-KS and resultant carbon anion to form a C–C bond. It was confirmed, that a single amino acid substitution in the active site would render the KS inactive.[35] Further, it was established that both methyl groups at C2′ position come from methionine,[20] but the presence of only one MT (in module 6) led to the assumption that MT domain catalyzes the two C2′ methyl-transfer processes

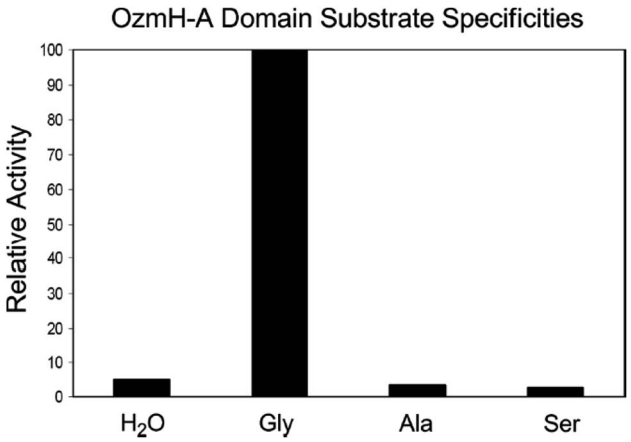

Fig. 4 Determination of OzmH A domain substrate specificities. The ATP-PP_i exchange reactions were performed using amino acids Gly, Ala and Ser as substrates and H_2O as a negative control (100% relative activity corresponds to 995 320 cpm).[25]

iteratively.[36] It was primary assumed that MT domain should be present in module 10 to account for the introduction of the methyl group at C6 position. However, the conserved *S*-adenosyl-L-methionine binding motif, leading to prediction of MT domain was unexpectedly found upstream in module 9.[36] On the basis of A domain specificity-conferring code, in harmony with isotope labeling studies[20] and supported by substrate specificity prediction by an *in vitro* amino acid-dependent radiolabel exchange assay it is predicted, that glycine is the substrate specificity for the A domain of OzmH (Fig. 4).[25]

2.2.3 Genes encoding PKSs. The *ozmQ*, *ozmN*, *ozmJ* and *ozmK* were identified as the four PKS genes of *ozm* cluster (Fig. 5). Together they encode six PKS modules. The *ozmQ* gene encodes OzmQ protein (842 amino acids) which consists of two domains: KS and ACP, constituting module 2. The *ozmN* gene encodes OzmN protein (4971 amino acids) which can be subdivided into three modules (modules 3–5). OzmN protein includes three KS, three DH, three KR, three ACP and one MT domain. The *ozmJ* gene encodes OzmJ protein (2926 amino acids) as a complex PKS which consists of two KS, two ACP, DH, enoyl reductase (ER), and KR. The OzmJ protein represents module 11, which is probably responsible for the incorporation of an unusual methoxymalonyl-ACP extender unit to afford the C3–C4 section of oxazolomycin A. The first of KS in OzmJ has a catalytic triad of Cys–His–His, the second KS possesses a Cys–Thr–His triad that might be inactive due to the change of a critical histidine residue for malonyl-ACP decarboxylation.[33,34] Both ACPs in OzmJ contain the serine residue required for post-translational attachment of the 4′-phosphopantetheine group. Otherwise, the OzmK protein (1202 amino acids) is characterized with the domain organization ACP-KS-MT-ACP to constitute module 12. However, N-terminal ACP contains a leucine substitution for serine at the 4′-phosphopantetheine attachment site, rendering it inactive, whereas the C-terminal ACP with conserved motif should be fully functional.[25]

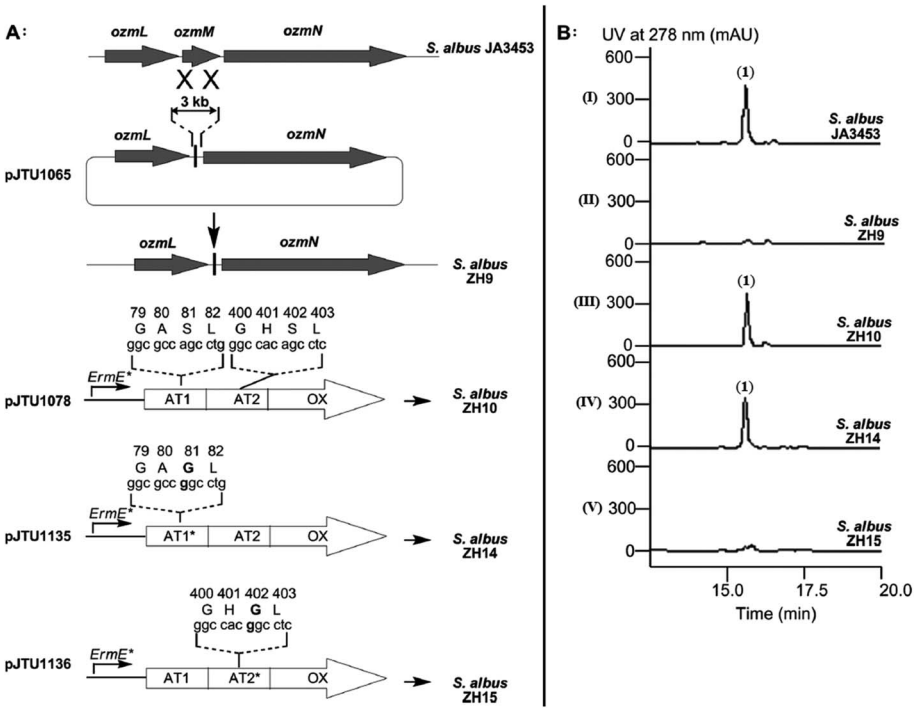

Fig. 5 Deletion of *ozmM* and complementation of the *ozmM* mutant with either intact *ozmM* or *ozmM-AT1* (Ser81 to Gly) or *ozmM-AT2* (Ser402 to Gly) mutant and their effect on the biosynthesis of oxazolomycin A. (A) Schematic representation of constructs for the generation of the ZH9 deletion mutant strain and its genetic complementation strains ZH10, ZH14 and ZH15. Details of side-specific mutagenesis with OzmM-AT1 and OzmM-AT2 are shown. (B) HPLC analysis of oxazolomycin A (**1**) production in: (I) *Streptomyces albus* JA3453; (II) ZH9 mutant; (III) ZH10 mutant; (IV) ZH14 mutant and (V) ZH15 mutant.[25]

2.2.4 Genes encoding enzymes for methoxymalonyl-ACP biosynthesis. In 2006 Zhao *et al.* reported, that *ozmBCDEFG* gene subcluster constitutes a cotranscribed operon required for biosynthesis and incorporation of the methoxymalonyl-ACP extender unit into oxazolomycin A because the numbers of nucleotides between the stop and start codon of the adjacent genes are all too small to code any regulatory elements for transcriptional initiation.[26] Five of the six genes (exception *ozmC*) are absolutely conserved among methoxy malonyl-ACP biosynthetic loci. The OzmG (287 amino acids) closely resembles to the hydroxyacyl-coenzyme A dehydrogenase (HADH) family of enzymes. The OzmF (221 amino acids) is a probable *O*-methyltransferase, OzmE (93 amino acids) is a probable ACP and OzmD (366 amino acids) is an acyl-coenzyme A dehydrogenase (ACDH). Dorrestein *et al.* reported,[22] that OzmB (366 amino acids) acts as a bifunctional glyceryl transferase/phosphatase belonging to the haloacid dehalogenase (HAD) superfamily of enzymes.[25]

2.2.5 Genes encoding discrete AT enzymes. The *ozmC* gene encodes a unique enzyme OzmC (325 amino acids), that has not been found in other methoxymalonyl-ACP biosynthesis loci of type I PKSs. Previous experiments[7,18] confirmed, that OzmC plays a crucial role in biosynthesis of oxazolomycin A. Therefore, OzmC is served as a candidate for the discrete AT loading of the methoxymalonyl-ACP extender to module 11 (Fig. 6). Further, discrete AT enzyme encoded by *ozmM* gene was characterized in the *ozm* cluster. The OzmM (1039 amino acids) contains tandem AT domains (AT1 and AT2) and oxidoreductase domain (OX) (Fig. 6). It was initially postulated, that both ATs in OzmM are specific for the methoxymalonyl-ACP (OzmM-

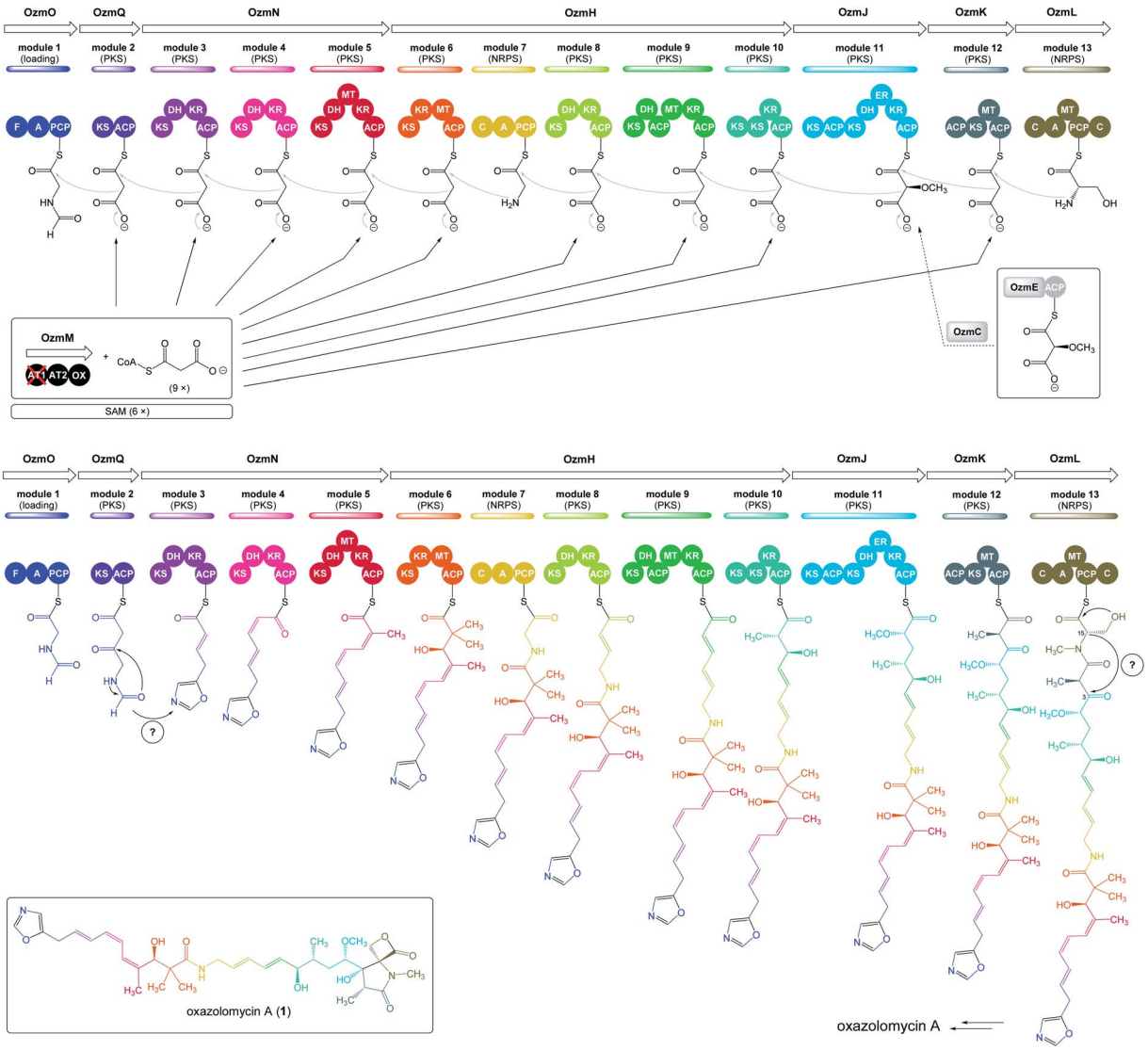

Fig. 6 Proposed model of oxazolomycin A biosynthesis in *Streptomyces albus* JA3453. Used abbreviations: A, adenylation domain; ACP, acyl carrier protein domain; AT1, N-terminal acyl transferase domain of OzmM; AT2, central acyl transferase domain of OzmM; C, condensation domain; DH, dehydratase domain; ER, enoyl reductase domain; F, formylation domain; KR, ketoreductase domain; KS, ketosynthetase domain; MT, methyltransferase domain; OX, oxidoreductase domain; PCP, peptide carrier protein domain; ?, unknown domain; SAM, *S*-adenosyl methionine.[25]

AT1) and malonyl-CoA (OzmM-AT2) extender unit. However, it was experimentally proven by Zhao *et al.*, that only OzmM-AT2 is necessary, whereas OzmM-AT1 is dispensable for production of the oxazolomycin A.[25] When the catalytic active site of OzmM-AT2 was specifically mutated (exchange of Ser402 to Gly), the biosynthesis of oxazolomycin A in resultant strain *Streptomyces albus* ZH15 was completely abolished. The Ser402 residue in active site of OzmM-AT2 employs to form the acyl-*O*-intermediate before transferring acyl groups from their CoA substrate to the nucleophile recipient ACP. Likewise, abolished biosynthesis of oxazolomycin A was observed, when OzmM was deleted entirely (*Streptomyces albus* strain ZH9). In contrast, mutation in OzmM-AT1 (exchange of Ser81 to Gly) caused no changes in the level of oxazolomycin A production (*Streptomyces albus* strain ZH14), resulting that OzmM-AT1 is cryptic or serves as an inactive domain. Based on the similarity to other discrete AT domains, the OzmM-AT2 domain is most likely responsible for the loading of the malonyl-CoA extender unit to all of the oxazolomycin's AT-less PKS modules except for module 11.[25]

2.2.6 Genes encoding resistance, regulatory proteins and proteins of unknown function. The *ozmA* gene encodes a putative multidrug transporter and deduced gene product *ozmS* belongs to the lysine exporter (LysE) family of transporters.[26,37] Therefore, both OzmA (482 amino acids) and OzmS (214 amino acids) may confer oxazolomycin resistance in *Streptomyces albus* JA3453 *via* drug transport. The *ozmR* and *ozmU* genes encode hypothetical regulatory proteins. The OzmR (308 amino acids) shows significant similarity to the LysR family of regulators, whereas OzmU (929 amino acids) belongs to the *Streptomyces* antibiotic regulatory protein (SARP) family of regulators. Although, OzmT (439 amino acids) resembles other Thr-tRNA synthetases, its exact roles still need to be determined.[25] The N-terminal of *ozmP* gene shows some resemblance to a subfamily of ATP pyrophosphatase and members of the superfamily ATP sulfurylase.[38] The gene *ozmP* along with *ozmO* and *ozmQ* constitute an operon that may be co-transcribed because the gaps between these three genes are too small to encode a promoter, but the exact role of OzmP (382 amino acids) for oxazolomycin A biosynthesis is still elusive.[25]

2.2.7 Hypothetical biosynthesis of methoxymalonyl-ACP. The hypothetical biosynthesis of methoxymalonyl-ACP is proposed as follows. The primary metabolite 1,3-bisphosphoglycerate (**19**) is transformed by OzmB into a phosphoglyceryl-S-OzmB intermediate (**20**). Then removes the phosphate group to afford 3-glyceryl-S-OzmB (**21**) (acting as a phosphatase). Subsequent transformation of glyceryl group (acting as a glyceryl transferase) to ACP of OzmE forms glyceryl-ACP (**22**). Following oxidation by OzmG, a 3-hydroxyacyl-coenzyme A dehydrogenase and then by OzmD, an acyl-coenzyme A dehydrogenase led to hydroxymalonyl-ACP (**24**). Finally, a methyl group is transferred by an OzmF, *O*-methyltransferase to generate methoxymalonyl-ACP intermediate (**25**) as an unusual polyketide extender unit (Scheme 1).[22,23,25]

2.2.8 Proposed biosynthesis of oxazolomycin A in Streptomyces albus JA3453. Detailed analysis of genes in the *ozm* cluster led to a model for biosynthesis of oxazolomycin A reported by Zhao *et al.*,[25] featuring PKSs (OZMJKMNQ), NRPSs (OzmO and OzmL) and a hybrid NRPS-PKS megasynthase (OzmH). It is proposed that the biosynthesis of oxazolomycin A is initiated by OzmO. It is assumed, that the OzmO A domain first activates glycine and loads it onto the OzmO PCP domain. Then the F domain of OzmO formylates on glycyl-S-PCP, to give formyl-glycyl-S-PCP. The enzyme responsible for the conversion of formyl-glycyl-S-PCP into the oxazole ring is still unknown, as is the timing of the cyclization process.

Bioinformatic analysis failed to predict such a cyclase gene or domain, within the *ozm* cluster. However, the OzmP, adjacent to and co-transcribed with OzmO, whose function could not be assigned to date, may be involved in oxazole ring biosynthesis. Further it is assumed, that intermediate could be condensed with malonyl-CoA on the OzmQ (module 2). Condensation with other three malonyl-CoAs takes place on OzmN (modules 3–5), along with *C*-methylation to C4′ position mediated by MT domain (module 5). Transportation to large protein OzmH involves condensation with malonyl-CoA and assumed double *C*-methylation to C2′ position by MT domain (module 6). After condensation with glycine (module 7) and with three malonyl-CoAs (modules 8–10), other *C*-methylation into C6 position occurs within OzmH. Although an MT domain should be present in module 10, as deduced from the structure of oxazolomycin A, it was unexpectedly identified in module 9. This gene organization may be explained as domain mispositioning, reflecting complex domain–domain interactions for polyketide-catalyzed methylation. Condensation with a methoxymalonyl-ACP is realized on OzmJ (module 11). After translocation to

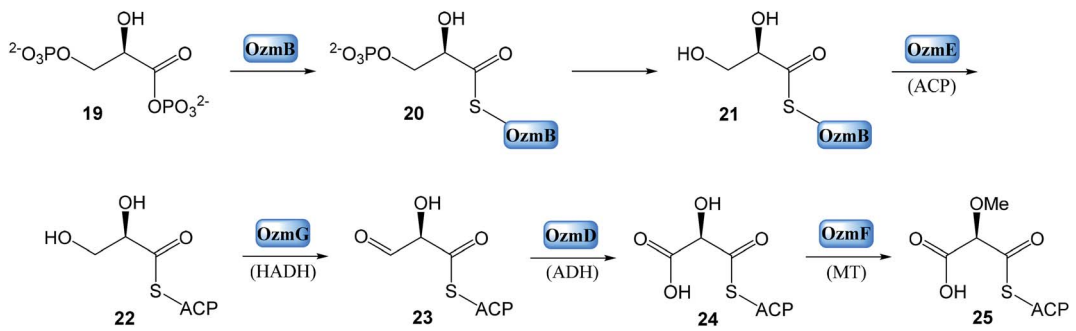

Scheme 1 Proposed pathway for methoxymalonyl-ACP extender unit biosynthesis in *ozm* cluster.

OzmK, a condensation with malonyl-CoA and *C*-methylation to C2 position takes place (module 12).

Finally, the biosynthesis of oxazolomycin A is terminated on OzmL. The amino acid serine is activated by the A domain and covalently bound to the PCP. Further, N-terminal C domain catalyzes formation of the peptide bond between seryl-S-PCP and the preceding acyl-S-ACP intermediate, followed by *N*-methylation by the MT domain. The C domain residing at the C terminus was proposed to release the full-length hybrid peptide polyketide product from PCP, giving the four-membered β-lactone ring, because no thioesterase domain was identified in the *ozm* cluster. Although the C-terminal C domain lacks a catalytic triad for condensation, it does have the Asp residue in both C domains and heterocyclase domains, which are subtypes of C domains. The heterocyclase domains catalyze not only peptide bond formation, but also subsequent cyclization of Cys, Ser or Thr, to afford a thiazoline or oxazoline ring. Although the C-terminal C domain in OzmL lacks the crucial His that is believed to be indispensable for condensation of aminoacyl-ACP and peptidyl-ACP, it may be still functional. Especially given, that this domain is not expected to catalyze peptide bond formation but only cyclization of the Ser side chain to form a β-lactone ring. Some of characterized C domains have been demonstrated[39,40] to catalyze ester bond formation. A similar function would be envisioned for the OzmL C-terminal C domain to be involved in β-lactone ring formation. However, a cyclase may be required for C3–C15 bond formation to afford the heterocyclic γ-lactam ring, but no apparent candidate gene was identified by bioinformatic analysis in the *ozm* cluster (Fig. 6).[25]

This oxazolomycin A NRPS-PKS megasynthase was also characterized with many features that appear to violate the typical "co-linearity rule" for NRPS or PKS domain organization, including domain redundancy (presence of two ACPs flanking the MT and KR domain in module 9; tandem KSs in module 10; two ACPs and two KSs in module 11) and mispositioning (presence of MT domain in module 9 except assumed module 10).[25,41,42] The example of domain redundancy has been

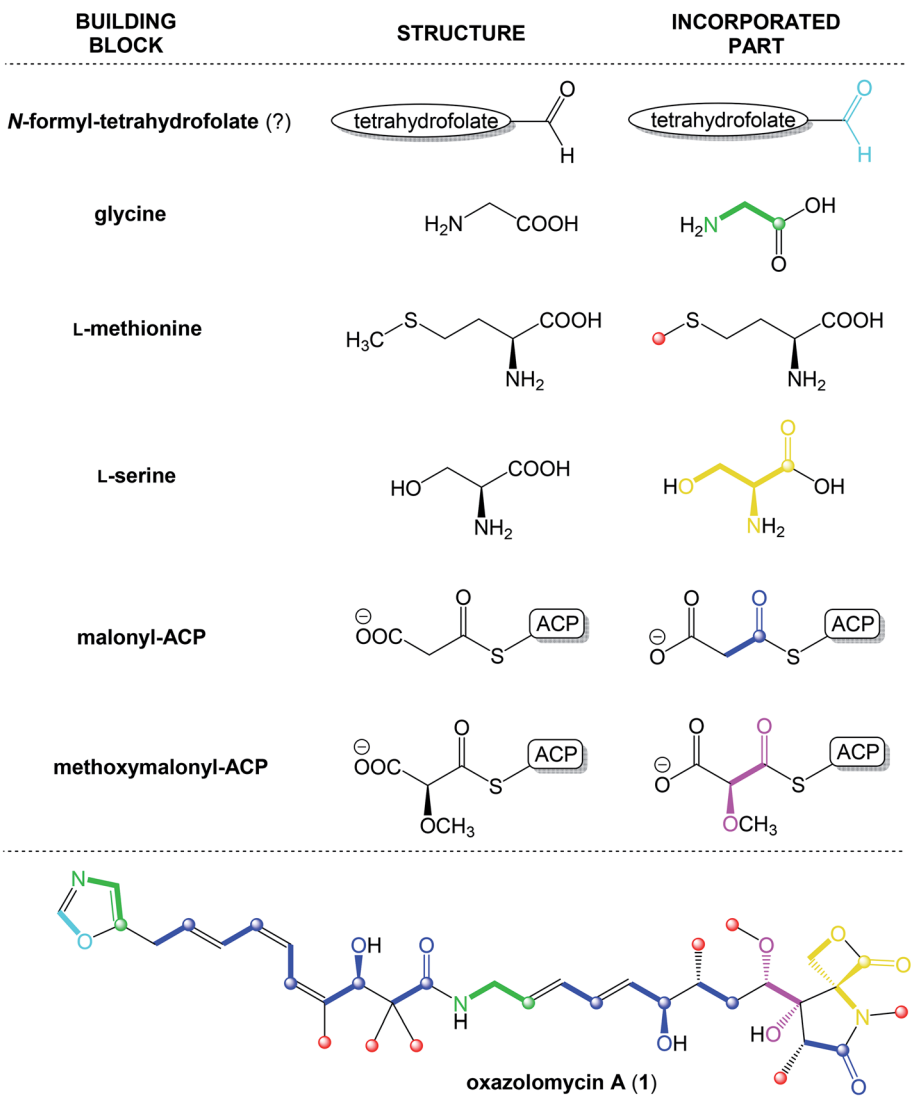

Fig. 7 Proposed biosynthetic origin of oxazolomycin A (**1**) according to labeling data and analysis of genes in *ozm* cluster.

confirmed experimentally where the catalytic Cys residue of the tandem KSs of OzmH module 10 were site-specifically mutated to Gly.[25,35]

According to results from labeling data[20] and analysis of genes in the *ozm* cluster,[25] presumably a whole structure of oxazolomycin A is constructed from 6 different building blocks (Fig. 7).

3 Biological activity of oxazolomycins and their fragments

3.1 Biological activity of oxazolomycin fragments

3.1.1 Proposed influence of right-hand fragment on the bioactivity of oxazolomycins. Since their discovery all members of oxazolomycin family exhibit interesting biological properties.

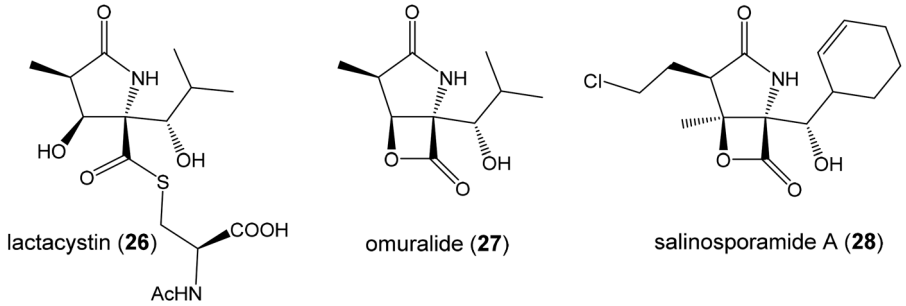

Fig. 8 Known proteasome inhibitors with pyroglutamate core.

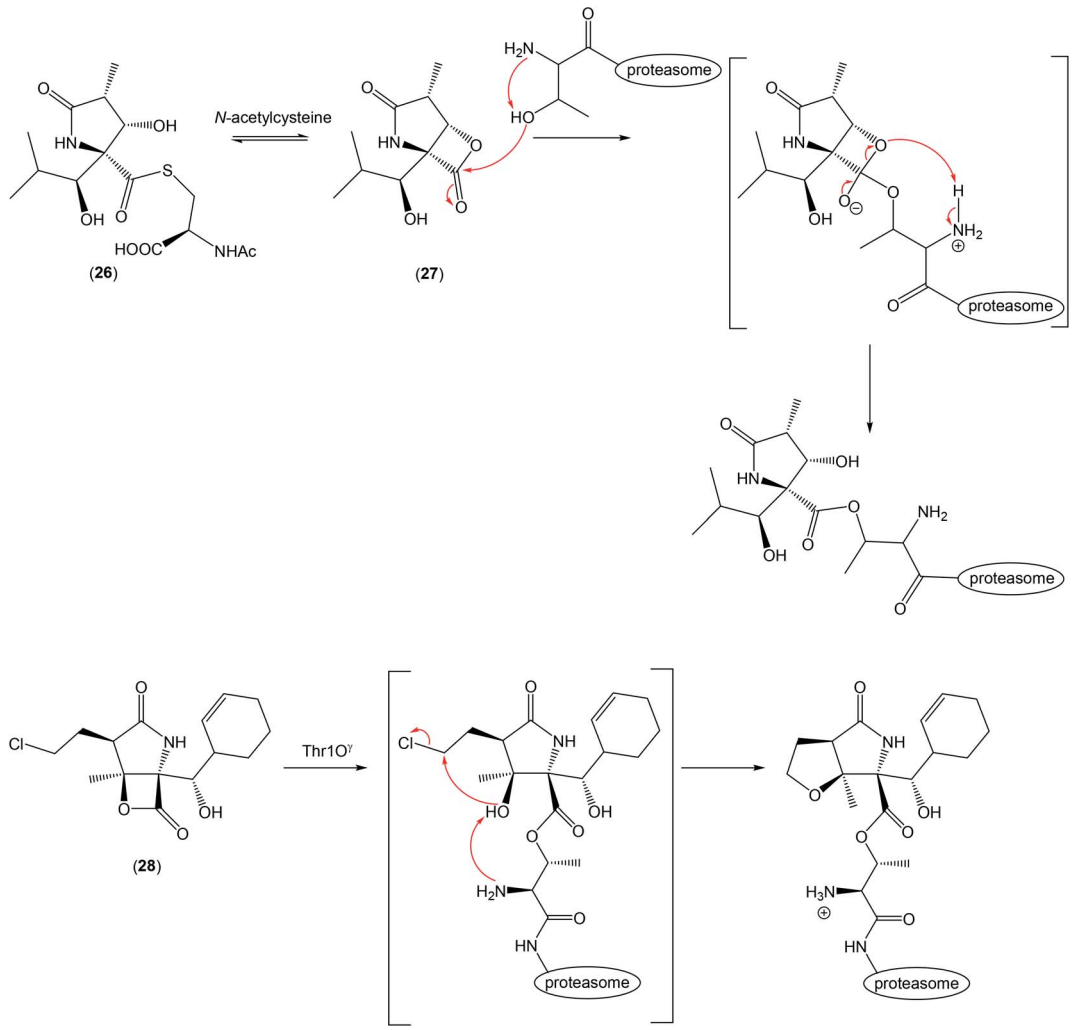

Scheme 2 Pyroglutamate derivatives and their binding in 20S proteasome.

The pyroglutamate core of right-hand fragment draws much attention due to the structural similarities with pyroglutamate core of known proteasome inhibitors,[43] such as omuralide (**27**) and salinosporamide A (**28**) (Fig. 8).[44] The β-lactone-γ-lactam moiety of **28** is responsible for inactivation of 20S proteasome by acetylation of Thr1O$^{\gamma}$ in the active site.[45] Lactacystin (**26**) is a monocyclic γ-lactam, which is inactive to proteasome, but after cyclization generate active lactacystin β-lactone, also known as omuralide (**27**),[46] which forms covalent binding to active site of proteasome (Scheme 2).[47] These findings support the hypothesis of the similar bioactivity for oxazolomycins with β-lactone-γ-lactam core.

Several studies evaluated SAR properties of right-hand fragment derivatives of oxazolomycins. It was reported, that the intrinsic antibacterial activity of simple pyroglutamates[48,49] and tatramates[50] is low. However further reports suggested,[51,52] that homologation to longer chain side-units restores bioactivity. Anwar *et al.* observed that a change as small as the introduction of a methyl substituent improves bioactivity in tetramates.[53] The right-hand fragment derivatives were evaluated against *Staphylococcus aureus* and *Escherichia coli* using the hole-plate method. Although quantitative MIC values are not available, these *in vivo* assays give outcomes enabling rapid assessment of the effect of structural variations of the fragment modification. Moreover, chemical informatics analysis of prepared derivatives was reported. Selected structures are shown in Fig. 9, their bioactivity and chemical informatics analysis are summarized in Table 2.

Holloway *et al.* prepared series of substituted tetramates **29–36** with antibacterial properties.[52] Significant activity against *S. aureus* was observed for substituted tetramate **29**, however against *E. coli* no bioactivity was observed. The tatramates **30**, **31**, **32** and bicyclic derivatives **34**, **35** exhibited similar bioactivities, whereas activity of primary alcohol **33** was lightly reduced. Bicyclic enamine **36** was inactive against *S. aureus*, however the activity against *E. coli* was found. Chemical informatics analysis is shown in Table 2.[52] Additionally, SAR analysis of pyroglutamate core derivatives was evaluated by Angelov *et al.* on different structural modifications of oxazolomycin's right-hand fragment.[54] The compounds **37–44** (Fig. 9) were the only products with activity against both *S. aureus* and *E. coli*, although out of the compounds with the correct relative configuration for oxazolomycin A, only **39**, **43** and **44** were active.

Most of the active compounds prepared by Angelov *et al.* have clog *P* values in the range 1.8–2.5 and % PSA values (polar surface area parameter (PSA)/molecular surface area parameter (MSA) × 100%) close to 14, with a potency of some 1–4% relative to the cephalosporin reference standard (Table 2). However, the compounds **43** and **44** were clearly different, being very much polar, with clog *P* values in the range −0.01 to 0.5 and % PSA values close to 21. It is noteworthy, that substitution of Bn group in benzyloxymethyls **37**, **38**, **40** and **42** to Me group afforded corresponding methoxymethyls, which might be considered as mimics structurally closest to the oxazolomycin's right-hand fragment. However, all of these methoxymethyls were inactive or only weakly active. It was assumed, that better activity of benzyloxymethyl structures **37**, **38**, **40** and **42** than corresponding methoxymethyls was a result of improved cell membrane permeability. It is interesting, that most active

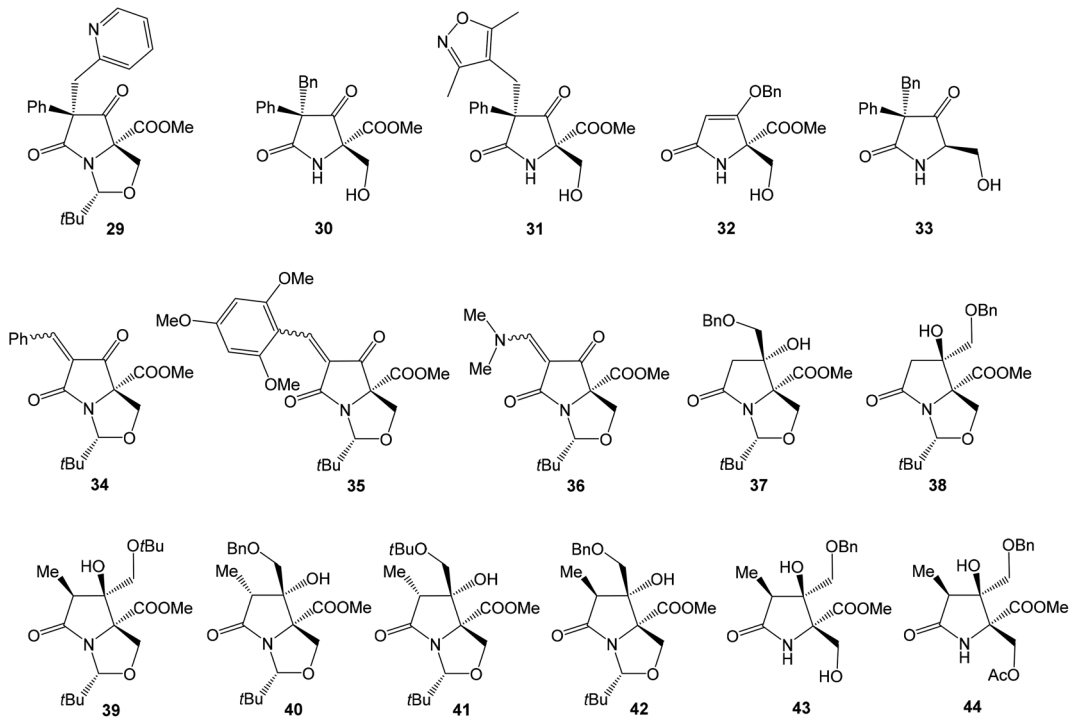

Fig. 9 Selected bioactive right-hand fragment derivatives.

Table 2 Chemical informatics analysis and bioassay of selected right-hand fragment derivatives

				Bioactivity				
				S. aureus		*E. coli*		
Compound	Log P^a	PSA[a]	% PSA[b]	Zone size [mm]	Relative potency[c]	Zone size [mm]	Relative potency[c]	Reported by
Oxazolomycin A (**1**)	1.61	171.7	17.9	—	—	—	—	Angelov *et al.*[54]
Oxazolomycin B (**3**)	1.61	171.7	17.9	—	—	—	—	Angelov *et al.*[54]
Oxazolomycin C (**4**)	1.61	171.7	17.9	—	—	—	—	Angelov *et al.*[54]
16-Methyloxazolomycin (**5**)	2.03	171.7	17.1	—	—	—	—	Angelov *et al.*[54]
Curromycin A (**6**)	1.72	180.1	16.6	—	—	—	—	Angelov *et al.*[54]
Curromycin B (**7**)	2.10	171.7	16.5	—	—	—	—	Angelov *et al.*[54]
KSM-2690 B (**8**)	2.03	171.7	17.1	—	—	—	—	Angelov *et al.*[54]
KSM-2690 C (**9**)	2.03	171.7	17.1	—	—	—	—	Angelov *et al.*[54]
Lajollamycin (**10**)	2.66	191.5	18.4	—	—	—	—	Angelov *et al.*[54]
29[d]	3.75	85.8	13.8	25	—	Inactive	—	Holloway *et al.*[52]
30[d]	2.45	92.7	18.8	15	—	18	—	Holloway *et al.*[52]
31[d]	1.15	118.7	22.8	14	—	19	—	Holloway *et al.*[52]
32[d]	−0.04	84.9	22.4	15	—	19	—	Holloway *et al.*[52]
33[d]	2.45	66.4	15.8	12	—	14	—	Holloway *et al.*[52]
34[d]	3.34	72.9	14.8	15	—	18	—	Holloway *et al.*[52]
35[d]	2.87	100.6	15.7	15	—	19	—	Holloway *et al.*[52]
36[d]	1.33	76.2	16.1	Inactive	—	18	—	Holloway *et al.*[52]
37[e]	1.97	85.3	14.4	15	3.8	18	0.087	Angelov *et al.*[54]
38[e]	2.14	85.3	14.4	13	0.91	19	0.08	Angelov *et al.*[54]
39[e]	1.84	85.3	14.0	11[f]	1.7	12[f]	0.035	Angelov *et al.*[54]
40[e]	2.51	85.3	13.8	13	2.6	18	0.087	Angelov *et al.*[54]
41[e]	1.84	85.3	14.0	11[f]	1.7	12[f]	0.035	Angelov *et al.*[54]
42[e]	2.51	85.3	13.8	15	3.8	15	0.055	Angelov *et al.*[54]
43[e]	−0.01	105.1	21.8	11	—	18	0.06	Angelov *et al.*[54]
44[e]	0.45	111.2	20.4	13	0.88	18	0.07	Angelov *et al.*[54]

[a] Log *P*, PSA and MSA calculated using Marvin. [b] % PSA = (PSA/MSA) × 100%. [c] Expressed as zone size per mg ml^{-1}, relative to cephalosporin C standard. [d] Using 100 μl of 4 mg ml^{-1} solution (DMSO). [e] Using 100 μl of 4 mg ml^{-1} solution (6 : 4, DMSO : H_2O). [f] Halo only.

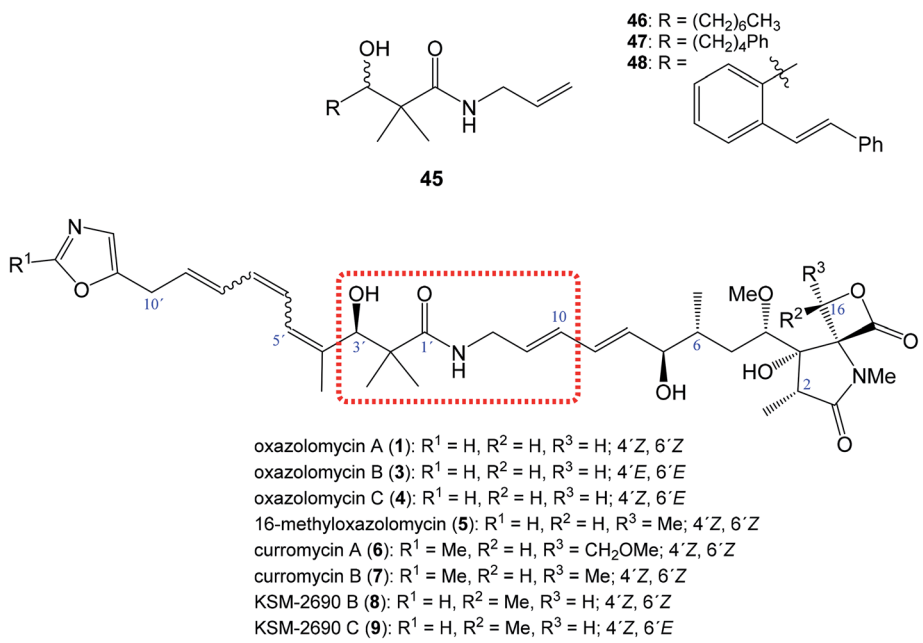

Fig. 10 Position of structural subunit **45** in the structure of oxazolomycins responsible for U-shaped conformation and its derivatives **46**–**48** prepared by Bagwell *et al.*

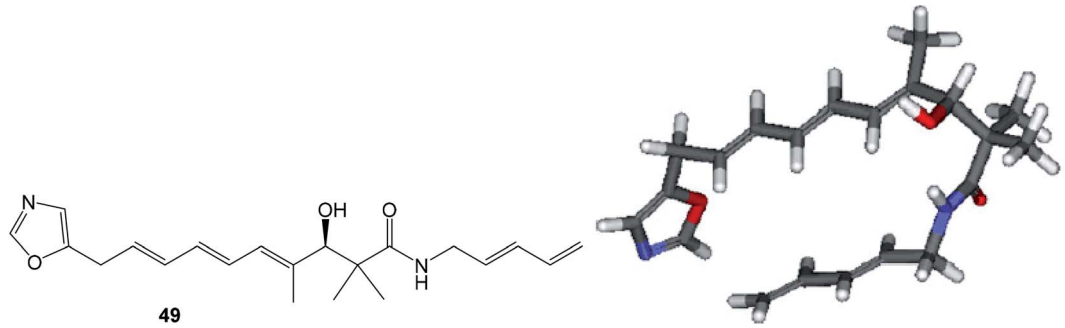

Fig. 11 Structure and calculated minimum energy conformation of amide **49**.

compounds prepared by Angelov *et al.* had chemical informatics values which correlated with the corresponding values for oxazolomycins described in Table 2. However, it is important to note, that only compounds **39**, **43** and **44** have correct relative configuration to oxazolomycins.[54]

Moreover, Koomsiri *et al.* reported, that antibacterial activity (Fig. 16) of oxazolomycin A (**1**) is more potent than oxazolomycin A2 (**14**) and bisoxazolomycin (**15**).[10] It is proposed, that β-lactone ring in right-hand fragment of oxazolomycin A plays an important role in the antibacterial activity.[10] This assumption is in accordance with proposed β-lactone-γ-lactam core importance for biological activity.[46,47]

3.1.2 Proposed influence of central fragment on the bioactivity of oxazolomycins. Bagwell *et al.* reported importance of 3-hydroxy-2,2-dimethylpropanamide structural subunit (**45**; Fig. 10), which is localized close to central fragment in the structure of oxazolomycins.[55] They suggested that *gem*-dimethyl amide motif of oxazolomycins is likely to enforce a U-shaped structure on the basis of Thorpe–Ingold effect,[56] and that this might be an important effect for the bioactivity. The minimum conformational energy of structure **49** (Fig. 11), which represents truncated structure of oxazolomycin B (**3**) confirmed that geminal dimethylamide motif induced a U-turn shape of the structure. Such structure is likely to be stabilized by a hydrogen bond as a result of the predicted close proximity (2.07 Å) of the NH and HO–C3′ groups (oxazolomycin's numbering). The molecular model of inthomycin B (**17**) (Fig. 12), which is a primary amide lacking the dienyl substituent indicated, that corresponding NH–O distance is the same (2.07 Å), but the structure is clearly linear. Finally, the molecular model of oxazolomycin B (**3**) (Fig. 13) calculated, that NH–O distance is much longer (4.07 Å), which is too long for effective H-bond, although the structure clearly preferred U-shaped conformation.

Bagwell *et al.* further reported, that appropriately substituted 3-hydroxy-2,2-dimethylpropanamide motif present in oxazolomycins can exhibit antibacterial activity itself. Selected compounds **46**, **47** and **48** (Fig. 10) were evaluated against *Staphylococcus aureus* and *Escherichia coli* to provide their bioactivity (Table 3).[55] The bioassay against *S. aureus* showed, that compound **46** is inactive, however derivatives **47** and **48** were active. It was found, that the most active structure **47** (MIC 4 mg ml^{-1})[55] is approximately 80-fold less active than KSM-2690 B (**8**) (MIC 50 μg ml^{-1}).[7] However, higher level of the activity were found against *E. coli*. The MIC of selected compounds **46–48** was found to be in range 0.5–1 mg ml^{-1}.[55] Since the reported MIC values for *E. coli* using oxazolomycins A–C (**1**, **3** and **4**) were found 100 μg ml^{-6}, the most active compounds **47** and **48** resulted approximately only 5–10 times weaker.[55] These results suggest, that structural subunit **45** present in structure of oxazolomycins could plays an additional role for final bioactivity.

3.1.3 Proposed influence of left-hand fragment on the bioactivity of oxazolomycins. Inthomycins A–C (**16–18**) represent left-hand fragment of oxazolomycin family members, except for lajollamycins (**10–13**). The inthomycins display a wide range of biological activities. Omura *et al.* reported, that inthomycin A (**16**) showed selective antimicrobial activity against cellulose-containing *Phytophthora parasitica* (MIC 125 μg ml^{-1}) and *Phytophthora cactorum* (MIC 31.3 μg ml^{-1}).[57] The herbicidal activity of **16** was evaluated on the inhibition of

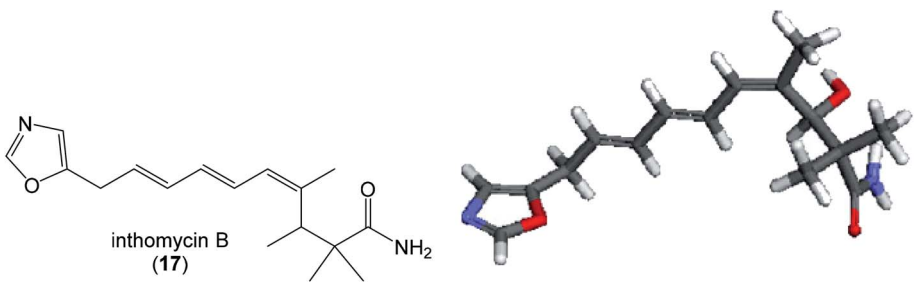

Fig. 12 Structure and calculated minimum energy conformation of inthomycin B (**17**).

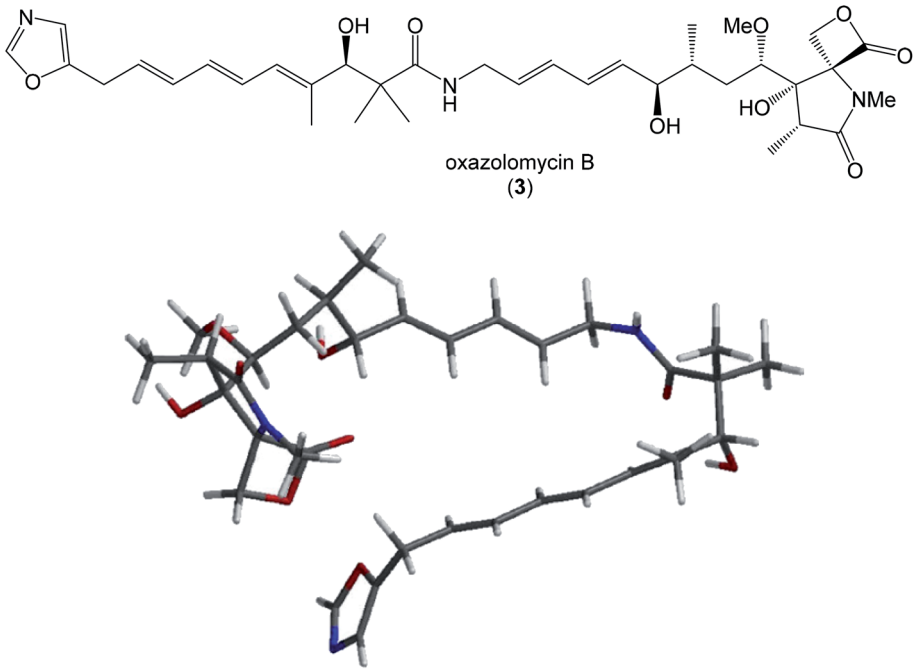

Fig. 13 Structure and calculated minimum energy conformation of oxazolomycin B (**3**).

Table 3 Bioassay of selected structural subunit derivatives **46–48** prepared by Bagwell *et al.*[55]

		Bioactivity[b]					
		S. aureus			*E. coli*		
Compound	Log P^a	Zone size [mm]	Relative potency[c]	MIC[d]	Zone size [mm]	Relative potency[c]	MIC[d]
46	3.73	Inactive	—	—	22	0.01	1.0
47	4.08	17	0.08	4	23	0.01	0.5
48	4.74	14	0.06	nd[e]	20	0.01	0.5

[a] Log *P* calculated using ChemBioDraw Ultra 11.0. [b] Hole plate bioassay at 4 mg ml^{-1} (7 : 3, DMSO : H_2O). [c] Expressed as zone size per mg ml^{-1}, relative to cephalosporin C standard. [d] Estimated by seriál dilution until no inhibition zone is observed. [e] nd = not determined.

radish seedlings (*Raphanus sativus* L.) growth in laboratory test tubes with MIC of 25 μg per tube.[57] Further, it was reported that no mice died after oral administration of **16** at dose 100 mg kg^{-1}.[57] Other study reported by Omura *et al.* showed, that **16** acts as an inhibitor of cellulose biosynthesis.[58] In 2009 Kawada *et al.* reported, that **16** and inthomycin B (**17**) inhibit the growth of human prostate cancer DU-145 cells by modulating tumor–stromal cell interactions.[40] The study involves using an *in vitro* coculture system, in which prostate cancer cell growth is upregulated by prostate stromal cells (PrSC). It was found, that both **16** and **17** strongly inhibited the growth of DU-145 cells when in coculture with PrSC compared to DU-145 cells culture alone. The effect on PrSC growth was not observed (Fig. 14).[59]

Inthomycins as the structural subunits of oxazolomycins are interesting compounds with wide range of biological activities. It is assumed, that some of the beneficial biological properties of inthomycins could resemble to bioactivity of oxazolomycins. Unfortunately, direct and comprehensive evaluation of the biological properties of inthomycins and oxazolomycins is still missing to date.

3.2 Biological activity of oxazolomycins

3.2.1 Antialgal activity. Kim *et al.* reported antialgal activity of 16-methyloxazolomycin (**5**) against *Chlorella vulgaris* IFO 15941 (MIC 10 μg ml^{-1}).[5] Unfortunately, no other antialgal activity has been reported to date. However, a positive result reported by Kim *et al.*[5] indicated a potential for other family members in this area.

3.2.2 Antibacterial activity. Most of the members of oxazolomycin family were tested against different bacterial species. It was observed that some oxazolomycins exhibit activity against Gram positive as well as against Gram negative bacterial strains. Early after oxazolomycin A (**1**) discovery Kawai *et al.* reported its antibacterial activity selectively against *Agrobacterium*

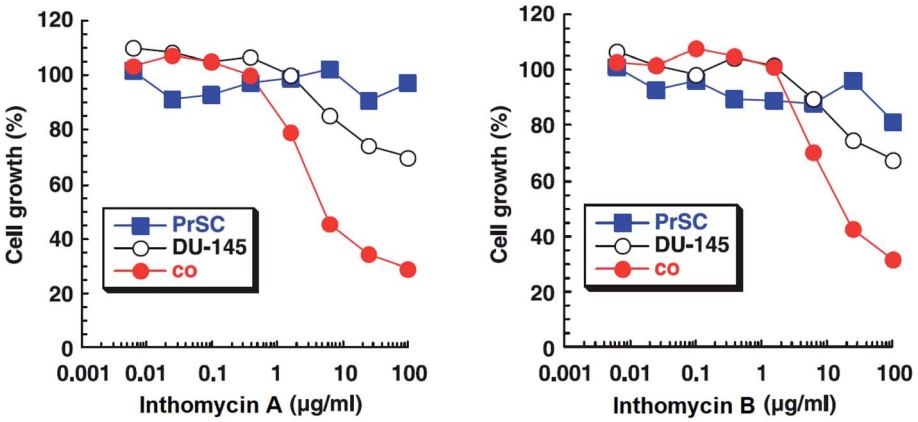

Fig. 14 Effects of inthomycin A (**16**) and inthomycin B (**17**) on the growth of DU-145 cells alone (black open circles), DU-145 cells cocultured with PrSC (red filled circles) and PrSC alone (blue filled squares) were determined using rhodanile blue staining.[59]

Table 4 The values of MIC for oxazolomycin A (**1**), B (**3**) and C (**4**) in bacterial strains

	Minimum inhibitory concentration (MIC) [μg ml^{-1}]						
	Agrobacterium rhizogenes IFO 13257	*Agrobacterium tumefaciens* EHA 101	*Agrobacterium tumefaciens* IFO 13263	*Bacillus subtilis*	*Escherichia coli*	*Pseudomonas putida* IFO 3738	*Rhizobium loti* IFO 13336
Oxazolomycin A (**1**)	25.0	6.3	3.1	>100	>100	50.0	>100
Oxazolomycin B (**3**)	>100	100	>100	>100	>100	—	>100
Oxazolomycin C (**4**)	>100	>100	>100	>100	>100	—	>100

tumefaciens IFO 13263 (MIC 3.1 μg ml^{-1}).[60] Lower antibacterial activity of **1** was observed against *Agrobacterium rhizogenes* IFO 13257 (MIC 25.0 μg ml^{-1}) and *Pseudomonas putida* IFO 3738 (50.0 μg ml^{-1}). However, the activity of **1** against *Bacillus subtilis* IFO 3007, *Escherichia coli* OP50, *Mycobacterium avium* IFO 3154, *Rhizobium meliloti* IFO 13336 and *Staphylococcus aureus* IFO 3060 was not observed (MIC > 100 μg ml^{-1}). Kawai *et al.* further observed no inhibitory effect of neooxazolomycin (**2**) against *Agrobacterium tumefaciens*.[60] Ryu *et al.* reported, that 16-methyloxazolomycin (**5**) showed an interesting antibacterial activity against *Bacillus subtilis* IAM 1069 (MIC 5.0 μg ml^{-1}).[5]

The biological activities of oxazolomycin A (**1**), oxazolomycin B (**3**) and oxazolomycin C (**4**) were mutually compared by Kanzaki *et al.* on following bacteria: *Agrobacterium tumefaciens* IFO 13263, *Agrobacterium tumefaciens* EHA 101, *Agrobacterium rhizogenes* IFO 13257, *Rhizobium loti* IFO 13336, *Escherichia coli* and *Bacillus subtilis* (results are summarized in Table 4).[6] As seen in Table 4, oxazolomycins **3** and **4** were inactive against tested bacteria, whereas **1** showed some activity against *Agrobacterium rhizogenes* IFO 13257 and significant activities against *Agrobacterium tumefaciens* IFO 13263 and *Agrobacterium tumefaciens* EHA 101. Noteworthy, oxazolomycins **1**, **3** and **4** are geometric isomers with structural diversity in their left-hand fragment (inthomycin subunit). These results suggest biological importance of left-hand fragment considering identical central and right-hand fragment of tested oxazolomycins.

Antibacterial activities of curromycin A (**6**) and B (**7**) were reported as very similar. Early in 1985 Ogura *et al.* reported,[61] that biological activities of **7** were almost identical with **6**.[3] For example significant bioactivity of **7** against *Bacillus subtilis* IAM 1026 (MIC 3.9 μg ml^{-1}) but lower against *Pseudomonas cepacia* M-0527 (MIC 50.0 μg ml^{-1}) were reported.[61] Similarly, identical weak antimicrobial activity for both **6** and **7** was reported by Ikeda *et al.* against *Micrococcus luteus* FDA16 (MIC 25 μg ml^{-1}) and *Pseudomonas aeruginosa* A3 (MIC 50 μg ml^{-1}).[4] Solutions of 2.5 μg ml^{-1} of **6** and **7** in 1/15 M phosphate buffer (pH = 6.8)

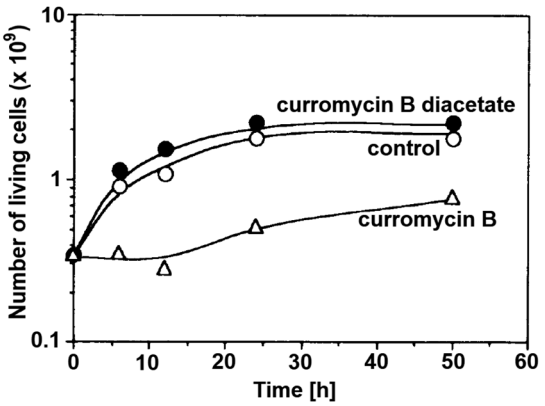

Fig. 15 Effect of curromycin B (**7**) and curromycin B diacetate against *Agrobacterium tumefaciens* growth on an inoculated potato tuber disk. Bacterial cells in the absence (○) and the presence of curromycin B diacetate (●) or curromycin B (Δ) were counted 0, 6, 12, 24 and 48 h after inoculation.[62]

Table 5 Summarized antibacterial activity of curromycins

	Minimum inhibitory concentration (MIC) [μg ml^{-1}]							Inhibition zone[b] [mm]
	Agrobacterium tumefaciens IFO 13263	*Bacillus subtilis* IAM 1026	*Bacillus subtilis* IFO 3007	*Escherichia coli* OP50	*Micrococcus luteus* FDA16	*Pseudomonas aeruginosa* A3	*Pseudomonas cepacian* M-0527	*Staphylococcus aureus* FDA 209P
Curromycin A (**6**)	6.3	~3.9[a]	>100	100	25	50	~50[a]	20.0
Curromycin B (**7**)	6.3	3.9	>100	100	25	50	50	21.5

[a] Values reported for **6** were described as "almost identical" with **7**. [b] Using cylinder plate method with concentration 2.5 μl ml^{-1}, reported as a diameter of inhibition zone.

showed hazy inhibition zones 20.0 mm for **6** and 21.5 mm for **7** against *Staphylococcus aureus* FDA 209P using cylinder plate method.[4] Kanzaki *et al.* also reported identical biological activities for both curromycins.[62] No substantial bioactivity of **6** and **7** against *Escherichia coli* OP50 (MIC 100 μg ml^{-1}) nor against *Bacillus subtilis* IFO 3007 (MIC >100 μg ml^{-1}) was reported. The strong inhibitory activity was observed against *Agrobacterium tumefaciens* IFO 13263 (MIC 6.3 μg ml^{-1} for both curromycins), approximately half MIC when compared to oxazolomycin A. In addition, once both hydroxy groups in **6** and **7** (at C7 and C3′ positions) were acetylated, corresponding curromycin diacetates had no antibacterial activity against the three species of bacteria (MIC > 100 μg ml^{-1}). And Kanzaki *et al.* compared effect of **7** and its diacetate against *Agrobacterium tumefaciens* growth on an inoculated potato tuber disk. No inhibitory effect was observed for curromycin B diacetate in contrary to active curromycin B (Fig. 15). The antibacterial activity of curromycins is summarized in Table 5.

Otani *et al.* examined KSM-2690B (**8**) and KSM-2690C (**9**) by using a paper disk diffusion method (concentration 50 μg ml^{-1}, 8 mm in diameter).[7] Interestingly, **8** showed antibacterial activity against *Micrococcus luteus* ATCC 9341 (15.0 mm, hazy zone), *Bacillus subtilis* PCI 219 (23.0 mm) and the highest activity against *Staphylococcus aureus* Smith (25.0 mm, hazy zone), whereas no growth inhibition of **9** was observed.[7] Since **8** and **9** are geometric isomers, which differ only in their left-hand fragment, and thus there is apparent importance of left-hand fragment suitable orientation for increased antimicrobial activity.

Potts *et al.* revealed light-sensitivity of lajollamycin (**10**).[8] For example, a DMSO solution of **10** (50 μM) degraded rapidly at room temperature when exposed to light, with only 25% of the parent compound remaining after 1 h. In contrast, **10** was stable in DMSO for at least 32 h, when protected from light. Thus, appropriate precautions were taken to protect the compound from light during bioassays. The results proved antimicrobial activity of **10** against both drug-sensitive and drug-resistant microorganisms. Remarkable bioactivity of **10** was observed against methicillin-sensitive (MIC 4 μg ml^{-1}) and methicillin-resistant (MIC 5 μg ml^{-1}) strains of *Staphylococcus aureus*. Higher activity was observed against penicillin-sensitive (MIC 2 μg ml^{-1}) and penicillin-resistant (MIC 1.5 μg ml^{-1}) *Streptococcus pneumoniae* strains. Lower bioactivity was observed against *Enterococcus faecium* for both vancomycin-sensitive (MIC 14 μg ml^{-1}) and vancomycin-resistant (MIC 20 μg ml^{-1}) strains. Lajollamycin (**10**) is also active against *Escherichia coli* IMP-type (MIC 12 μg ml^{-1}). The antibacterial activity of **10** is summarized in Table 6.[8]

The antibacterial activity of lajollamycins **10**, **11**, **12** and **13** was evaluated by Oh *et al.* against various bacterial strains such as *Bacillus subtilis* ATCC 6633, *Escherichia coli* ATCC 35270, *Kocuria rhizophila* NBRC 12708, *Proteus hauseri* NBRC 3851, *Salmonella enterica* ATCC 14028 and *Staphylococcus aureus* ATCC 6538p, but no significant inhibitory activity (MIC > 128 μg ml^{-1}) was observed.[9]

Comprehensive evaluation of oxazolomycin A (**1**), oxazolomycin A2 (**14**) and bisoxazolomycin (**15**) on bacterial strains was

Table 6 Antibacterial activity of lajollamycin (**10**)

	Minimum inhibitory concentration (MIC) [μg ml^{-1}]							
	Enterococcus faecalis vancomycin-resistant	*Enterococcus faecalis* vancomycin-sensitive	*Staphylococcus aureus* methicillin-resistant	*Staphylococcus aureus* methicillin-sensitive	*Streptococcus pneumoniae* penicillin-resistant	*Streptococcus pneumoniae* penicillin-sensitive	*Escherichia coli* IMP-type
Lajollamycin (**10**)	20	14	5	4	1.5	2	12

investigated by Koomsiri *et al.* using paper disk method.[10] Oxazolomycins were applied on paper disc (diameter 6 mm) at the concentrations of 30, 10, 3 and 1 μg per disc (Table 7). Oxazolomycins were found inactive against *Mycobacterium smegmatis* ATCC 607 and *Pseudomonas aeruginosa* IFO 3080. The bioassays against *Bacillus subtilis* ATCC 6633 revealed that activity of **1** increases with higher concentration, but oxazolomycins **14** and **15** were completely inactive. Evaluation of *Escherichia coli* NIHJ showed bioactivity of **1** at all tested concentrations, whereas compound **14** displayed growth inhibition only at higher concentrations. Dimeric oxazolomycin **15** was inactive at all tested concentrations. Lower activity of **1**, compared to activity against other tested strains was observed against *Kocuria rhizophila* ATCC 9341. No growth inhibition against this strain was observed for **14**, however application of dimeric **15** resulted in some activity. The inhibition of *Staphylococcus aureus* ATCC 6538p with **1** was observed for all tested concentrations, whereas oxazolomycins **14** and **15** displayed activity only at higher concentrations (10 and 30 μg per disc). The highest antibacterial activity of **1** was obtained in bioassays against *Xanthomonas campestris* pv. *oryzae* KB 88. Interestingly, compounds **14** and **15** also displayed such activity, although apparently reduced.

In general, the widest antibacterial activity was observed for oxazolomycin A (**1**). Oxazolomycins **14** and **15** displayed activity only at higher concentrations. The comparison of antibacterial activities at higher tested concentration (30 μg per disc) is demonstrated in Fig. 16. Oxazolomycin **15** is the only dimeric member of oxazolomycin family and as such its different antibacterial activity (lower in this case) from **1** or **14** can be presumed. However, compounds **1** and **14** are structurally related oxazolomycins. The right-hand fragment of **1** (spirocyclic β-lactone-γ-lactam) and **14** (monocyclic γ-lactam) represents the only structural difference. From this point of view, β-lactone ring in structure of oxazolomycin A (**1**) seems to play an important role for the increase of antibacterial activity.[10]

3.2.3 Antifungal activity. Koomsiri *et al.* investigated the antifungal activity of oxazolomycin A (**1**), A2 (**14**) and bisoxazolomycin (**15**) against *Aspergillus niger* ATCC 6275, *Candida albicans* ATCC 64548, *Mucor racemosus* IFO 4581 and *Saccharomyces cerevisiae* ATCC 9763 using the paper disc method (disc diameter = 6 mm, applied concentrations: 1, 3, 10 and 30 μg per disc).[10] However, no antifungal activity was observed. Antifungal activity of lajollamycins **10–13** was evaluated by Oh *et al.* against *Aspergillus fumigatus* and *Candida albicans*, but the lajollamycins also did not exhibit bioactivity.[9]

3.2.4 Antiviral activity. Tonew *et al.* investigated effect of **1** against Coxsachie A9, herpes simplex type 1, influenza A (WSN, H1N1) and vaccinia (Lister).[63] It was observed that **1** significantly reduced the plaque formation of enveloped DNA and RNA viruses by more than 90% in the range of the maximally tolerated dose. In one-step growth cycle assays **1** prevented the replication of herpes simplex type 1, influenza A and vaccinia viruses in dose-dependent manner. The observed MIC values of **1** against herpes simplex type 1, influenza A and vaccinia viruses were determined at the same level (MIC 15.6 μg ml^{-1}). However, inhibition of Coxsackie A9 by **1** was not observed.[63]

Table 7 Antibacterial activity of oxazolomycin A (**1**), A2 (**14**) and bisoxazolomycin (**15**)

	Concentration [μg per disc]	Diameter of inhibition zone [mm]							
		Bacillus subtilis ATCC 6633	*Escherichia coli* NIHJ	*Kocuria rhizophila* ATCC 9341	*Mycobacterium smegmatis* ATCC 607	*Pseudomonas aeruginosa* IFO 3080	*Staphylococcus aureus* ATCC 6538p	*Xanthomonas campestris* pv. *oryzae* KB 88
Oxazolomycin A (**1**)	**30**	31	28	16	*Inactive*	*Inactive*	26	45
	10	30	27	15	*Inactive*	*Inactive*	24	42
	3	25	25	10	*Inactive*	*Inactive*	24	13
	1	18	20	*Inactive*	*Inactive*	*Inactive*	20	27
Oxazolomycin A2 (**14**)	**30**	*Inactive*	15	*Inactive*	*Inactive*	*Inactive*	24	16
	10	*Inactive*	*Inactive*	*Inactive*	*Inactive*	*Inactive*	17	12
	3	*Inactive*	*Inactive*	*Inactive*	*Inactive*	*Inactive*	*Inactive*	10
	1	*Inactive*	*Inactive*	*Inactive*	*Inactive*	*Inactive*	*Inactive*	*Inactive*
Bisoxazolomycin (**15**)	**30**	*Inactive*	*Inactive*	11	*Inactive*	*Inactive*	17	14
	10	*Inactive*	*Inactive*	8	*Inactive*	*Inactive*	13	9
	3	*Inactive*	*Inactive*	*Inactive*	*Inactive*	*Inactive*	*Inactive*	9
	1	*Inactive*	*Inactive*	*Inactive*	*Inactive*	*Inactive*	*Inactive*	*Inactive*

Curromycins were investigated by Ohno *et al.* against replication of human immunodeficiency virus (HIV) in both acute and chronic infection.[64] Reverse transcriptase assay[65] was performed to estimate the concentration of viral particles in the culture supernatant. MTT assay,[66] based on the mitochondrial reduction of 3-(4,5-dimethylthiazol-2-yl)-2,5-diphenyl tetrazolium bromide, was utilized to determine the number of living cells. The 50% effective concentrations (EC_{50}) of **6** and **7** for HIV-1 IIIB replication (reverse transcriptase assay on primary infected human lymphoid cells) were determined as 2.5 μg ml^{-1} and 5 μg ml^{-1}. Azidothymidine (AZT) treatment also showed concentration dependent inhibition in this assay system (Fig. 17). To exclude the possibility that curromycins directly inhibit reverse transcriptase in the reverse transcriptase assay system, p24 antigen was monitored by capture ELISA, to study the production of HIV antigens with treatment of curromycins. The OD values, which represent the antigen expression exhibited the same tendency with reverse transcriptase values (data not reported).[64] Therefore, these agents did not have effect on reverse transcriptase directly. The 50% inhibitory concentration (IC_{50}) values of MTT on primary infected human lymphoid cells were at 6.5 μg ml^{-1} for **6** and 20 μg ml^{-1} for **7**. Furthermore, the antiviral activity of curromycins was examined in chronically infected U937 cells[67] and it was proved that curromycins have anti-HIV activity in chronically infected cells. In this case the ratio of IC_{50} and EC_{50} was greater than 10. The results suggest that curromycins are more effective in chronically infected monocytoid cells than in primarily infected lymphoid cells. Lower effect was observed with AZT in chronic assay system (Fig. 18). The chronic assay results further indicated that curromycins affect the later steps in the virus replication cycle.[64]

3.2.5 Cytotoxic activity. After discovery of oxazolomycin A (**1**) Uemura *et al.* observed its cytotoxic activity against mouse leukemia P388 cells, as well as *in vivo* activity against Ehrlich ascites carcinoma.[1] Similarly, after discovery of neo-oxazolomycin (**2**) by Uemura *et al.*, the cytotoxic activity against Ehrlich ascites carcinoma was reported.[2] Unfortunately, the experimental data of cytotoxicity screening were not reported in these studies.[1,2]

Structural determination of curromycin A (**6**) and B (**7**) reported by Ogura *et al.* involved some biological assays.[3,61] Curromycin **6** showed cytotoxic activity against Fried leukemia cells and against mouse melanoma B16. Significant bioactivity against mouse leukemia P388 (IC_{50} 0.06 μg ml^{-1}) was observed.[3] Moreover, Hayakawa *et al.* evaluated the cytotoxic activity of **6** against human gastric carcinoma MKN45 in nutrient-deprived and normal medium using the MTT method.[68] The bioassay in nutrient-deprived medium (Earle's salt solution supplemented with 10% fetal bovine serum) showed potency of **6** against MKN45 (IC_{50} 15 ng ml^{-1}). The growth of MKN45 cells in a normal medium (Dulbecco's modified Eagle's medium with 10% fetal bovine serum) was inhibited by **6** at the range of IC_{50} 20-20 000 ng ml^{-1}, although no cell death was observed.[68] Curromycin **7** showed cytotoxic activity against mouse melanoma B16 (IC_{50} 2.5 μg ml^{-1}). Further, cytotoxicity against mouse leukemia P388 for **7** (IC_{50} 0.12 μg ml^{-1}) was lower than reported for **6**, but still significantly different from a control.[3]

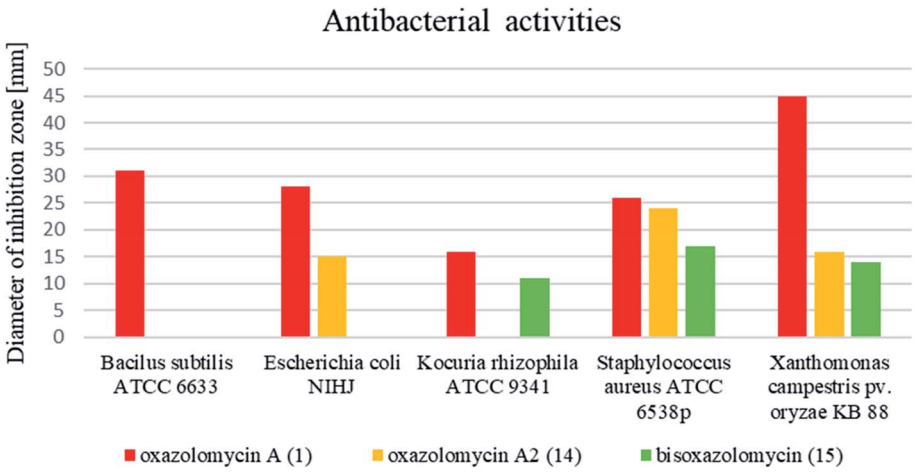

Fig. 16 Comparison of antibacterial activity of oxazolomycins **1**, **14** and **15** using disc diffusion method at the concentration 30 μg per disc.

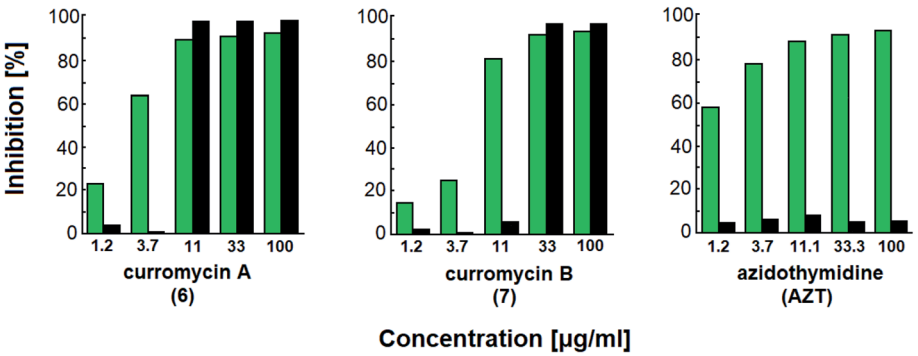

Fig. 17 Effect of curromycin A (**6**), B (**7**) and azidothymidine (AZT) on primary infected human lymphoid cells. Green columns: % inhibition of reverse transcriptase; black columns: % inhibition of MTT.[67]

Kim *et al.* reported cytotoxic activity of 16-methyloxazolomycin (**5**) against human lung adenocarcinoma A549 cells (IC_{50} 4.6 μg ml^{-1}).[5] Mouse leukemia P388 was inhibited by **5** (IC_{50} 0.23 μg ml^{-1}). Despite lower bioactivity of **5** against P388 compared to curromycins, it seems that oxazolomycins express significant activity against selected leukemia cell line (Fig. 19).

Cytotoxic activity of KSM-2690 B (**8**) and C (**9**) was evaluated by Otani *et al.* against human bladder carcinoma T24 cells.[7] Both oxazolomycins **8** and **9** were active and exhibited the same cytotoxic effects (IC_{50} 10 μg ml^{-1}). The cytotoxicity of lajollamycin (**10**) was demonstrated on mouse melanoma cell line B16–F10 growth (EC_{50} 9.6 μM) reported by Potts *et al.*,[8] whereas

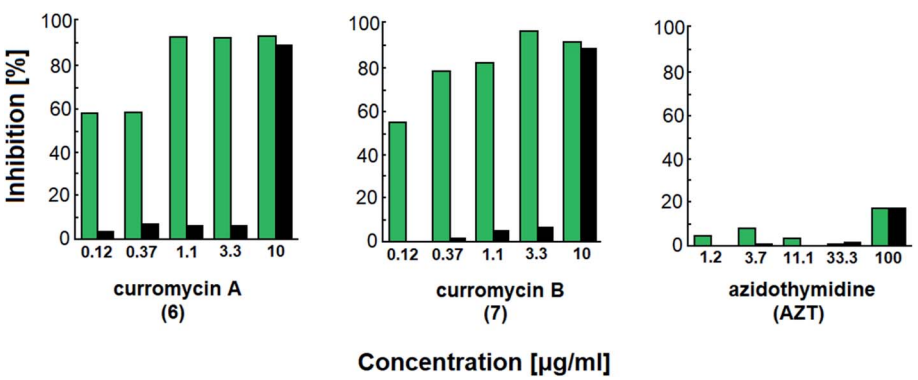

Fig. 18 Effect of curromycin A (**6**), B (**7**) and azidothymidine (AZT) in chronic replication assay. Green columns: % inhibition of reverse transcriptase; black columns: % inhibition of MTT.[67]

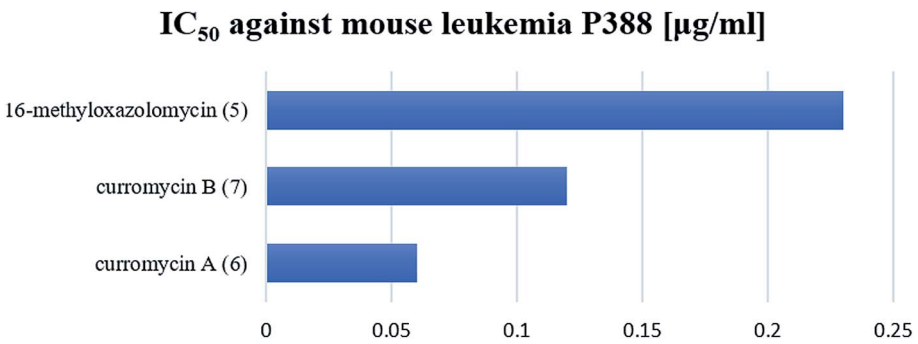

Fig. 19 Cytotoxic activity of curromycin A (**6**), B (**7**) and 16-methyloxazolomycin (**5**) against mouse leukemia P388.

further study reported by Oh *et al.*[9] showed that lajollamycins (**10–13**) did not exhibit cytotoxic activity against human breast carcinoma MDA-MB-231, colorectal carcinoma HCT 116, gastric carcinoma SNU-638, hepatic adenocarcinoma SK-HEP-1, leukemia K562 nor lung adenocarcinoma A549 cell lines (IC_{50} > 100 μM).

Koomsiri *et al.* compared the cytotoxicity of oxazolomycin A (**1**), A2 (**14**) and bisoxazolomycin (**15**).[10] The highest cell growth inhibition activity against human leukemia HL60 cell line was observed for **1** (IC_{50} 0.6 μM), followed by dimeric structure **15** (IC_{50} 7 μM) and monocyclic oxazolomycin **14** (IC_{50} 20 μM; Fig. 20). The results suggest spirocyclic β-lactone-γ-lactam core significance for cytotoxic activity, similarly to antibacterial activity discussed above, but further comprehensive experiments are needed to confirm this hypothesis.

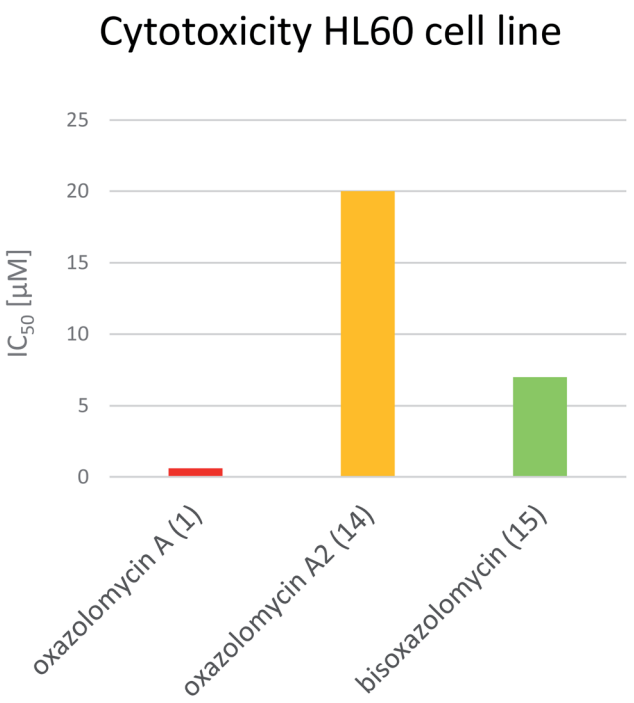

Fig. 20 Comparison of IC_{50} values for oxazolomycin A (**1**), A2 (**14**) and bisoxazolomycin (**15**) against human leukemia HL60.

3.2.6 Regulation of enzymatic activity. As described above, Oh *et al.* observed no antifungal activity of lajollamycins **10–13** against *Candida albicans*.[9] But interestingly, the lajollamycins displayed moderate inhibition activity against *Candida albicans* isocitrate lyase, which is closely related to fungal pathogenicity because of its diverse metabolic pathway.[9,69] Resemble bioactivity was reported for **10** (IC_{50} 42 μM), **11** (IC_{50} 40 μM), and **12** (IC_{50} 50 μM; Fig. 21). The lower inhibition was observed for **13** (IC_{50} 120 μM).

Hayakawa *et al.* investigated[68] the effect of curromycin A (**6**) on GRP78 gene expression by the luciferase reporter assay using human fibrosarcoma HT1080 cells transformed with the luciferase gene under the control of the GRP78 promoter (HT1080 GL).[70] It was reported that **6** dose-dependently inhibited the luciferase expression (IC_{50} 4.3 ng ml^{-1}) in the presence of 10 mM of 2-deoxyglucose (Fig. 22).[68]

3.2.7 Inhibition of crown gall formation. The phytopathogenic bacterium *Agrobacterium tumefaciens* is the causative agent for crown gall disease on a broad range of plant species.[59] According to antibacterial activity of oxazolomycin members against *Agrobacterium tumefaciens*,[60,62] some oxazolomycins were evaluated toward the inhibition of crown gall formation. The effect of oxazolomycin A (**1**) was examined by Kawai *et al.*

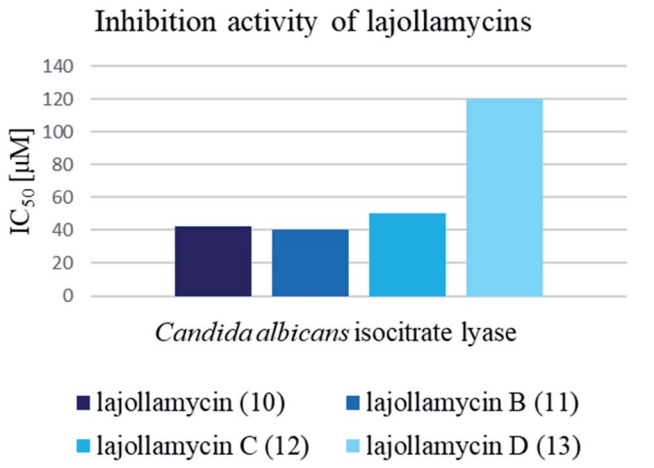

Fig. 21 Inhibition activity *Candida albicans* isocitrate lyase by lajollamycins **10–13**.

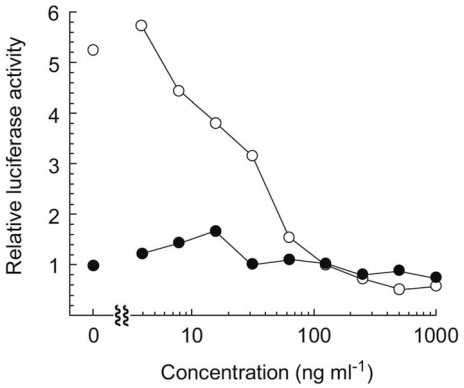

Fig. 22 Effect of curromycin A (**6**) on the luciferase expression in HT1080 G-L cells. HT1080 G-L cells were treated with **6** in the presence (○) or absence (●) of 2-deoxyglucose (10 mM) for 18 h at 37 °C. The relative luciferase activity compared with non-treated control was measured with a luminometer.

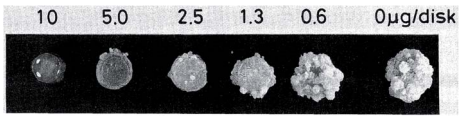

Fig. 23 Effect on crown gall formation of oxazolomycin A (**1**) administered simultaneously with the inoculation of *Agrobacterium tumefaciens*.[60]

using the potato tuber disc assay.[60] Simultaneous administration of **1** with the inoculation of *Agrobacterium tumefaciens* resulted in the inhibition of crown gall formation at a dose of 2.5 μg per disc, but resulted in necrosis of the potato disc surface at a dose of 10 μg per disc presuming its phytotoxicity (Fig. 23).[60] The minimum inhibitory dose (MID) of **1** against crown gall formation was reported on the level 0.8 μg per disc.[6]

Kawai *et al.* further examined effect on crown gall formation of oxazolomycin A (**1**) administrated a certain period after the inoculation of *Agrobacterium tumefaciens* (Table 8).[60] It was observed that administration of oxazolomycin A (**1**) 3 h after the inoculation inhibited crown gall formation at a dose of 5.0 μg per disc and the surface of the potato disc was necrosed at a dose of 10.0 μg per disc. Increase of the interval between the inoculation and the administration of the agent resulted in observation of small crown gall formation at a dose of 10.0 μg per disc, the potato disc being no longer necrosed and forming as many crown galls as the control. The necrosis was also observed for cycloheximide at 1.3 μg per disc, where no formation of crown gall was found. The administration of cycloheximide at any time after the inoculation caused no necrosis of the potato disc at a dose of 2.5 μg per disc. As a result of these data, Kawai *et al.* concluded, that cycloheximide was strongly phytotoxic to both the nontransformed and transformed plant cells. In contrast to cycloheximide, oxazolomycin **1** had toxicity against nontransformed plant cells as well as against *A. tumefaciens*, while it had no toxicity toward transformed plant cells whose genome integrated the T-DNA of *A. tumefaciens*. This indicates, that **1** might be used for distinguishing between the transformed and nontransformed plant cells.

The similar experiments were accomplished with the strong antibacterial agents against *A. tumefaciens*, tetracycline and chloramphenicol. These two antibiotics administrated 72 h

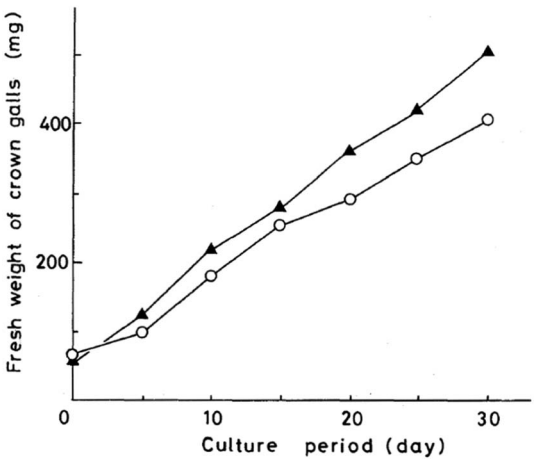

Fig. 24 Growth curves of crown gall tissue on solid Murashige–Skoog medium. Oxazolomycin A (○) at 100 μg ml^{-1}; carbenicillin (▲) at 1000 μg ml^{-1}.

Table 8 Effect of oxazolomycin A (**1**), tetracycline and chloramphenicol administration after the inoculation of *A. tumefaciens* on crown gall formation. The data represents a percentage of inhibited potato disc

	Dose [μg per disc]	Time interval between the inoculation and administration							
		0 h	3 h	6 h	12 h	24 h	72 h	120 h	192 h
Oxazolomycin A (**1**)	**10.0**	100%	75%	50%	50%	0%	0%	0%	0%
	5.0	100%	75%	0%	0%	0%	0%	0%	0%
	2.5	75%	75%	0%	0%	0%	0%	0%	0%
Tetracycline	**10.0**	100%	100%	100%	100%	100%	100%	100%	50%
	5.0	100%	100%	100%	100%	100%	75%	75%	25%
	2.5	75%	50%	50%	100%	50%	0%	0%	0%
Chloramphenicol	**10.0**	100%	100%	100%	100%	100%	100%	75%	100%
	5.0	100%	100%	75%	100%	75%	50%	25%	0%
	2.5	75%	25%	25%	25%	25%	25%	25%	0%

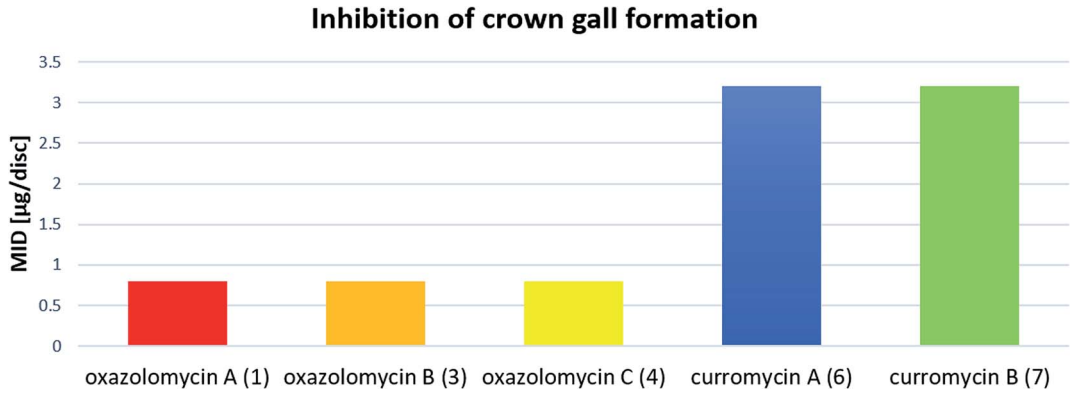

Fig. 25 Effect of oxazolomycins and curomycins against crown gall formation.[62]

after the inoculation still inhibited crown gall formation and they inhibited the multiplication of crown gall even when administered after 8 days (192 h; Table 8). These results suggested that both antibiotics were toxic toward not only *A. tumefaciens*, but also toward transformed cells. The results reported by Kawai *et al.* suggested that oxazolomycin A (**1**) inhibited the earliest step in crown gall formation, therefore **1** may be used as a chemical probe in studying the early stages of crown gall formation. Kawai *et al.* further examined, that neooxazolomycin (**2**) is inactive against crown gall formation, probably due to the lack of a β-lactone ring.[60]

Kawai *et al.* further provided application of oxazolomycin A (**1**) for a sterilization of crown gall in experiments on the transformation of plant cells by *A. tumefaciens*.[60] In these experiments, transformed cells must be firstly purged from *A. tumefaciens* by culturing on Murashige–Skoog medium containing antibiotics (*i.e.* carbenicilin). Despite the ability of carbenicillin to completely remove the bacterium, a high concentration of the antibiotic is needed, because of its weak activity against *A. tumefaciens*. Kawai *et al.* proposed, that **1** as the selective antibiotic against *A. tumefaciens* and with no toxicity toward transformed plant cells could be useful for removing the bacterium. This possibility was examined by transferring crown gall to a solid Murashige–Skoog medium containing **1**. It was observed, that **1** inhibited growth of any bacteria at a concentration of 100 μg ml^{-1}, while commonly used carbenicillin at 1000 μg ml^{-1}. A nearly equal rate of crown gall growth was obtained on the medium containing the respective concentrations of these compounds (Fig. 24). However, **1** at concentration 50 μg ml^{-1} had a bactericidal effect only on the growth of *A. tumefaciens* and the resulting infestation of other bacteria spoiled the crown galls. Therefore Kawai *et al.* concluded, that this antibiotic could be useful for sterilizing the transformed plant cells, but would be better used together with other antibiotics.[60]

Kanzaki *et al.* evaluated the inhibitory activity of oxazolomycin B (**3**) and C (**4**) against crown gall formation.[6] It was observed that both geometric isomers **3** and **4** of **1** showed comparable bioactivity (MID 0.8 μg per disc). These results indicate that the oxazolomycin's geometry of left-hand fragment is not significant for the inhibition of crown gall formation.

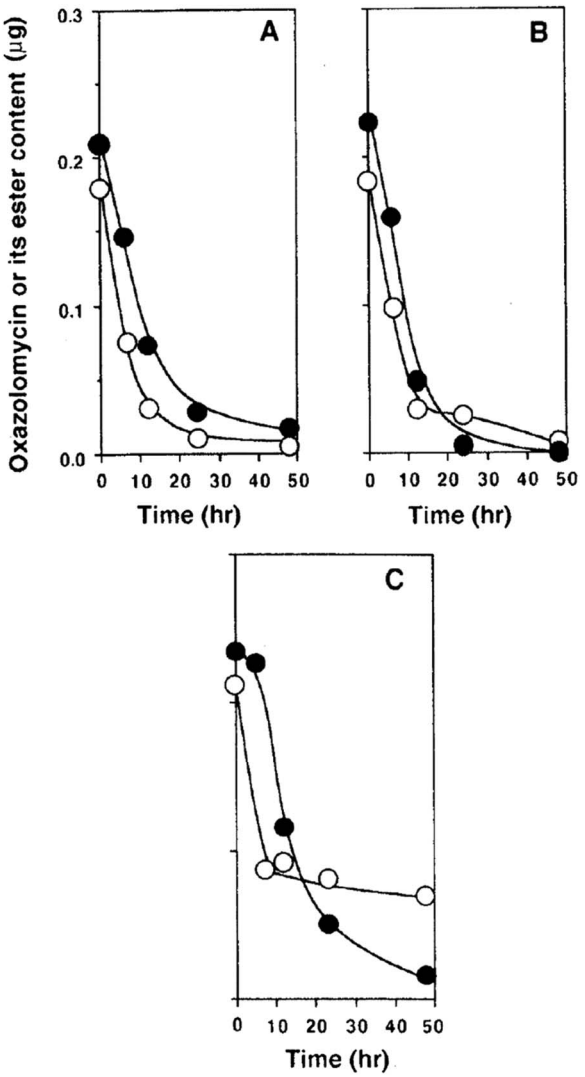

Fig. 26 Decay of oxazolomycin A (●) and oxazolomycin A dipropionate (○) in the process of crown gall formation. The compounds were administered to potato tuber discs inoculated with *A. tumefaciens* (**A**), to potato tuber discs (**B**) or to a culture of *A. tumefaciens* (**C**).[71]

The inhibitory effect of curromycin A (**6**) and B (**7**) against crown gall formation was investigated by Kanzaki *et al.*[62] The both curromycins **6** and **7** showed strong, but little reduced activity (MID 3.2 μg per disc) against crown gall formation than **1**. Kanzaki *et al.* suggested, that strong and selective activity of **6** and **7** against *A. tumefaciens* possibly resulted in an inhibition of crown gall formation (Fig. 25).

Kanzaki *et al.* further examined inhibition of crown gall formation by diesters derived from **6** and **7**, acylated on hydroxyl groups at C7 and C3′.[62] Curromycin diesters had similar (curromycin A diacetate; MID 3.2 μg per disc) or lower (curromycin B diacetate and curromycin B dipropionate; MID 6.3 μg per disc for both) bioactivity compared to natural curromycins. In contrast to curromycins, the curromycin esters had no inhibitory antibacterial activity against *A. tumefaciens* (Fig. 15). These results indicated that the inhibitory activity of the curromycin esters against crown gall formation was not related to growth inhibition of *A. tumefaciens*.[62]

Moreover, Kawazu *et al.* similarly examined the inhibition of crown gall formation by diesters derived from **1**, acylated on hydroxyl groups at C7 and C3′.[71] All evaluated esters: oxazolomycin A diacetate, oxazolomycin A dipropionate, oxazolomycin A dibutyrate including monoester oxazolomycin A monobutyrate (acylated at hydroxyl group at C7 position) showed half inhibitory activity (MID 1.6 μg per disc) if compared to natural oxazolomycin A (**1**). Similarly, oxazolomycin A esters had no antibacterial activity against *A. tumefaciens*, in contrast to **1**.[71] These findings suggest that the curromycin esters[62] and oxazolomycin A esters[71] specifically inhibited some steps of plant transformation (but not *A. tumefaciens*) and therefore could be promising chemical probes for studying the mechanism of plant transformation mediated by *A. tumefaciens*.[62]

Kawazu *et al.* want to investigated, if the oxazolomycin A ester administrated to potato tuber disc was converted to oxazolomycin A (**1**) or other compounds.[71] The decay of the oxazolomycin A dipropionate administered to potato tuber disc inoculated with *A. tumefaciens* was examined and compared with **1**. Both compounds were rapidly decomposed, decreasing to about a half content after 6 h and to one tenth content after 24 h in the potato disc, irrespective of the presence or the absence of *A. tumefaciens*. However, these compounds decayed more slowly to about one fourth content after 24 h in the culture of *A. tumefaciens* (Fig. 26). Under examined conditions, oxazolomycin A dipropionate was not converted to **1** or *vice versa*. The results suggested that the unique activity of the esters was not caused due to biological deesterification.[71]

3.2.8 Phytotoxic activity. Kawazu *et al.* observed the activity of oxazolomycin A (**1**) against germination of *Medicago sativa* (MID 12.5 μg per disc).[71] The same study reported that **1** caused necrosis of potato tuber disc (MID 5 μg per disc). Kanzaki *et al.* evaluated the phytotoxic activity on seeds germination of *Medicago sativa* on geometric isomers of **1**.[6] The phytotoxicity of oxazolomycin B (**3**) decreased to one half (MID 25.0 μg per disc) and of oxazolomycin C (**4**) to one fourth (MID 50.0 μg per disc) compared to activity of **1** against *Medicago sativa* seeds germination. The necrosis of potato tuber disc was also caused by **3** (MID 6.3 μg per disc) and **4** (12.5 μg per disc). Kanzaki *et al.* further reported the phytotoxic activity of curromycins.[62] Same activity against the germination of *Medicago sativa* was observed for both curromycins (MID 12.5 μg per disc). Similarly, both curromycins caused the necrosis of potato tuber disc at same dose (MID 50 μg per disc). Phytotoxic activities of oxazolomycins are summarized in Fig. 27.

Kawazu *et al.* evaluated phytotoxic activity of following oxazolomycin A diesters (acylated on hydroxyl groups at C7 and C3′): oxazolomycin A diacetate, oxazolomycin A dipropionate, oxazolomycin A dibutyrate and mono ester oxazolomycin A

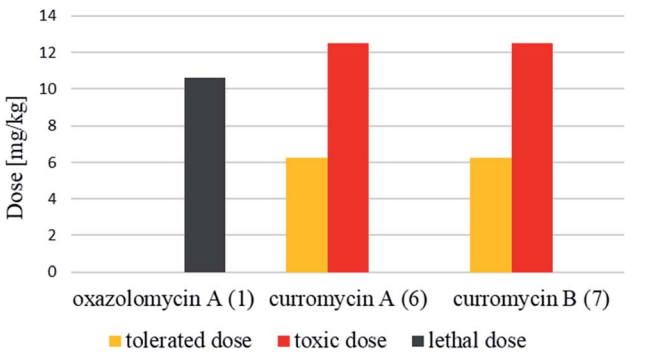

Fig. 28 Tolerated, toxic and lethal doses of oxazolomycin A (**1**) and curromycins A (**6**) and B (**7**).

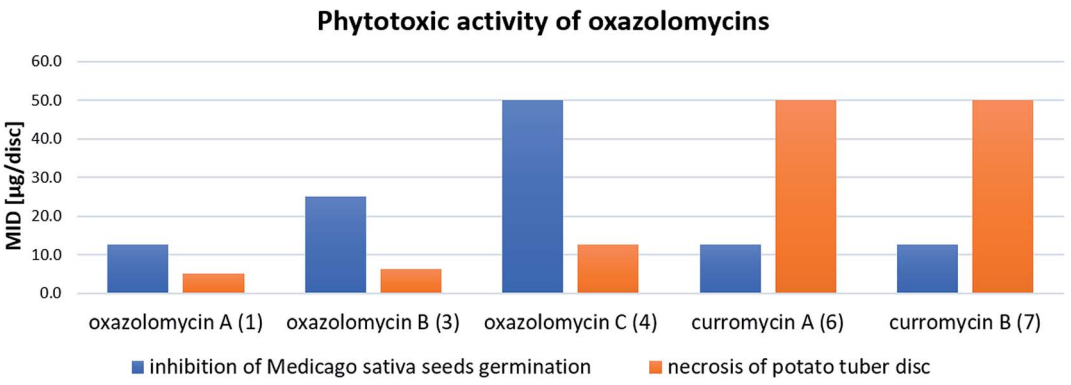

Fig. 27 Summary of reported phytotoxic activity of oxazolomycins.

monobutyrate (acylated on hydroxyl group at C7) against seeds germination of *Medicago sativa*, but no activity (MID > 100 μg per disc) was observed.[71] Any of oxazolomycin A esters caused necrosis on potato tuber disc even at dose of 50 μg per disc. Following curromycin diesters (acylated on hydroxyl groups at C7 and C3′): curromycin A diacetate, curromycin B diacetate and curromycin B dipropionate, were investigated by Kanzaki *et al.* toward phytotoxic activity, but no necrosis of potato tuber disc nor activity against seeds germination of *Medicago sativa* were observed.[62]

3.2.9 Tolerated, toxic and lethal dose. The lethal dose (LD_{50}) of oxazolomycin A (**1**) was determined using *i.p.* administration in mice by Mori *et al.* at level 10.6 mg kg^{-1}.[1] Both curromycins, **6** and **7** administered *via i.p.* injection expressed the same values for tolerated and same levels of toxic doses in mice, as reported by Ikeda *et al.*[4] The tolerated dose in mice was determined at level 6.25 mg kg^{-1} for both curromycins, whereas toxic dose (TD_{50}) was specified as 12.5 mg kg^{-1} (Fig. 28).

4 Total syntheses of oxazolomycins

4.1 Total synthesis of neooxazolomycin by Kende

4.1.1 Synthesis of the left-hand fragment of neooxazolomycin by Kende. The first enantioselective total synthesis of neooxazolomycin (**2**) was reported by Kende *et al.* in 1990.[13] (*Z*)-3-Bromo-2-methyl-2-propenol (**50**)[72] was used as the starting material, which underwent *O*-silylation with TMSCl to the silyl ether **51**. Pd-catalyzed coupling[73] with (trimethylsilyl) acetylene further provided enyne **52**. Acid promoted selective desilylation of TBS-protecting group to primary alcohol **53** and sequential oxidation with MnO_2 produced (*Z*)-configured aldehyde **54**. The diastereoselective Reformatsky-type condensation of aldehyde **54** with tin(II) enolate prepared *in situ* from chiral acyloxazolidinone **55** by use of $SnCl_2$ and $LiAlH_4$ in THF[74] provided expected 1,3-oxazine-2,4-dione **56** in 95% yield,[75] with desired (3′*R*)-configuration (neooxazolomycin numbering) in excellent diastereoslectivity (*de* > 99%) and complete retention of the alkene (*Z*)-geometry.[75] In following two reactions, removal of chiral auxiliary and *C*-silyl group has been performed. Exposition of compound **56** to 30% H_2O_2 and LiOH[76] produced amide **57** in 13% yield and carboxylic acids **58** and **59** in 87% yield and 24 : 1 ratio. The mixture of carboxylic acids **58** and **59** was hydrolyzed with LiOH, to provide acid **59** in 85% yield. Homochiral Evans oxazolidinone was recovered in 69% yield. Transformation of carboxylic acid **59** to enantiomerically pure (*ee* > 99%) methyl ester **60** was achieved with CH_2N_2 in Et_2O. Enantiomeric purity of ester **60** was determined by use of chiral shift reagent Eu(hfc)$_3$ employing racemic mixture **60** as

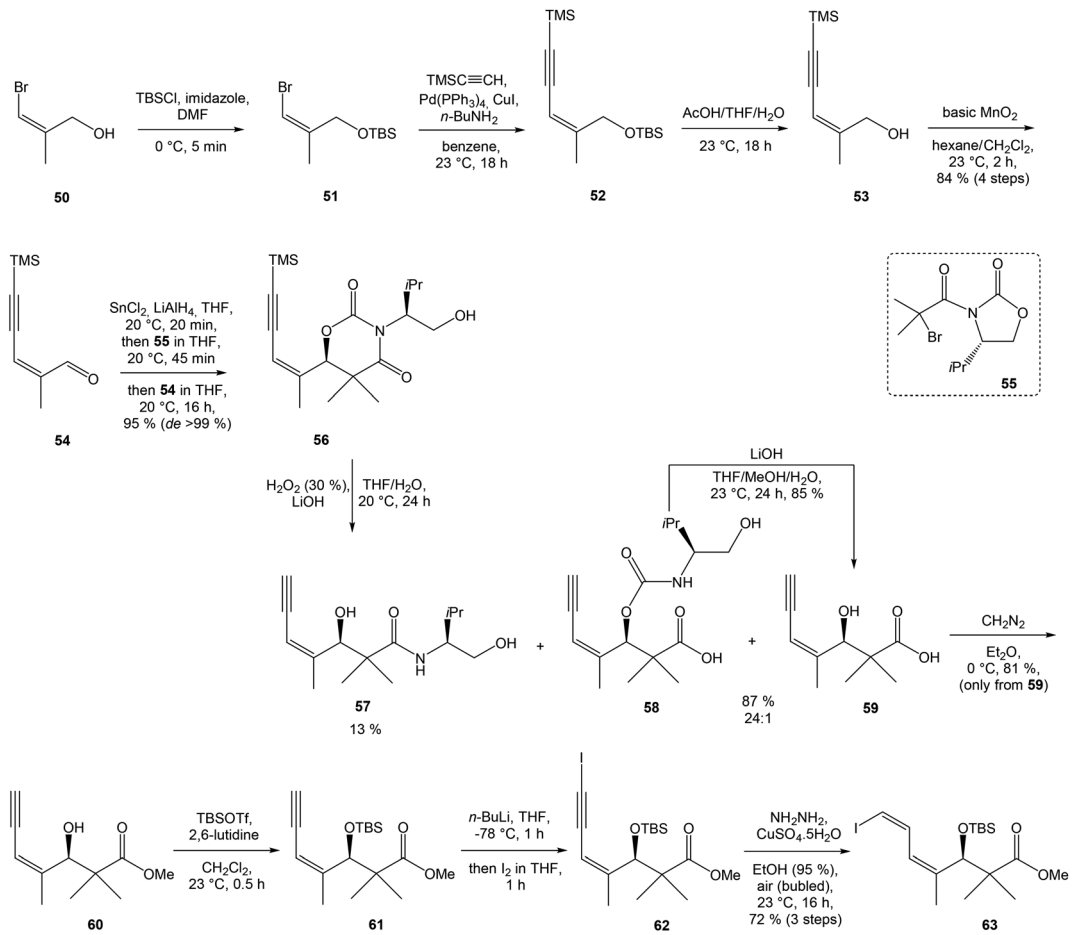

Scheme 3 Synthesis of Stille cross coupling partner **63** for left-hand fragment of neooxazolomycin by Kende.

standard. After protection of secondary hydroxy group in ester **60** with TBSOTf and 2,6-lutidine, corresponding silyl ether **61** underwent iodination reaction in presence of *n*-BuLi and I_2 in THF to iodide **62**. Diimide reduction[77] of iodoacetylene **62** gave (*Z*,*Z*)-diene iodide **63** in 72% yield after 3 steps from **60** (Scheme 3).

To introduce the oxazole ring into the structure, ethyl diethoxyacetate and lithiated methyl isocyanide ($LiCH_2NC$) under the conditions of Schöllkopf condensation[78] provided 5-substituted oxazole acetal **64** in 86% yield. Acidic hydrolysis of **64** with HCl, followed by reduction with $NaBH_4$ led to the oxazole methanol **65** in 68% yield. Alcohol was transformed in the Appel reaction by use of NBS and Ph_3P to the unstable bromide **66**, which was directly conjugated with the organocuprate **67** [79] to give the (*E*)-configurated vinyl stannane **68** in 49% yield. The Stille cross coupling conditions[80] applied on the mixture of (*E*)-stannane **68** and (*Z*,*Z*)-diene iodide **63** provided desired (*Z*,*Z*,*E*)-configurated triene ester **69** with complete retention of all alkene geometries in 79% yield. Desilylation of silyl ether group with 50% HF/CH_3CN gave secondary alcohol **70** in 92% yield, without any isomerization of the conjugated triene system. Hydrolysis of ester **70** under basic conditions with LiOH in the mixture $THF/MeOH/H_2O$ led to the β-hydroxy acid **71** in 94% yield. This hydrolysis required hydrogen bonding from free β-hydroxyl group, while TBS-protected ester **69** could not be hydrolyzed. Acetylation of hydroxyl group in β-hydroxy acid **71** was carried out using Ac_2O in pyridine to give corresponding protected acid **72** in excellent 99% yield. Acid **72** represents the left-hand fragment of the target neooxazolomycin structure (Scheme 4).

4.1.2 Synthesis of the right-hand and middle fragment of neoozaxolomycin by Kende. Readily available anhydrogalactoside **73** [81] was used as the starting material, as well as the source of chirality on the route to synthesis of the right-hand fragment of neooxazolomycin. Methyl group introduction and contemporary *trans*-diaxial epoxide opening was carried out with MeLi and MeMgCl in THF/Et_2O[82] to produce diol **74** in 95% yield. No Payne rearrangement product was observed in this reaction. Glycoside **74** subsequently underwent four reaction steps including: (I) selective equatorial hydroxyl group silylation with $i\text{-}Pr_3SiOTf$ and 2,6-lutidine, (II) transformation of the axial hydroxyl group to the imidazole thiocarbamate with $S{=}C(Im)_2$ followed by radical deoxygenation,[83] (III) desilylation of silyl ether with TBAF, (IV) formation of acetonide with acetone/$FeCl_3$,[84] to provide deoxy acetonide **75** in 64% overall yield in 4 steps.

Further four reaction steps: (I) benzyl protecting group removal under conditions of $Pd(OH)_2$-catalyzed reductive debenzylation, (II) oxidation of primary hydroxyl group under Swern conditions to corresponding aldehyde, (III) following oxidation with $KMnO_4$ buffered by 5% NaH_2PO_4 in *t*-BuOH to carboxylic acid, (IV) diazomethane esterification led to methyl ester **78** in 70% yield over four steps from **75**. Cyclocondensation[85] of ester **78** and dianion of amidomalonate **79**

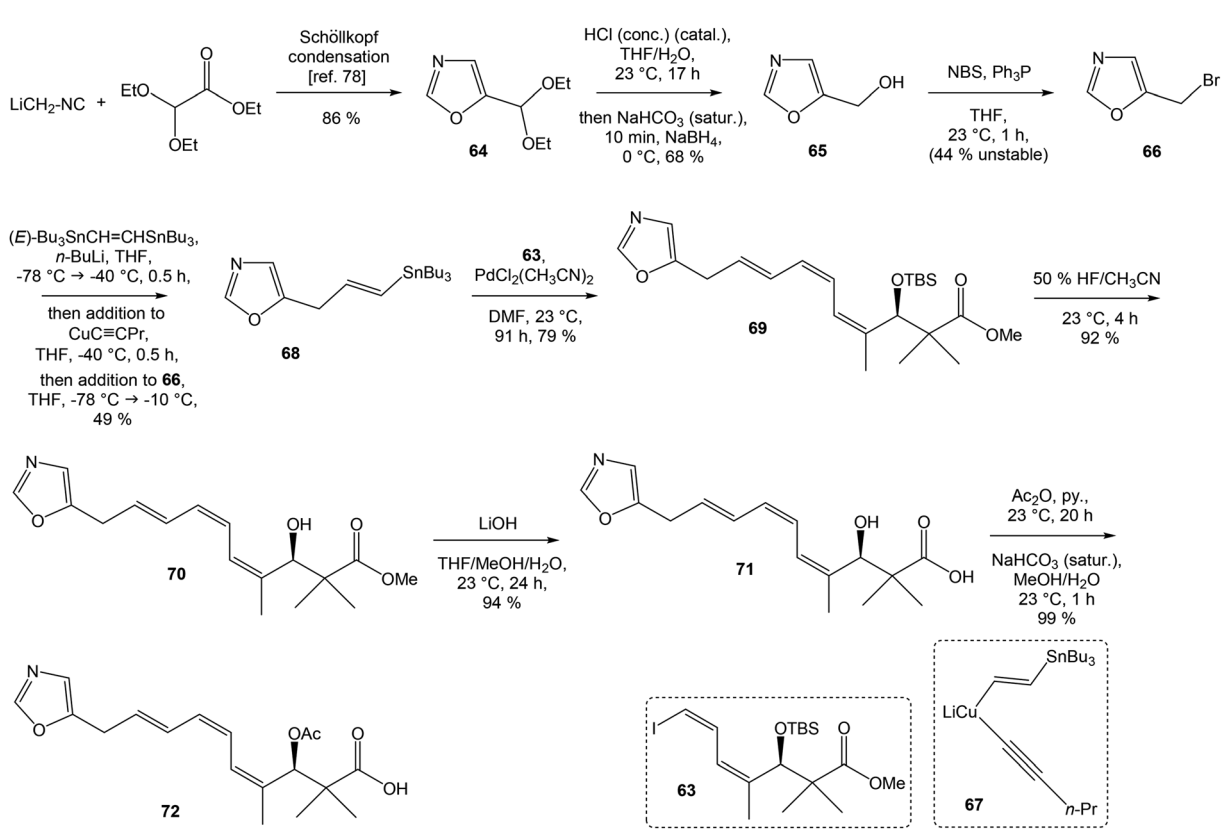

Scheme 4 Synthesis of the left-hand fragment derivative **72** of neooxazolomycin by Kende.

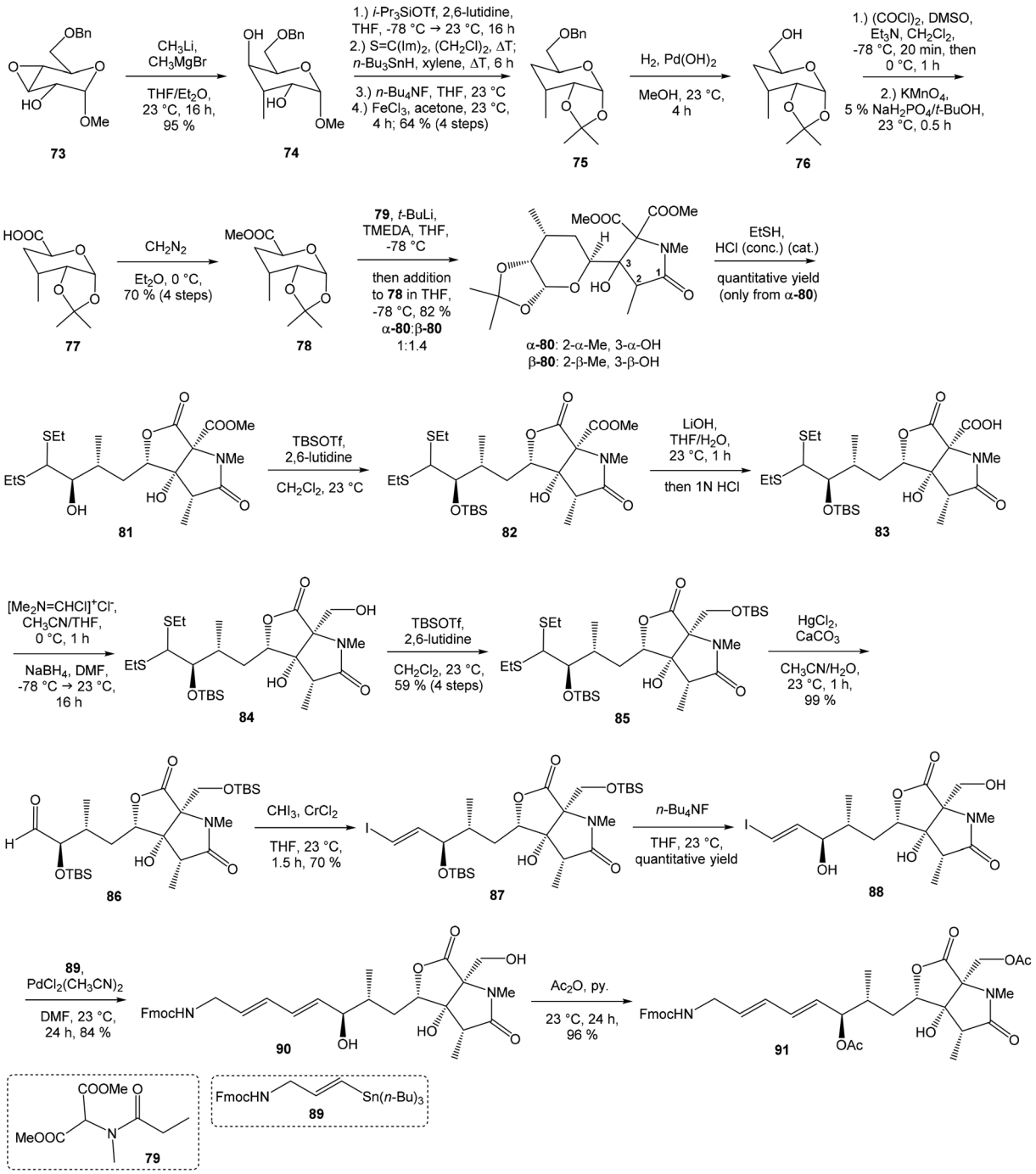

Scheme 5 Synthesis of the right-hand and middle fragment derivative **91** of neooxazolomycin by Kende.

with *t*-BuLi and TMEDA in THF at −78 °C gave a mixture of γ-lactames **α-80** and **β-80** in ratio 1 : 1.4 and 82% yield (cumulative yield based on recovered ester **78**). Desired γ-lactam **α-80** was separated and transformed to bicyclic lactam–lactone **81** with EtSH and catalytic amount of HCl in almost quantitative yield. Following *O*-silylation of secondary hydroxyl with TBSOTf and 2,6-lutidine, basic hydrolysis of methyl ester with LiOH and Fujisawa reduction[86] provided diol **84.** In order to confirm the structure, intermediate **84** was converted to the known triacetate, prepared by Uemura *et al.*[2] from **92.** The silylation of primary alcohol group with TBSOTf and 2,6-lutidine led to thioacetal **85** in 59% overall yield from **81.** Modification of thioacetal group **85** to the aldehyde **86** was performed with $HgCl_2$ and $CaCO_3$ in CH_3CN/H_2O in excellent 99% yield. The reaction performed on the aldehyde **86** with CH_3I and $CrCl_2$ gave a 70% yield of desired (*E*)-vinyl iodide **87.**[87] Completely desilylation with TBAF in THF provided triol **88** in quantitative yield. Following coupling of the (*E*)-vinyl triol **88** under Stille conditions[80] and the Fmoc-amino protected propenylstannane **89** prepared from propargylamine was made in following

sequence: (I) FmocCl, pyridine, CH_2Cl_2 and (II) Bu_3SnH/AIBN,[88] and afforded (*E*,*E*)-dienylamide **90** in 84% yield. Double *O*-acetylation with Ac_2O in pyridine produced diacetate **91** in 96% yield, which represents combined right-hand and middle fragment of the neooxazolomycin structure (Scheme 5).

4.1.3 Finalization of the total synthesis of neooxazolomycin by Kende. To finalize Kende's total synthesis of neooxazolomycin, protected acid **72** gave in the reaction with *N*,*N*-bis(2-oxo-3-oxazolidinyl)phosphorodiamidic acid chloride and Et_3N the activated anhydride,[89] to which a solution of the free amine prepared from the Fmoc diacetate **91** by DBU deprotection[88] was added. This procedure provided after 1 hour 60% yield of neooxazolomycin triacetate **92**, which spectroscopic analysis was in full agreement with naturally derived **92**.[2] Final basic hydrolysis of triacetate **92** with LiOH, followed by acidification afforded a 67% yield of pure neooxazolomycin (**2**) (Scheme 6). The final compound of Kende's total synthesis was identical with an authentic sample of the natural neooxazolomycin supplied by Dr D. Uemura of Shizuoka University in Japan.[13] Evaluation of the samples was performed by 300 MHz ^{1}H NMR, IR, TLC (silica gel and reverse phase) in several solvent system, HPLC and mass spectrometry comparison.[13]

4.2 Total synthesis of neooxazolomycin by Hatakeyama

Kende's total synthesis of neooxazolomycin, reported in 1990,[13] remained for many years the only total synthesis of oxazolomycins. However, Hatakeyama *et al.*[16] reported in 2007 second total synthesis of the neooxazolomycin (**2**), in which the major challenge consisted in the stereoselective construction of the right-hand fragment.

4.2.1 Synthesis of the left-hand fragment of neooxazolomycin by Hatakeyama. The left-hand fragment of neooxazolomycin was constructed in a remarkable improvement of the overall yield, compared with the synthesis reported by Kende *et al.*[13] As the starting material, 2,2-diethoxyethanol **93** was used, which in the reaction with KSCN under acidic conditions[90] afforded resulting oxazole-2-thiol, followed by butylation to thioether **94** in 79% yield in 2 steps. After copper-mediated propargylation of **94** [91,92] 2,5-disubstituted oxazole **95** in 94% yield was isolated. Following desulfurization with RANEY® Ni provided 5-substituted oxazole **96** in 92% yield. Desilylation performed with AgOTf gave 73% yield of alkyne **97**. The hydrostannylation under Bu_3SnH/AIBN conditions led to stannane **98** in 88% yield, as a mixture of (*E*/*Z*)-isomers in ratio 6 : 1. The Stille cross coupling of stannane **98** and (*Z*,*Z*)-diene iodide **63** prepared by Kende procedure,[13] afforded an inseparable mixture of (*E*/*Z*)-isomers of triene **99** in 79% yield. After desilylation with 47% HF/CH_3CN, followed by recrystallization, a geometrically pure (*Z*,*Z*,*E*)-configurated triene ester **70** was obtained. Basic hydrolysis of ester **70** and acetylation, previously reported by Kende[13] afforded protected acid **72** with 80% yield in 3 steps from **99** (Scheme 7).

4.2.2 Synthesis of the right-hand and middle fragment of neooxazolomycin by Hatakeyama. The stereoselective synthesis

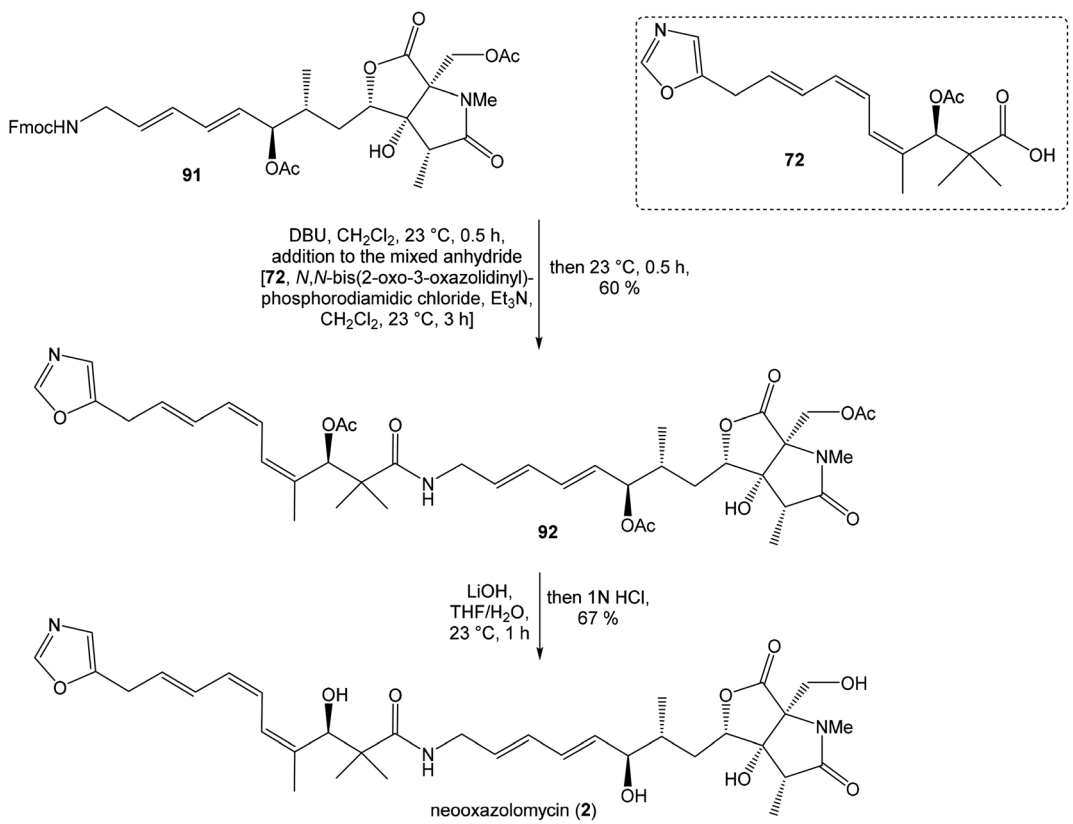

Scheme 6 Finalization of the total synthesis of neooxazolomycin (**2**) by Kende.

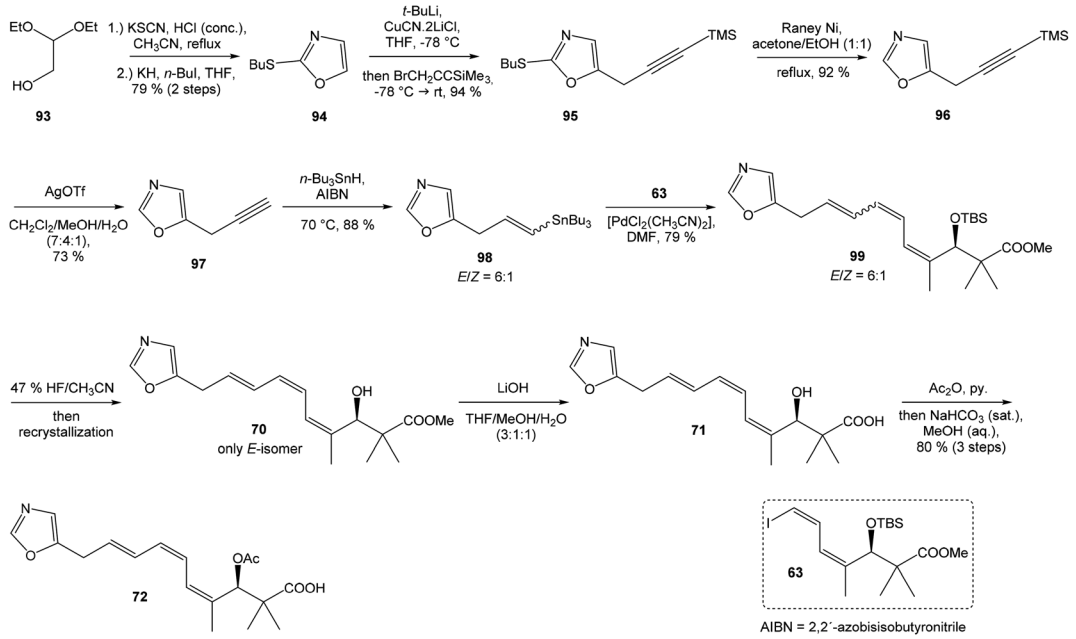

Scheme 7 Synthesis of the left-hand fragment derivative **72** of neooxazolomycin by Hatakeyama.

of right-hand fragment of neooxazolomycin started by the coupling of alkyne **101** [93] with triflate **102**,[94,95] both prepared from (*S*)-hydroxy-2-methylpropanoate **100**. Alkynol **103** was prepared *via* desilylation with TBAF in THF in 81% yield after 2 steps. Protection of the primary hydroxyl group with tetramethyldisilazane to corresponding hydrodimethylsilyl ether **104** and following hydrosilylation catalyzed with [Pt(dvds)][96] in THF provided siloxane **105**. Exposure of the siloxane **105** to the mixture of I_2 and CsF in DMF/MeOH (5 : 1) gave (*E*)-iodoalkenol **106** with perfect stereoselectivity in 82% yield after 3 steps. Such combination of solvents and additives in the iodination step was found to be crucial for the selectivity within the preparation of desired (*E*)-configured iodoalkenol **106** (Scheme 8).

Oxidation of primary hydroxyl group to the carboxylic acid **107** was carried out under Jones oxidation conditions. Carboxylic acid was transformed using $SOCl_2$ in CH_2Cl_2 to the acyl chloride **108** and following reaction with dimethyl 2-(methylamino)malonate[97] provided amide **109** in 62% yield in 3 steps. Amide **109** was converted to pyrrolidinone **110** by treatment with $Pd(OAc)_2/Ph_3P$ in the presence of K_2CO_3 and TBABr in DMF/H_2O at 70 °C in 84% yield.[98] Double bond dihydroxylation under OsO_4/NMO conditions and concomitant lactonization yield to lactone **111** as the sole product in 88% (Scheme 8). Formation of other diastereomer was not observed. The high stereoselectivity can be explained by the preferred conformer of pyrrolidinone **110**, where the method using OsO_4 is restricted to the α-face. This hypothesis was supported by NOE experiments and molecular mechanics calculations.[16]

Hydrolysis of **111** was promoted with 4 M LiOH leading to carboxylic acid **112** and following Fujisawa reduction[86] give the diol **113** in 57% yield after 3 steps. To confirm the configuration of diol **113**, X-ray analysis of the corresponding mono-*tert*-butyldimethylsilyl ether was accomplished.[16] Protection of diol **113** to the dioxasilinane **114**, following reductive debenzylation with H_2 catalyzed with Pd/C in MeOH and Dess–Martin oxidation led to aldehyde **116** in 83% yield after 3 steps. Reaction between aldehyde **116** and diene iodide **117** under Nozaki–Hiyama–Kishi conditions[99] provided product **118** in 73% yield as a mixture of diastereomers ($R/S = 1 : 1$).[87] Although no diastereoselectivity was observed in Nozaki–Hiyama–Kishi reaction, high stereoselective formation ($R/S = 30 : 1$) of desired (*R*)-configurated secondary alcohol **120** was observed in two following reaction steps (oxidation with Dess–Martin periodinane, followed by reduction with L-selectride) in very good yield. Exposure of **120** to HF/pyridine mixture provided triol **90**, which after acetylation with Ac_2O in pyridine gave compound **91** in 92% yield after 2 steps, as a combined right-hand and middle fragment of neooxazolomycin (Scheme 8).[16]

4.2.3 Finalization of the total synthesis of neooxazolomycin by Hatakeyama. Hatakeyama's total synthesis of neooxazolomycin used previous synthetic route[13] to finalize the product. Thus, condensation of acid **72** and free amine was generated *in situ* from compound **91** and provided triacetyl **92** in 60% yield. Final deacetylation gave desired neooxazolomycin (Scheme 9), which spectroscopic (^{1}H and ^{13}C NMR) and chromatographic (TLC and HPLC) comparisons were identical with natural sample of the neooxazolomycin.[16]

4.3 Total synthesis of neooxazolomycin by Kim

Kim *et al.* reported in 2019 a total synthesis of neooxazolomycin (**2**) using a chirality-transfer strategy.[17] The six stereocenters of right-hand fragment were derived from D-**serine** by a series of chirality-transfer processes.

4.3.1 Synthesis of the left-hand fragment of neooxazolomycin by Kim. The synthesis of left-hand fragment started from the TBS-protected hydroxypivalic acid **121**,[100] which

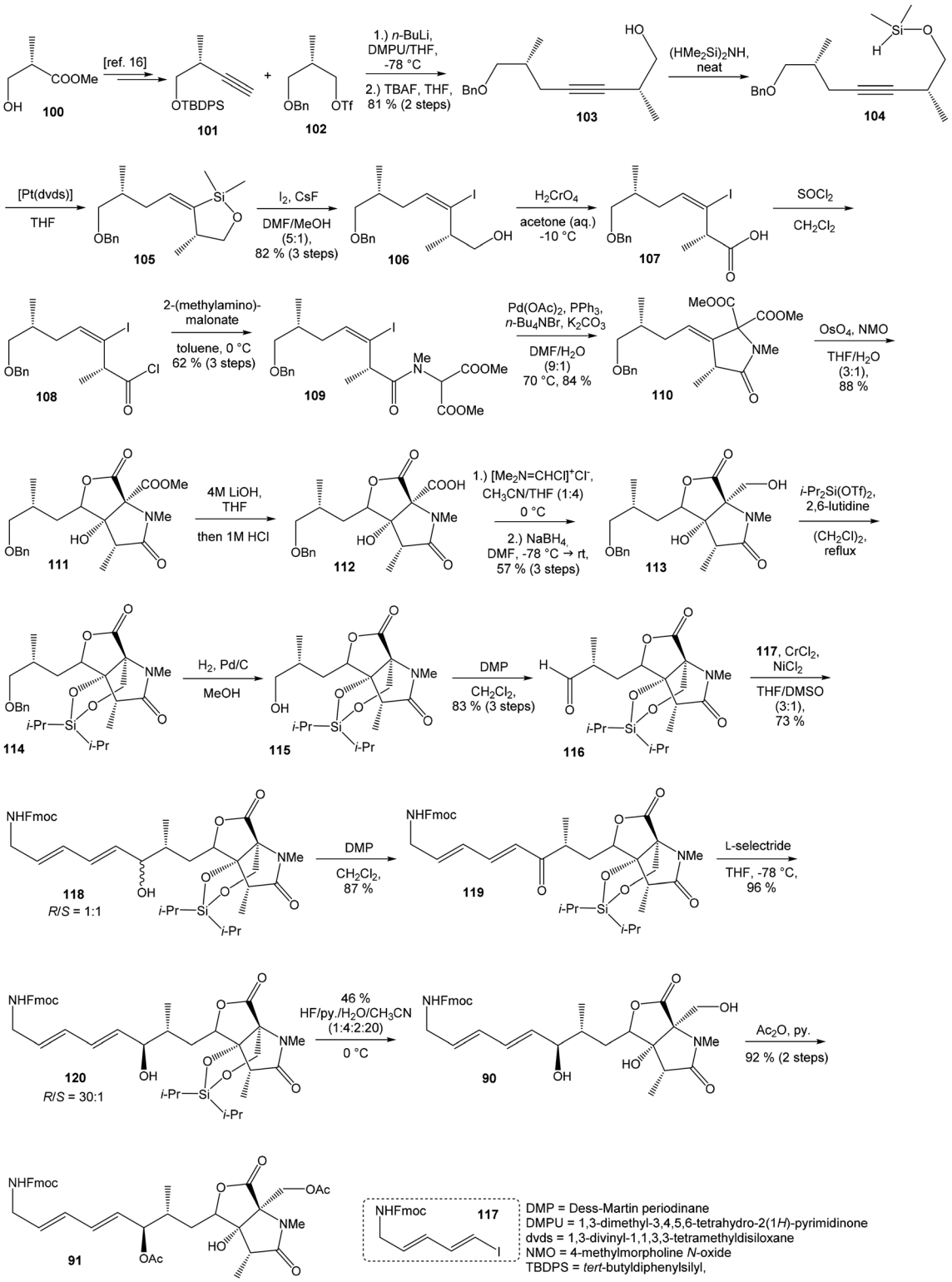

Scheme 8 Synthesis of the right-hand and middle fragment derivative **91** of neooxazolomycin by Hatakeyama.

in reaction with copper acetylide of propiolate afforded compound **122** in 86% after 2 steps.[101] Following asymmetric reduction of prochiral ketone **122** with (+)-DIP-chloride[102] was used for a preparation of (3′*R*)-configurated alcohol **123** in 72% yield, with 93% *ee*. Prepared hydroxyl group was protected with BzCl to provide 98% yield of alkyne **124**. The alkyne in next reaction with CuI and CH_3I in THF at −78 °C led to (*Z*)-configurated methyl ester **125** in 89% yield as a sole geometric isomer. Transformation of methyl ester group to aldehyde was achieved in two steps. The reduction of ester **125** with DIBAL-H

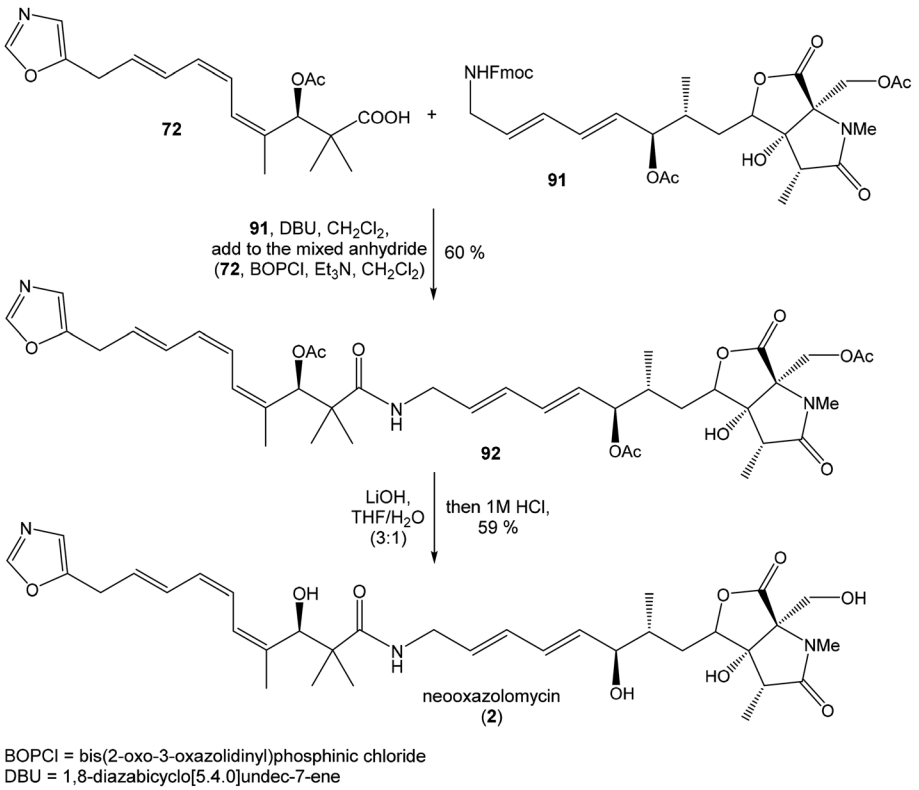

Scheme 9 Finalization of the total synthesis of neooxazolomycin (**2**) by Hatakeyama.

in THF gave corresponding primary alcohol **126** in 83% yield. Following oxidation with NMO, TPAP in CH_2Cl_2 produced aldehyde **127** in 98% yield. By application of Uenishi's protocol,[103] which involved a Corey–Fuchs dibromoolefination and Pd-catalyzed hydrogenolysis of aldehyde **127**, desired (*Z*,*Z*)-1-bromodiene **128** was selectively obtained. The Stille cross coupling of **128** with the known vinyl stannane **68** [104] afforded required oxazol triene **129** in 70% yield without significant isomerization of any double bond. The unidentified geometric isomer was detected at trace levels (<1 : 30). Then TBS protecting group of oxazol triene was removed to produce corresponding primary alcohol **130** in 90% yield. The Swern oxidation led to aldehyde **131** in 96% yield, which after following Pinnick oxidation provided carboxylic acid **132** in 84% yield (Scheme 10).

4.3.2 Synthesis of the right-hand and middle fragment of neooxazolomycin by Kim. The right-hand fragment synthesis started from **D-serine**, which was transformed to Cbz-protected oxaproline *t*-butyl ester **133** in two steps.[105,106] The Cbz protecting group was removed under conditions of hydrogenolysis catalyzed with $Pd(OH)_2/C$ to provide *N*-deprotected oxaproline *t*-butyl ester **134** in 99% yield. Meanwhile, the nucleophilic substitution of chlorine in ethyl 4-chloroacetoacetate **135** with BnOH gave compound **136** in 86% yield. Subsequent monomethylation with CH_3I/K_2CO_3 in acetone afforded β-keto ester **137** in 88% yield. Basic hydrolysis with KOH in H_2O/MeOH afforded acid **138** in 98% yield. It was observed, that both coupling partners **138** and **134** are unstable, thus the amide coupling was conducted immediately after preparation of these species. Amide **139** was prepared in 76% yield as an inseparable mixture of C2 diastereomers (neooxazolomycin numbering) with diastereomer ratio (d.r.) 1.4 : 1 (Scheme 11).

Intramolecular aldol reaction was carried out with EtONa in EtOH and desired aldol product **140** was obtained with perfect enantioselectivity (>99% *ee*) in 61% yield. The configurations of the three contiguous stereocenters were unambiguously confirmed by XRD analysis.[17] To introduce the exocyclic carbon chain, the benzyl protection group was removed under conditions of catalytic hydrogenation with H_2, Pd/C in MeOH/AcOH (2 : 1) to produce primary alcohol **141** in 97% yield. Following oxidation with TEMPO, TCCA in CH_2Cl_2 gave aldehyde **142** in 84% yield. Various nucleophilic addition reactions were examined in following step. The best result was obtained when the Barbier reaction was conducted using In and TBAI in water to give **144** in 79% yield, in d.r. = 12 : 1 after spontaneous lactonization in EtOAc (Scheme 11). The stereocenter at C4 is epimeric to that of target natural product **2**, however this stereochemistry was useful in the induction of the desired C6 stereocenter by hydrogenation.[107,108]

Reduction of **144** with H_2, Pd/C in MeOH/AcOH (2 : 1) produced compound **145** in 99% yield. The stereochemistry of reduced product **145** was confirmed by XRD analysis.[17] The lactone ring opening was performed with *N*,*O*-dimethylhydroxylamine hydrochloride and i-PrMgCl in THF to give compound **146** in 92% yield. Inversion of hydroxyl group on C4 was achieved by sequential oxidation with NMO, TPAP in CH_2Cl_2 to

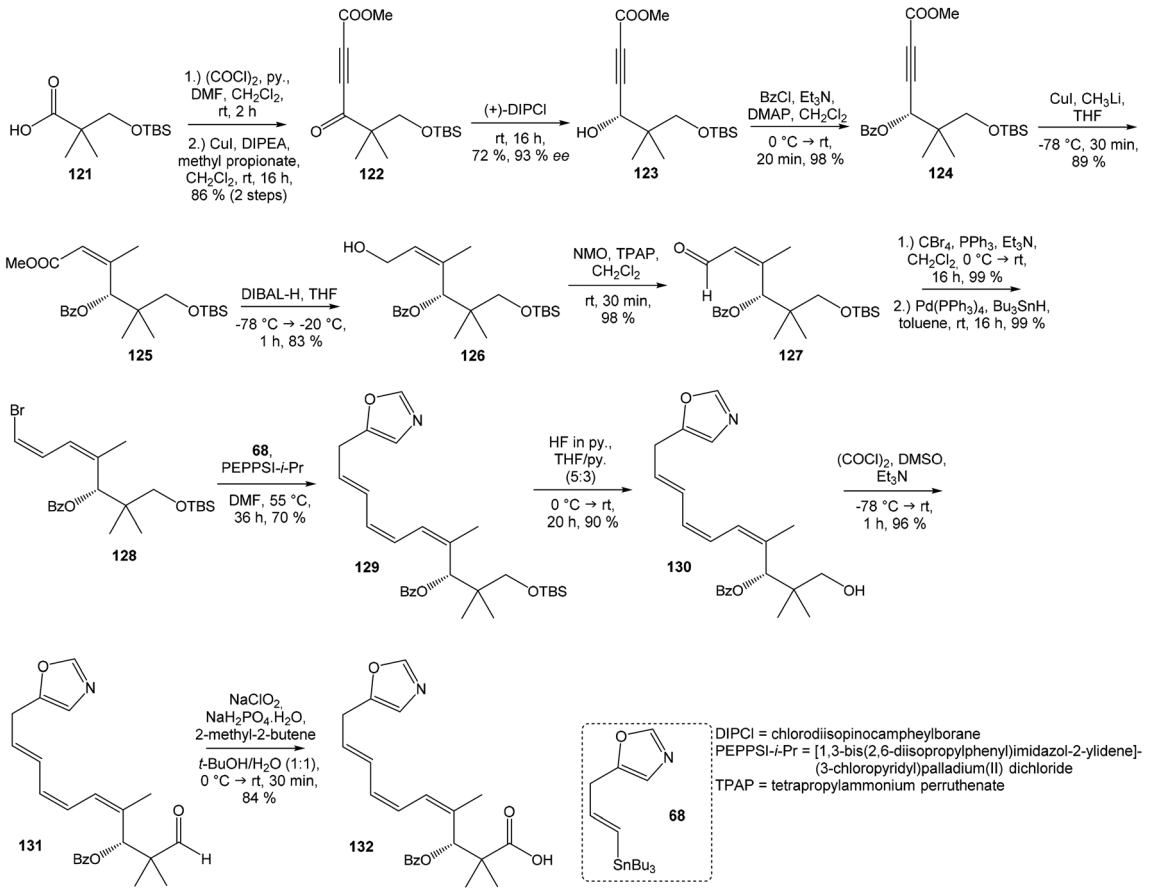

Scheme 10 Synthesis of the left-hand fragment derivative **132** of neooxazolomycin by Kim.

ketone **147** followed by stereoselective reduction with $CeCl_3 \cdot 7H_2O$, $NaBH_4$ in MeOH, to produce required epimer **148** in d.r. 15 : 1. Protection of secondary alcohol required careful selection of reaction conditions to avoid undesired lactonization. The protection was carried out with TMSCl and HMDS in pyridine and gave compound **149** in 94% yield without undesired lactonization. Next reaction was performed with dimethyl methylphosphonate, *n*-BuLi in THF and produced β-keto phosphonate **150** in 82% yield. Desilylation of **150** with TBAF in THF proceeded with concomitant lactonization to tricyclic **151** in 80% yield (Scheme 11).

The reductive ring opening of the oxaproline moiety was achieved with $Et_3SiH/FeCl_3$ to provide *N*-methylated bicyclic diol **152** in 51% yield.[109] The structure of bicyclic diol was confirmed by XRD analysis.[17] The hydroxyl groups were protected with $Si(^iPr)_2(OTf)_2$ and 2,6-lutidine to corresponding dioxasilinane **153** in 99% yield.[16] The Horner–Wadsworth–Emmons reaction of **153** with the aldehyde **154** in presence of $Ba(OH)_2$ in THF/H_2O (40 : 1) at −30 °C proceeded in 75% yield and produced ketone **155** with partially hydrolyzed dioxasilinane group. Under such reaction conditions, no isomerization at C6 was observed. The selective reduction of ketone **155** with L-selectride in THF was followed by immediate acetylation with Ac_2O in pyridine to give **157** in 75% yield (after 2 steps) in d.r. 4 : 1 (Scheme 11). Notably, no diastereoselectivity was observed in the formation of the C7 stereocenter when the primary hydroxy group was not protected.

4.3.3 Finalization of the total synthesis of neooxazolomycin by Kim. The both prepared compounds, left-hand fragment **132** and right-hand fragment **157**, were coupled to finalize the synthesis of **2**. Thus, BOP-mediated coupling between **132** and free amine generated *in situ* from **157** provided amide **158** in 51% yield. The silyl protecting group was removed during this coupling reaction. Deprotection of benzoate and acetate protective groups was performed with K_2CO_3 in MeOH. Unfortunately, the basic hydrolysis caused partial lactone ring opening. However, relactonization was simply achieved by treatment with acidic resin to give desired neooxazolomycin (**2**) in 90% yield (Scheme 12). Kim *et al.* reported[17] that spectral data and optical rotation of prepared **2** were in good agreement with those previously reported.[13,16]

4.4 Total synthesis of oxazolomycin A by Hatakeyama

Hatakeyama *et al.* reported in 2011 a total synthesis of other member of the oxazolomycin family. The total synthesis of oxazolomycin A (**1**) was based on the methodology previously developed by Hatakeyama *et al.*[16] in total synthesis of neooxazolomycin. Moreover, penultimate crude product in the Hatakeyama's total synthesis was in 2017 reported by Koomsiri

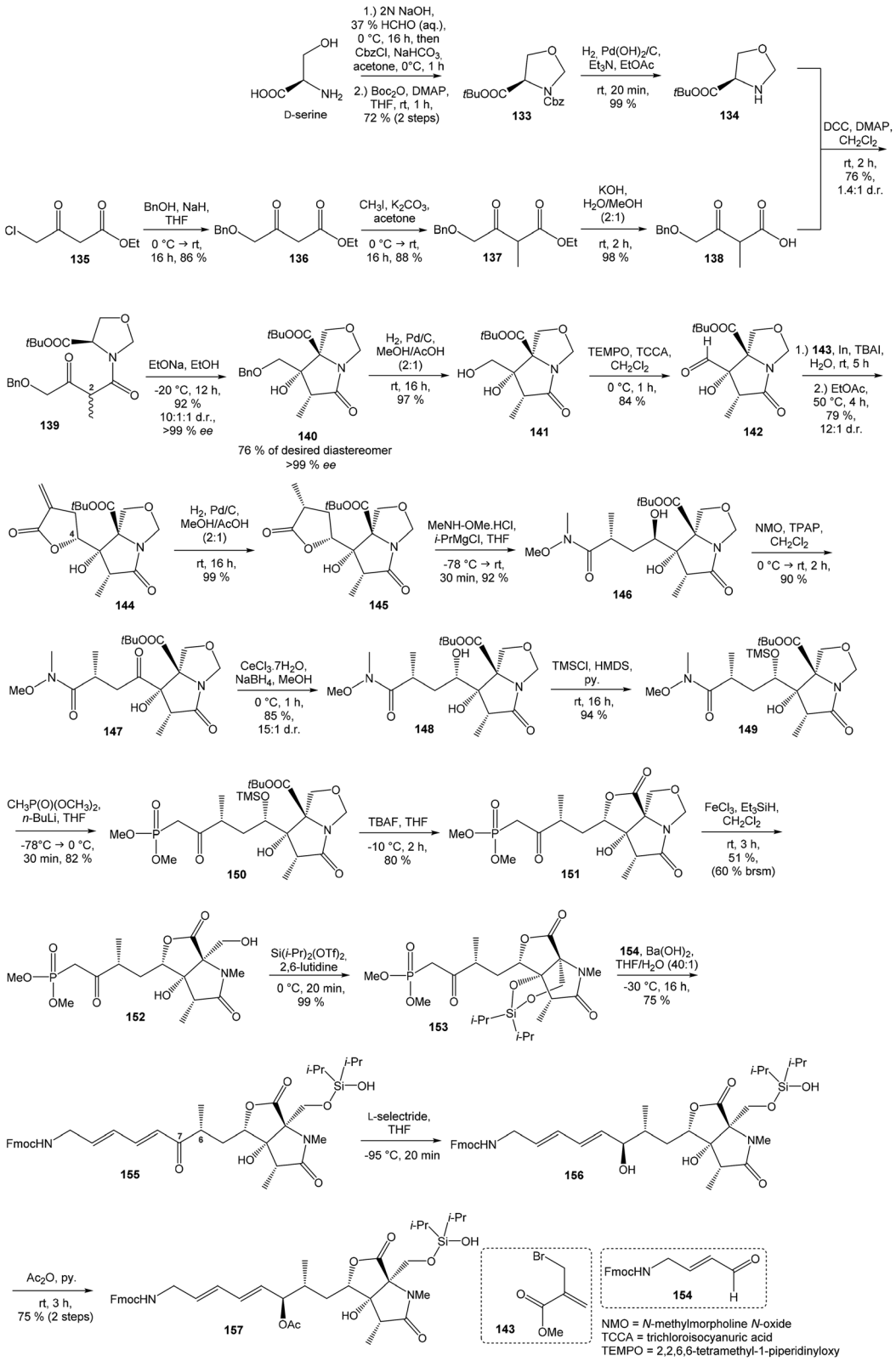

Scheme 11 Synthesis of the right-hand and middle fragment derivative **157** of neooxazolomycin by Kim.

et al.[10] as a novel member of oxazolomycin family named oxazolomycin A2. Thus, Hatakeyama *et al.* elaborated suitable methodology for total synthesis of oxazolomycin A2 (**14**) as well.

4.4.1 Synthesis of the left-hand fragment of oxazolomycin A by Hatakeyama. Synthesis of left-hand fragment of oxazolomycin A includes remarkable improvement of the previously

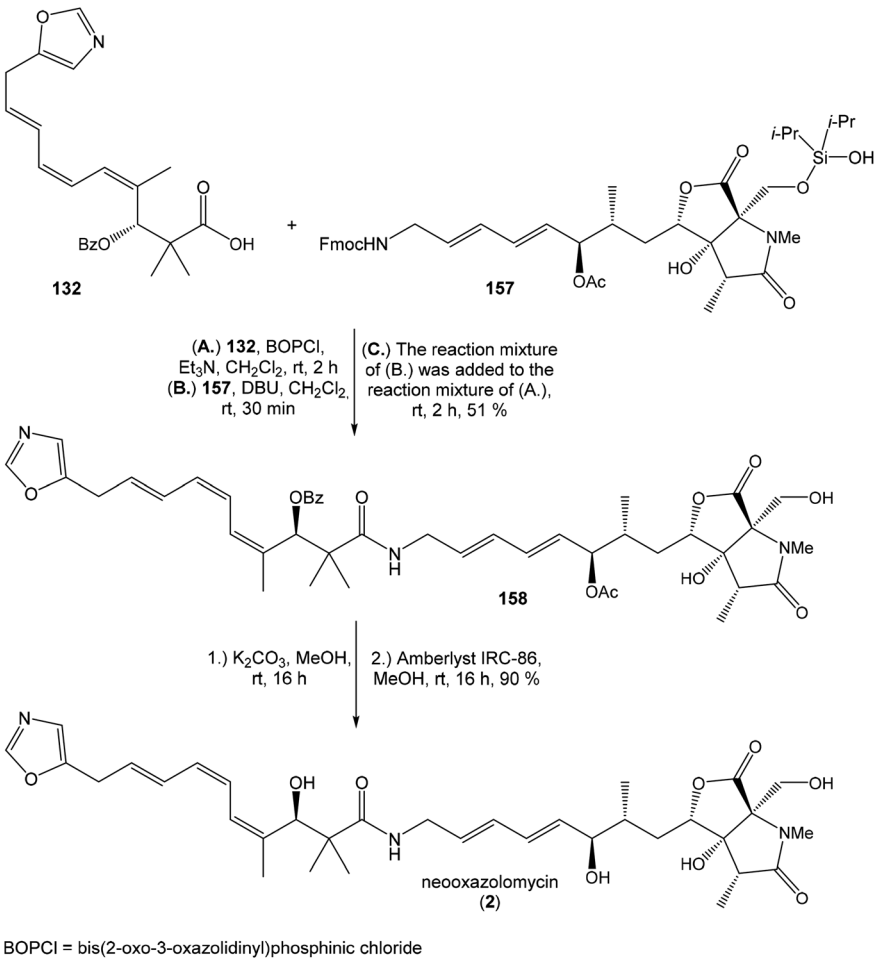

Scheme 12 Finalization of the total synthesis of neooxazolomycin (**2**) by Kim.

procedure reported by Hatakeyama *et al.*[16] As the starting material, propargyl alcohol was readily transformed[16] to aldehyde **54**. Following asymmetric cyclocondensation[110–113] of an aldehyde **54** was performed according to Nelson's protocol[112] *via* catalysis by *Cinchona* alkaloid **159** to give expected β-lactone **160** in 92% yield. Moreover, β-lactone **160** was prepared with excellent enantioselectivity (*ee* = 98%) and diastereoselectivity (*de* > 99%). Methanolysis of lactone **160** with MeONa in MeOH provided methyl ester **161** in 95% yield. Generation of the lithium enolate from the ester **160** and subsequent methylation afforded **162** in 84% yield.[114] After desilylation and hydroxyl group protection with TBSOTf and 2,6-lutidine in CH_2Cl_2, protected enyne **61** was obtained in 98% yield. The previously established procedure[16] was utilized to convert **61** to the iodoalkene **63** in 92% yield. Stille cross coupling between iodoalkene **63** and stannane **68** [115] using $Pd(PPh_3)_4$, CuI and CsF[116] in DMF provided (*Z*,*Z*,*E*)-triene **69** in 83% yield as a pure geometric isomer. Using a Pd(0) catalyst alone in Stille cross coupling always resulted in isomerization of triene system. Finally, desilylation, saponification and acetylation give to protected left-hand fragment **72** in 88% yield (after 3 steps) (Scheme 13).

4.4.2 Synthesis of the right-hand fragment of oxazolomycin A by Hatakeyama. As the starting material in Hatakeyama's synthesis of right-hand fragment of oxazolomycin A, (*S*)-3-hydroxy-2-methylpropionate was used. Conversion to alkynol **103** was performed using previously reported procedure.[16] Alkynol **103** was after Jones oxidation, followed by preparation of corresponding acid chloride and condensation with dimethyl 2-(methylamino)malonate[97] transformed to amide **165**. Coniaene type cyclization[117] catalyzed with $In(OTf)_3$ in the presence of DBU in toluene at reflux afforded lactam **110** in 91% as the sole product. The cyclization took place regioselectively and stereoselectively with complete (*E*)-selectivity and without epimerization. Exposure of lactam **110** to OsO_4/NMO conditions (as previously reported) installed three asymmetric centers in a single procedure leading to bicyclic γ-lactam-γ-lactone **111** in the quantitative yield.[16] Basic hydrolysis with consecutive acidification resulted in carboxylic acid **112**. Subsequent transformation to acyl chloride followed by $NaBH_4$ reduction produced alcohol **113** in 60% yield (Scheme 14).

Further, primary hydroxyl group was protected with MOMCl, lactone ring reduced with $NaBH_4$ and selective silylation with TBSOTf led to diol **168** that was prepared in 93%. Subsequent secondary hydroxyl group methylation of diol **168** using

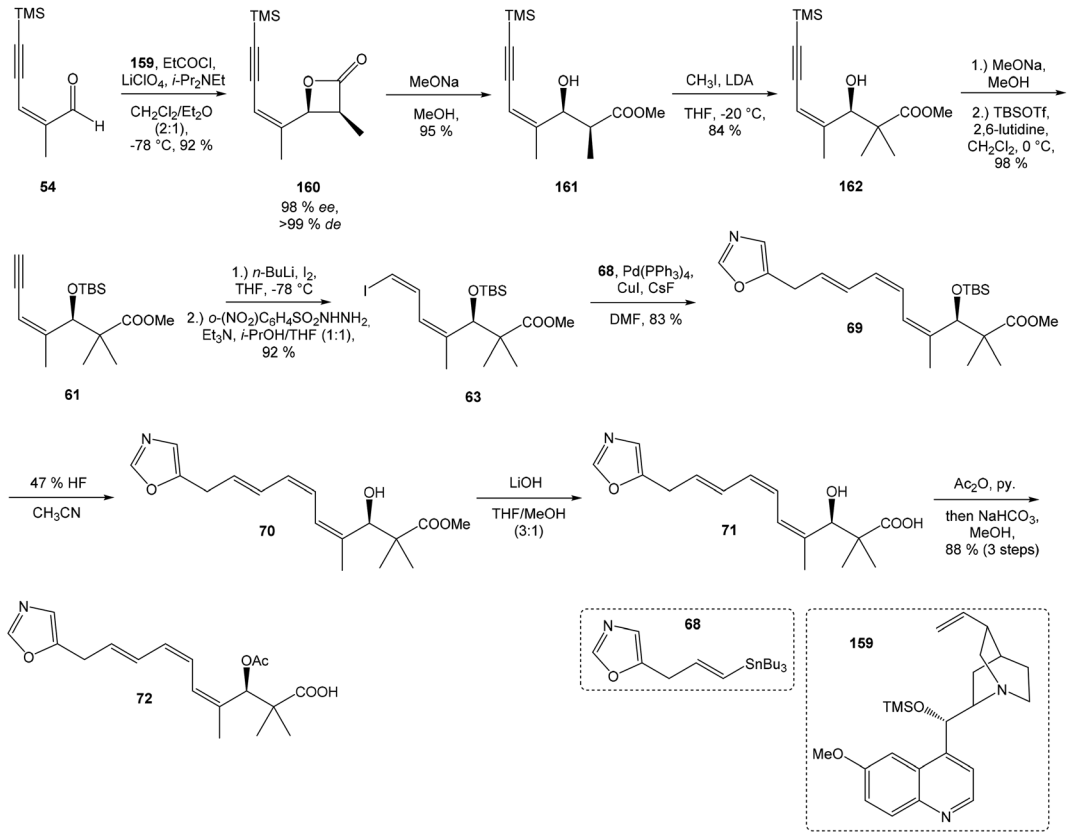

Scheme 13 Synthesis of the left-hand fragment derivative **72** of oxazolomycin A by Hatakeyama.

Meerwein reagent and proton sponge[118] provided alcohol **169** in 95% yield. Compound **169** was desilylated with TBAF, primary hydroxyl group underwent Jones oxidation followed by Pinnick oxidation that led to acid **171**. Cleavage of the MOM protecting group mediated with $ZrCl_4$ [119] gave β-hydroxy acid **172**, which was treated with triisopropylsilyloxymethyl(dodecyl)sulfane[120,121] in the presence of $CuBr_2$, TBABr and Et_3N and allowed the selective esterification yielding to ester **173** in 67% (in 5 steps). Remarkably, esterification reaction did not proceed selectively in the absence of Et_3N, although both the carboxylic acid and the primary alcohol groups were protected. The reaction of ester **173** with i-$Pr_2Si(OTf)_2$ and 2,6-lutidine in DCE led to dioxasilinane **174** in 90% yield. After reductive debenzylation of the compound **174** catalyzed with $Pd(OH)_2$, followed by Dess–Martin oxidation, aldehyde **176** was prepared in 92% yield (in 2 steps) (Scheme 14).

4.4.3 Synthesis of the middle fragment of oxazolomycin A by Hatakeyama. Allylamine was used as the starting material in Hatakeyama's synthesis of middle fragment. Protection of the amino group with FmocCl in dioxane provided protected amine **177** in 96% yield. Cross-metathesis reaction[122] of allyl **177** with acrolein, catalyzed with Hoveyda–Grubbs 2nd generation catalyst in CH_2Cl_2 gave aldehyde **154** in 85% yield. Finally, Takai's iodoalkenylation[87] mediated by CHI_3 and $CrCl_2$ in THF produced iodoalkene **117** in 66% yield, as a mixture of (*E*/*Z*)-isomers in ratio 8 : 1 (Scheme 15). Geometrically pure (*E*)-isomer **117** was isolated by recrystallisation from EtOAc. This reaction sequence involved only 3 reaction steps in good overall yield (54%), compared to previously reported[16] preparation of compound **117** from propargyl alcohol in 9 steps with only 18% overall yield.

4.4.4 Finalization of the total synthesis of oxazolomycin A by Hatakeyama. To finalize the oxazolomycin A synthesis, combination of the three prepared fragments, complete deprotection and the selective formation of the β-lactone ring was accomplished. Thus, the right-hand fragment **176** and the middle fragment **117** were firstly linked under conditions[99,123,124] of Nozaki–Hiyama–Kishi reaction. Using $CrCl_2$ and $NiCl_2$ in THF/DMSO, product was isolated in 81% yield as a mixture of (7*R*)-configurated **180** and its (7*S*)-epimer in ratio 3 : 2. Utilization of Dess–Martin oxidation followed by reduction with L-selectride provided desired (7*R*)-configurated alcohol **180** and its (7*S*)-epimer in ratio 4 : 1. Undesired (7*S*)-configurated alcohol was separated and again recycled by above mentioned oxidation–reduction procedure. Application of this sequence allowed to isolate desired alcohol **180** in 53% yield from aldehyde **176** (Scheme 16).

Protection of hydroxyl group with Ac_2O in pyridine led to protected compound **181** in 91% yield. Exposure of **181** to DBU in CH_2Cl_2 provided free amine which was directly condensed with the left-hand fragment **72** in presence of BOPCl and produced amide **182** in 68% yield. Deprotection of amide **182** with HF-pyridine, followed by basic hydrolysis with LiOH and subsequent acidification with ion-exchange resin gave tetrahydroxy

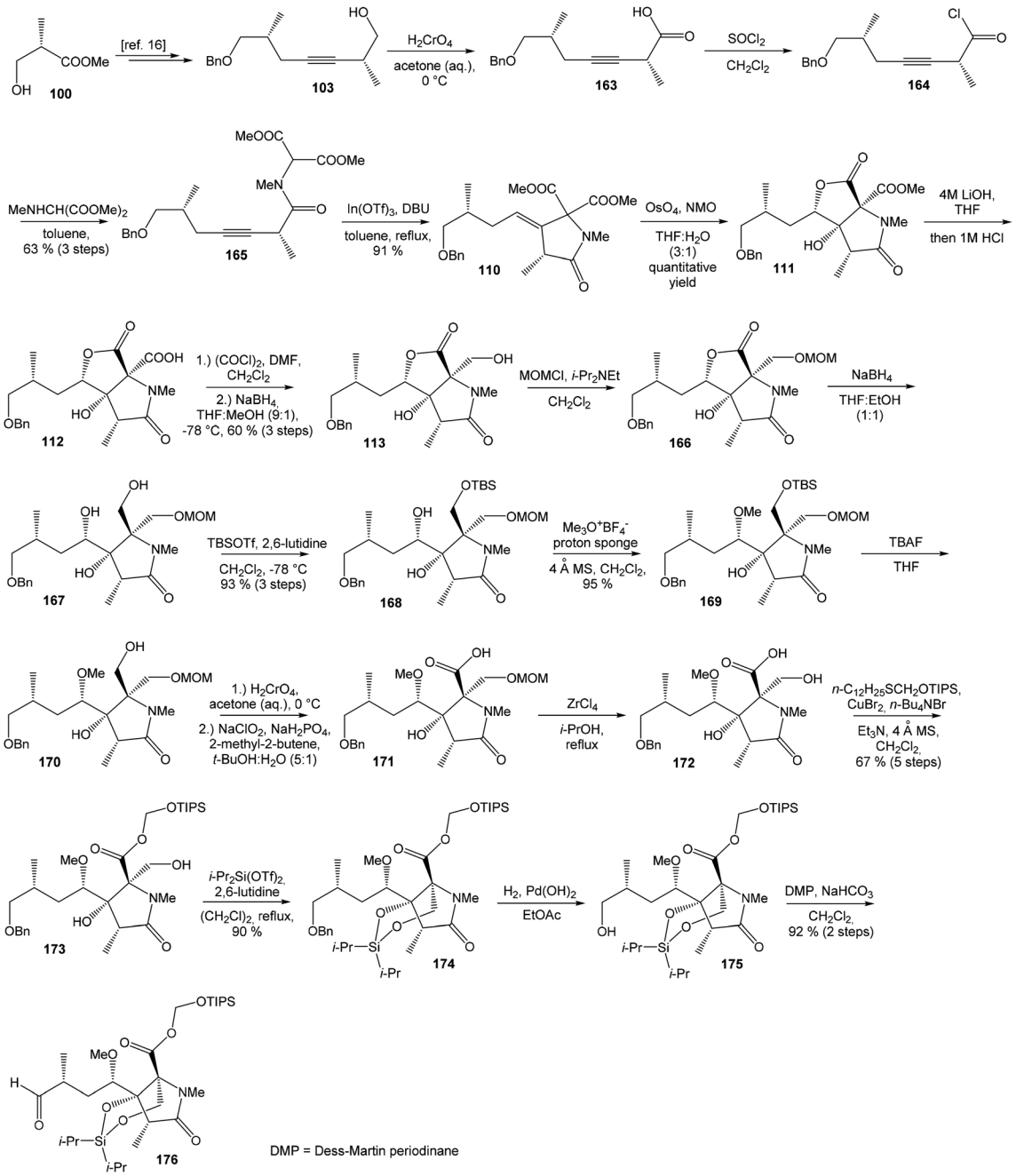

Scheme 14 Synthesis of the right-hand fragment derivative **176** of oxazolomycin A by Hatakeyama.

acid, which was later isolated by Koomsiri *et al.* as oxazolomycin A2 (**14**).[10] Then final treatment of crude **14** with HATU[125] in the presence of i-Pr_2NEt in THF provided final oxazolomycin A (**1**) in 40% yield from amide **182** (Scheme 16). The spectroscopic data of the prepared oxazolomycin **1** were identical with the previously reported data for natural oxazolomycin A.[1,6,60] The structure of final product **1** was confirmed by comparison of the spectral data of its diacetate with those reported previously.[1,60]

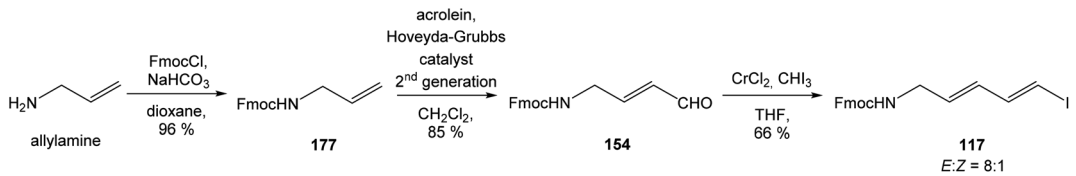

Scheme 15 Synthesis of the middle fragment derivative **117** of oxazolomycin A by Hatakeyama.

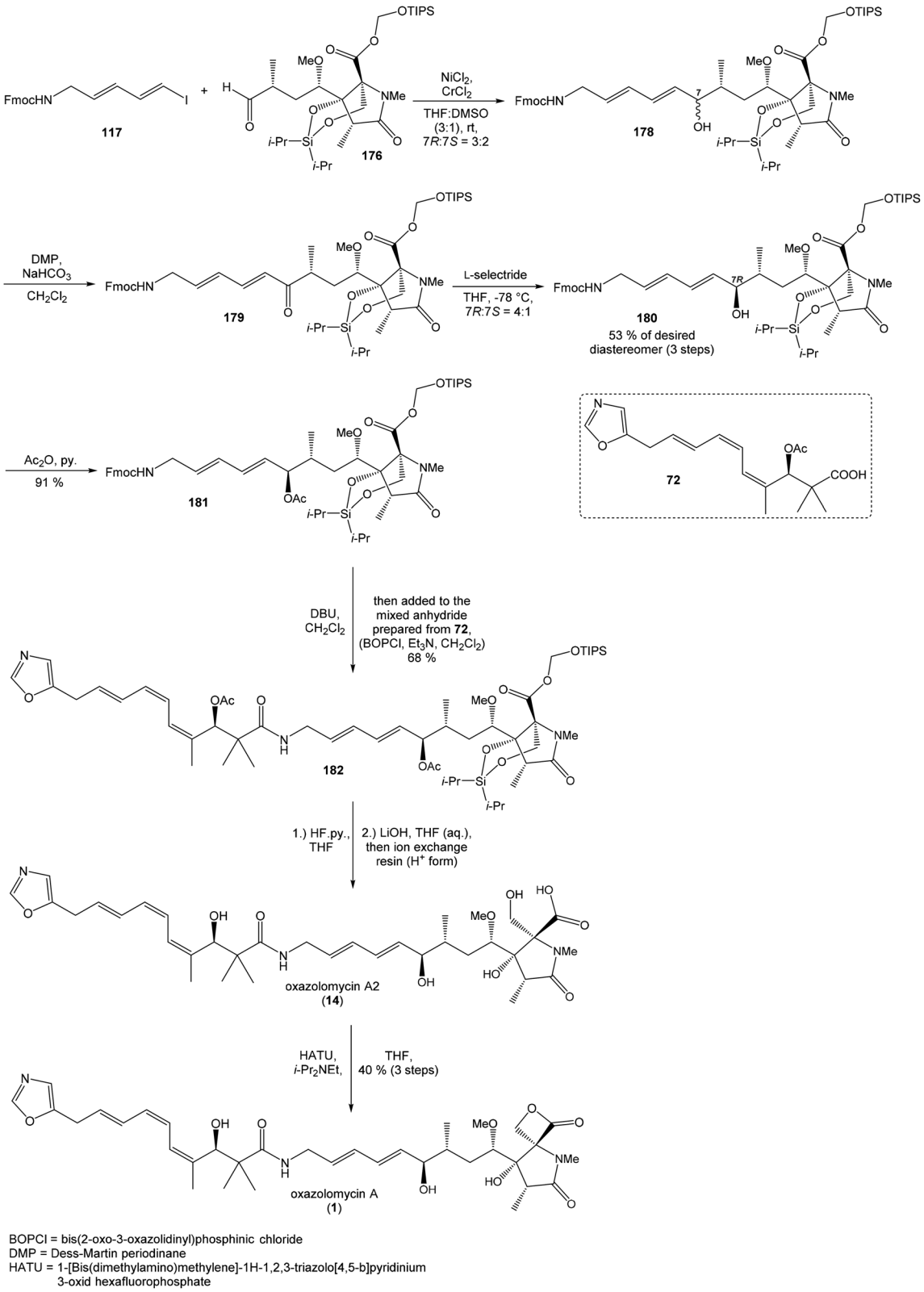

Scheme 16 Finalization of the total synthesis of oxazolomycin A (**1**) by Hatakeyama.

The first total synthesis of oxazolomycin A reported by Hatakeyama *et al.* involves 34 steps of the longest linear sequence in 1.4% overall yield from methyl (*S*)-3-hydroxy-2-methylpropionate. Moreover, synthesis of oxazolomycin A2 was achieved in 33 steps of the longest linear sequence in 1.4–3.5% overall yield from methyl (*S*)-3-hydroxy-2-

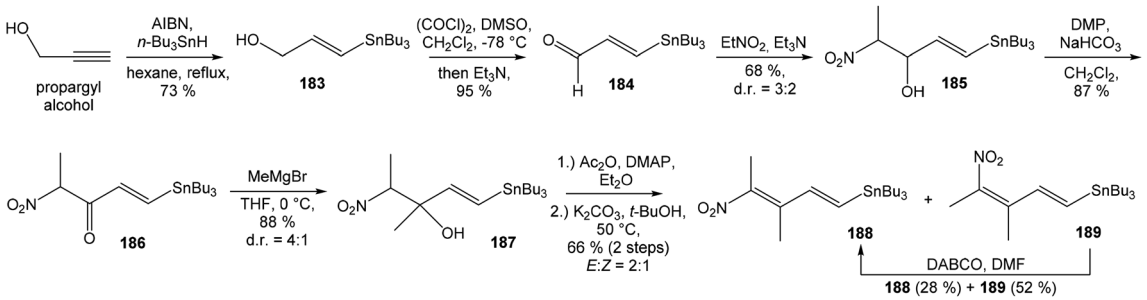

Scheme 17 Synthesis of the left-hand fragment precursor **188** of lajollamycin B by Hatakeyama.

methylpropionate. Unfortunately, oxazolomycin A2 in the Hatakeyama's total synthesis was not isolated but used as a crude product directly for next reaction. However, Hatakeyama *et al.* elaborated first consecutive total synthesis, which involved two different members of oxazolomycin family.[10,12]

4.5 Total synthesis of lajollamycin B by Hatakeyama

Hatakeyama *et al.* reported in 2019 the first total synthesis of lajollamycin B (**11**), nitrotetraene spiro-β-lactone-γ-lactame member of the oxazolomycin family.[15] This convergent synthesis involves preparation and conjugation of three fragments. Left-hand fragment represents nitrodienylstannane **188**, middle fragment **191** constitutes 7-iodoheptadienoic acid, right-hand fragment **181** has already been prepared for previous synthesis of oxazolomycin A reported by Hatakeyama *et al.*[12]

4.5.1 Synthesis of the left-hand fragment precursor of lajollamycin B by Hatakeyama. To achieve required nitrodienylstannane **188**, propargyl alcohol has been chosen as the starting material. According to the reported procedures[126,127] of hydrostannylation using Bu_3SnH and AIBN in hexane at reflux, propargyl alcohol was converted to *E*-vinylstannane **183** in 73% yield. Oxidation of alcohol **183** was achieved under Swern conditions, using $(COCl)_2$, DMSO, Et_3N in CH_2Cl_2 by which 95% of product was obtained as the aldehyde **184**. Prepared aldehyde **184** was exposed to $EtNO_2$ and Et_3N in Henry reaction to produce nitroalcohol **185** in 68% yield as a mixture of diastereomers in a ratio 3 : 2. Corresponding nitroketone **186** was prepared in 87% using oxidation with Dess–Martin periodinane. Following Grignard reaction with MeMgBr in THF at 0 °C gave tertiary alcohol **187** in 88% yield as a 4 : 1 mixture of diastereomers (Scheme 17).

Compound **187** was moved to next dehydration reaction to produce desired left-hand fragment **188**. Unfortunately, all examined experiments using MsCl/Et_3N and $SOCl_2$/pyridine as well as various other acidic conditions totally failed. Thus, compound **186** was dehydrated[128,129] *via* corresponding acetate, prepared with Ac_2O and DMAP in Et_2O, followed by using K_2CO_3 in *t*-BuOH at 50 °C. This procedure afforded desired (*E*)-isomer **188** and its (*Z*)-isomer **189** in 66% yield as a 2 : 1 mixture of (*E*/*Z*)-geometric isomers. After separation, undesired (*Z*)-isomer **189** was converted in reaction with DABCO to the mixture of (*E*)-isomer **188** in 28% yield and initial (*Z*)-isomer **189** in 52% yield (Scheme 17). It was observed that isomerization carried out at higher temperature led to largely decomposition of both products **188** and **189**. Unambiguously determination of the geometries of **188** and **189** was achieved by NOESY spectra.[15]

Hatakeyama and co-workers examined other synthetic strategies to prepare desired nitrodienylstannane **188**, *e.g.* synthesis starting with commercially available (*E*)-4-(dimethylamino)-3-buten-2-one or synthesis beginning from ethyl pyruvate. Unfortunately, such strategies did not provide satisfactory results.[15]

4.5.2 Combination of middle and right-hand fragment in the total synthesis of lajollamycin B by Hatakeyama. Intermediate **190** [19] was under conditions of saponification using LiOH in THF/MeOH/H_2O (3 : 1 : 1), followed by acetylation with Ac_2O in pyridine, quantitatively transformed to carboxylic acid **191**, which represents the middle fragment in total synthesis of lajollamycin B. Formerly prepared Fmoc-protected right-hand fragment **181** [12] was deprotected using DBU in CH_2Cl_2 to corresponding free amine, which was directly condensed with middle fragment **191**, using BOPCl and Et_3N and provided amide **192** in 62% yield. Following desilylation with HF/pyridine in THF and deacetylation using LiOH in THF (aq.) afforded tetrahydroxyacid **193**, which was treated with HATU[125] in presence of i-Pr_2NEt in THF and provided the key precursor **194** in 44% yield after 3 steps (Scheme 18).

4.5.3 Model study for the final Stille coupling. The Stille cross coupling reactions of intermediate **190** [19] with (*E*)-nitrodienylstannane **188** and (*Z*)-nitrodienylstannane **189**, served as a model study for the final step. These reactions were examined under Baldwin's conditions,[116,130] which had been found to cause no isomerization of the similar conjugated triene systems during the Stille coupling.[12,115] However, (*E*)-configurated tetrasubstituted terminal double bond isomerization of **188** took place to produce mixture of (*E*)-isomer **196** and (*Z*)-isomer **195** in 38% yield, in ratio 5 : 4. When amounts of $Pd(PPh_3)_4$ and CsF were decreased in the reaction with (*E*)-configurated **188**, it was found that yield increased to 73%, although isomerization of the terminal double bond was still presented for **196** : **195** in ratio 2 : 1. Similar reaction conditions applied on (*Z*)-configurated **189** provided mixture of **196** and **195** in 71% yield in ratio of 2.5 : 1. When the mixture of 2 : 3 of **188** and **189** was used as the starting material, mixture of products **196** and **195** was obtained in 76% yield in ratio 2 : 1 (Scheme 19). The results of these reactions are summarized in Table 9. Unfortunately,

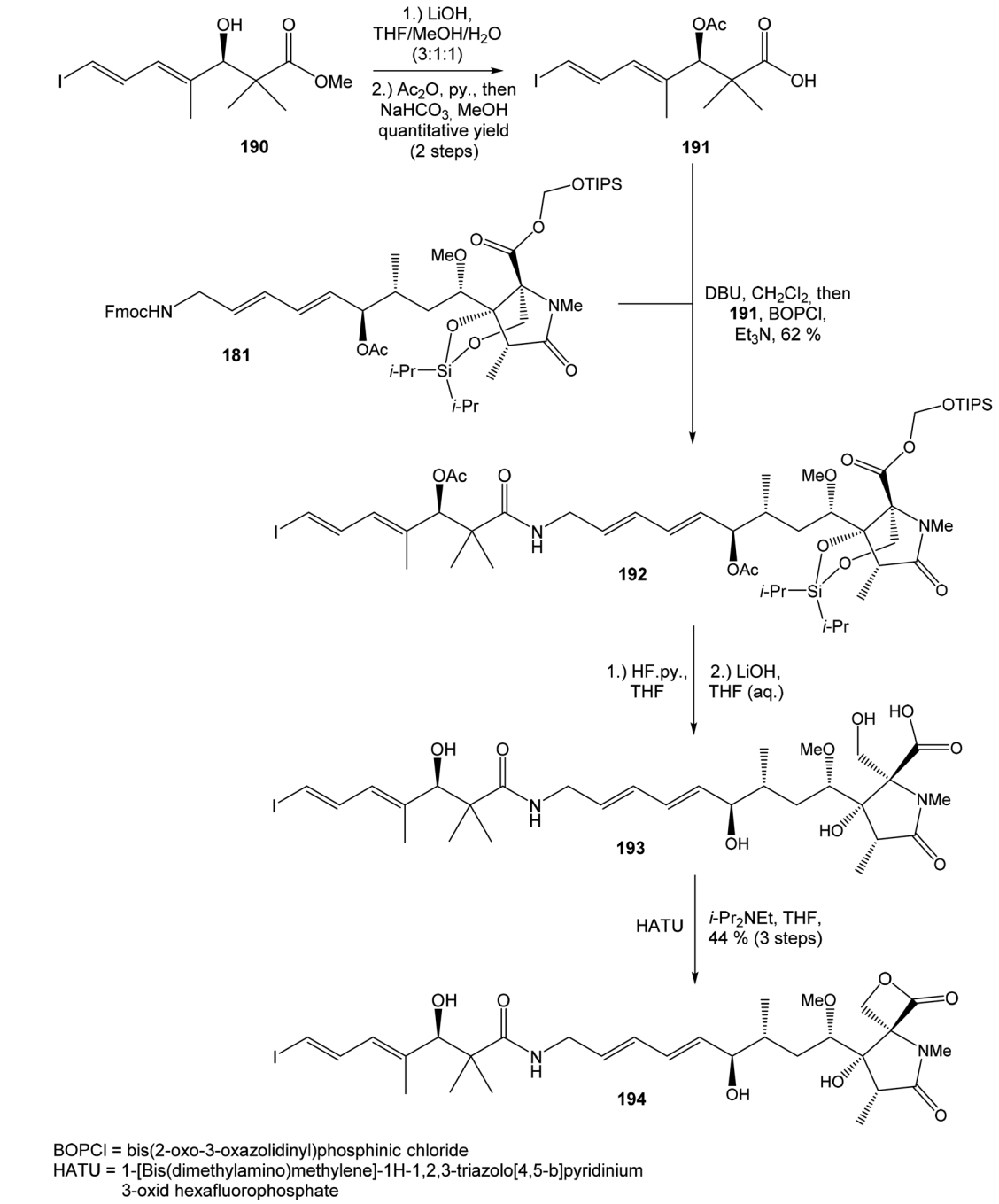

Scheme 18 Synthesis of the right-hand and middle fragment derivative **194** of lajollamycin B by Hatakeyama.

the mixture of **196** and **195** was not separable *via* chromatographic methods. Thus, geometries of the products **196** and **195** were determined directly from the prepared mixture, using COSY, HSQC, HMBC and NOESY spectral analysis.[15]

4.5.4 Finalization of the total synthesis and structural elucidation of lajollamycin B by Hatakeyama. Both formerly prepared structures of iodide **194** and (*E*)-nitrodienylstannane **188** reacted under Stille coupling conditions, in presence of $Pd(PPh_3)_4$, CuI and CsF. The expected mixture of (*E*)-configured compound **197** in 24% yield and (*Z*)-configured compound **11** in 22% yield was obtained as the final products of total synthesis of lajollamycin B (Scheme 20).

Surprisingly, the spectroscopic comparison (^{1}H and ^{13}C NMR) of unexpected (*Z*)-configurated compound **11** found it to be identical with those reported[9] as natural lajollamycin B, in contrary to expected (*E*)-configurated compound **197**. Furthermore, Hatakeyama and co-workers carefully reinvestigated COSY, HSQC, HMBC and ROESY spectra of lajollamycin B reported by Oh *et al.*[9] and found that key ROESY correlation between H9′ and Me-11′, confirming (*E*)-configuration was not

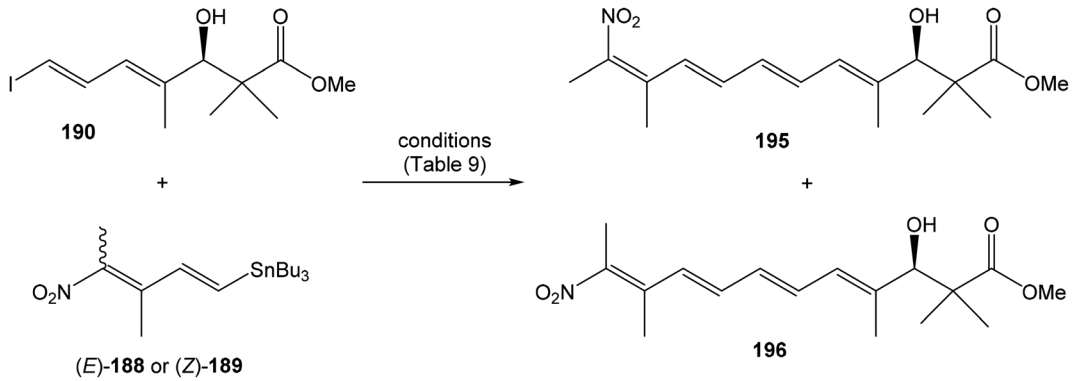

Scheme 19 Hatakeyama's model study for the final Stille coupling in the synthesis of lajollamycin B.

Table 9 Hatakeyama's conditions for a model study of Stille coupling

Entry	Conditions	Yield[a]	**195** : **196**[b]
1	**188** (1.1 equiv.), $Pd(PPh_3)_4$ (10 mol%), CuI (10 mol%), CsF (2 equiv.), DMF, rt, 1.5 h	38%	4 : 5
2	**188** (1.1 equiv.), $Pd(PPh_3)_4$ (2 mol%), CuI (10 mol%), CsF (20 mol%), DMF, rt, 26 h	73%	1 : 2
3	**189** (1.1 equiv.), $Pd(PPh_3)_4$ (1 mol%), CuI (10 mol%), CsF (20 mol%), DMF, rt, 5 h	71%	2 : 5
4	2 : 3 mixture of **188** and **189** (1.1 equiv.), $Pd(PPh_3)_4$ (2 mol%), CuI (10 mol%), CsF (20 mol%), DMF, rt, 71 h	76%	1 : 2

[a] Yield of the (*E*/*Z*)-mixture. [b] Determined by ^{1}H NMR.

observed.[9,15] Hatakeyama *et al.* unambiguously assigned stereostructures of prepared products **11** and **197** based on their NOESY spectra (Fig. 29).[15] Moreover, Hatakeyama and co-workers observed, that the nitrotetraene domain of **197** when compared to **196** and spectra of **11** when compared to **195** exhibited close similarities in ^{1}H and ^{13}C NMR.[15] These findings allowed Hatakeyama *et al.* to revise the initially assigned (*E*)-geometry of the terminal nitro-containing tetrasubstituted alkene in lajollamycin B to (*Z*)-geometry.

Hatakeyama *et al.* prepared the first total synthesis of lajollamycin B (**11**) and its (10′*E*)-isomer **197**. The synthesis involved conjugation of key intermediates as the right-hand fragment

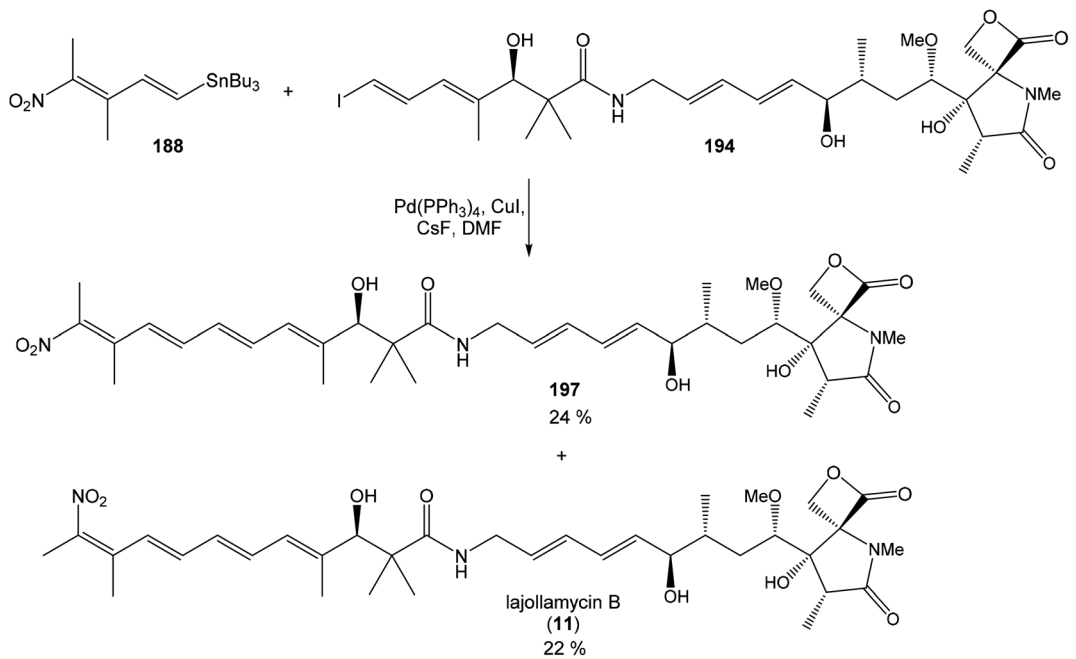

Scheme 20 Finalization of the total synthesis of lajollamycin B (**11**) by Hatakeyama.

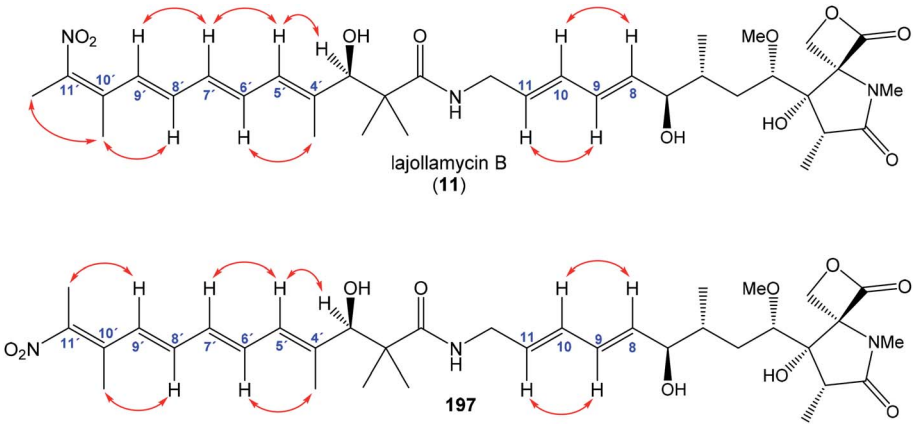

Fig. 29 NOESY correlations reported by Hatakeyama *et al.* for final products in the total synthesis of lajollamycin B.

181 and the middle fragment **191**, which was developed for synthesis of other members of oxazolomycin family.[12,16,43,131] This synthetical strategy represents applicable methodology for both lajollamycins and oxazolomycins. And importantly, the stereochemistry of natural lajollamycin B was revised and corrected.[15]

5 Formal synthesis of oxazolomycin family member

5.1 Formal synthesis of (+)-neooxazolomycin by Taylor

In 2011 Taylor *et al.* reported first formal synthesis of (+)-neooxazolomycin (**2**).[18] Talyor's formal synthesis of neooxazolomycin included the same late stage amide formation between left-hand fragment **71** (Scheme 25) and already combined right-hand and middle fragment **91**, which were prepared in both previously reported total syntheses by Kende and Hatakeyama.[13,16] The left-hand fragment **71** of neooxazolomycin, was readily available as an intermediate in formerly reported synthesis of inthomycin A.[115,132] Synthesis of the compound **91**, which represents combined right-hand and middle fragment of neooxazolomycin is described herein.

5.1.1 Synthesis of the middle fragment of neooxazolomycin by Taylor. Sulfide **198**, an intermediate in Taylor's methodological study of the synthesis of pentadienyl amines[133] was used as the starting material. The sulfide **198** underwent double Boc group deprotection in the presence of TFA in CH_2Cl_2 to give deprotected amine **199** in 90% yield. Re-protection reaction of free amine with Fmoc-Cl in THF/H_2O provided Fmoc sulfide **200** in 87% yield. As the final step in the preparation of the middle fragment of neooxazolomycin, oxidation to corresponding sulfone **201** was required. Thus, previously successful oxidation conditions (proved on similar substrates) were applied on sulfide **200**. Surprisingly, it was shown that the oxidation of this precursor is more complicated. It was proved that during the oxidation side product **202** is formed *via* [2,3]-sigmatropic rearrangement[134] and it is hydrolyzed to allylic sulfoxide **203**. Thus, a polyoxometallate-catalyzed[135] oxidation was used to overlap this issue. The high concentration and the excess of H_2O_2 (30 equiv.) increased the rate of the second oxidation relative to undesired [2,3]-sigmatropic

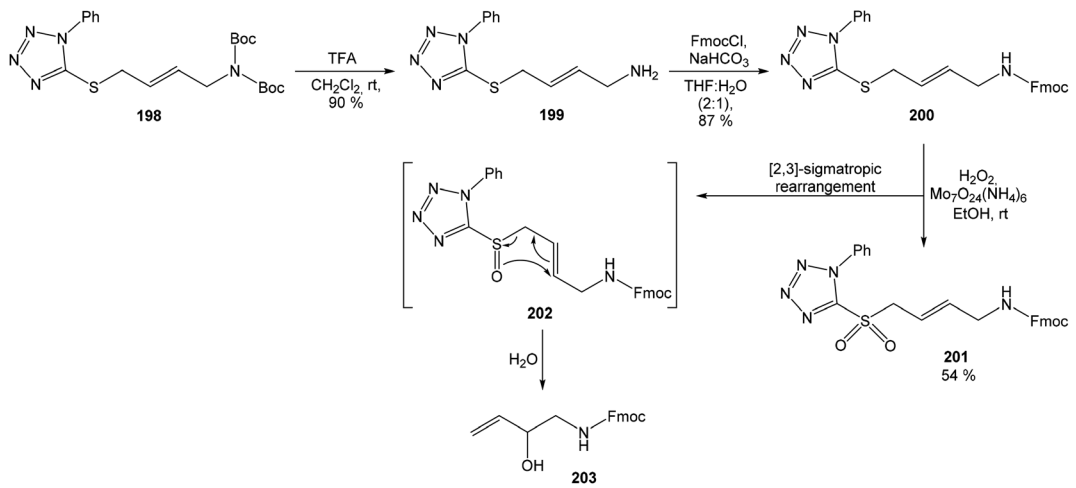

Scheme 21 Synthesis of the middle fragment derivative **201** of neooxazolomycin by Taylor.

rearrangement. Desired sulfone **201** was isolated in 54% yield (Scheme 21). The sulfone **201** prepared in 3 reaction steps from **198**, represents required partner for conjugation with right-hand fragment.

5.1.2 Synthesis of the right-hand fragment of neo-oxazolomycin by Taylor. Previous work reported by Moloney *et al.* for the synthesis of functionalized tetramic acids[136] was used as the inspiration for the right-hand fragment preparation. In this synthesis, **D-serine** was firstly methylated under Fieser conditions to its methyl ester, which was condensed with piv-aldehyde and in the presence of Et_3N in pentane afforded oxa-zolidine **204** in 95% yield as a mixture of *cis*/*trans*-isomers in ratio 1 : 1. *N*-Acetylation with acid chloride **205** with pyridine in CH_2Cl_2 provided *N*-acylated oxazolidine **206** in 92% yield as the mixture of diastereomers in ratio 1 : 1 (stereocenter on malo-nate moiety). Dieckmann condensation promoted by *t*-BuOK in *t*-BuOH led to regioselective cyclisation to desired bicyclic oxa-zolidine **207** in 93% yield. Compound **207** was prepared as a single diastereomer, albeit as a mixture of 9 : 1 enol/keto tautomers. Next reaction with Tf_2O and i-Pr_2NEt in CH_2Cl_2 at −50 °C gave corresponding triflate **208** in 70% yield (Scheme 22), which represents one of two partners for Stille cross coupling.

(Trimethylsilyl)propargyl alcohol was in 2 reaction steps transformed to required (*E*)-trisubstituted alkene **209** according to the procedure of Denmark and co-workers.[137] Sharpless epoxidation of alkene with $Ti(O^iPr)_4$, (+)-DIPT and TBHP in CH_2Cl_2 provided epoxide **210** in 85% as an enantiomeric mixture in ratio 95 : 5. Enantioselectivity of prepared epoxide **210** was determined by formation of Mosher's esters with both (*R*)- and (*S*)-MTPA-Cl. Corresponding esters **211** and **212** were determined by ^1H NMR analysis. Further, primary hydroxyl group in epoxide **210** was protected *via* bezylation with BnBr/NaH in THF to fully protected epoxide **213** in 85% yield. Epoxide **214** was obtained in 85% yield after desilylation under standard conditions with TBAF in THF. Lewis acid conditions

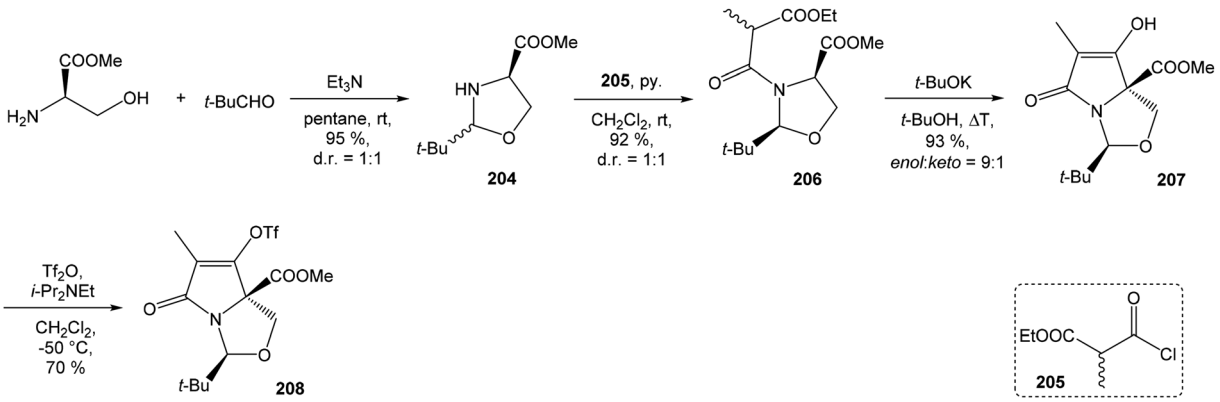

Scheme 22 Synthesis of bicyclic precursor for right-hand fragment **208** of neooxazolomycin by Taylor.

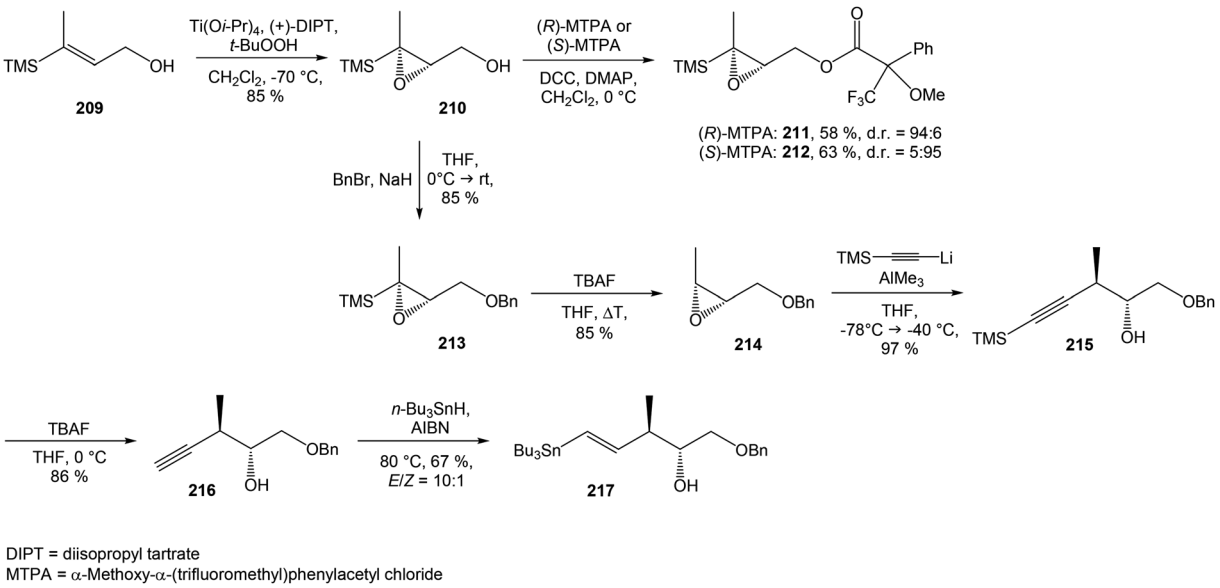

DIPT = diisopropyl tartrate
MTPA = α-Methoxy-α-(trifluoromethyl)phenylacetyl chloride

Scheme 23 Synthesis of Stille cross coupling partner **217** for right-hand fragment of neooxazolomycin by Taylor.

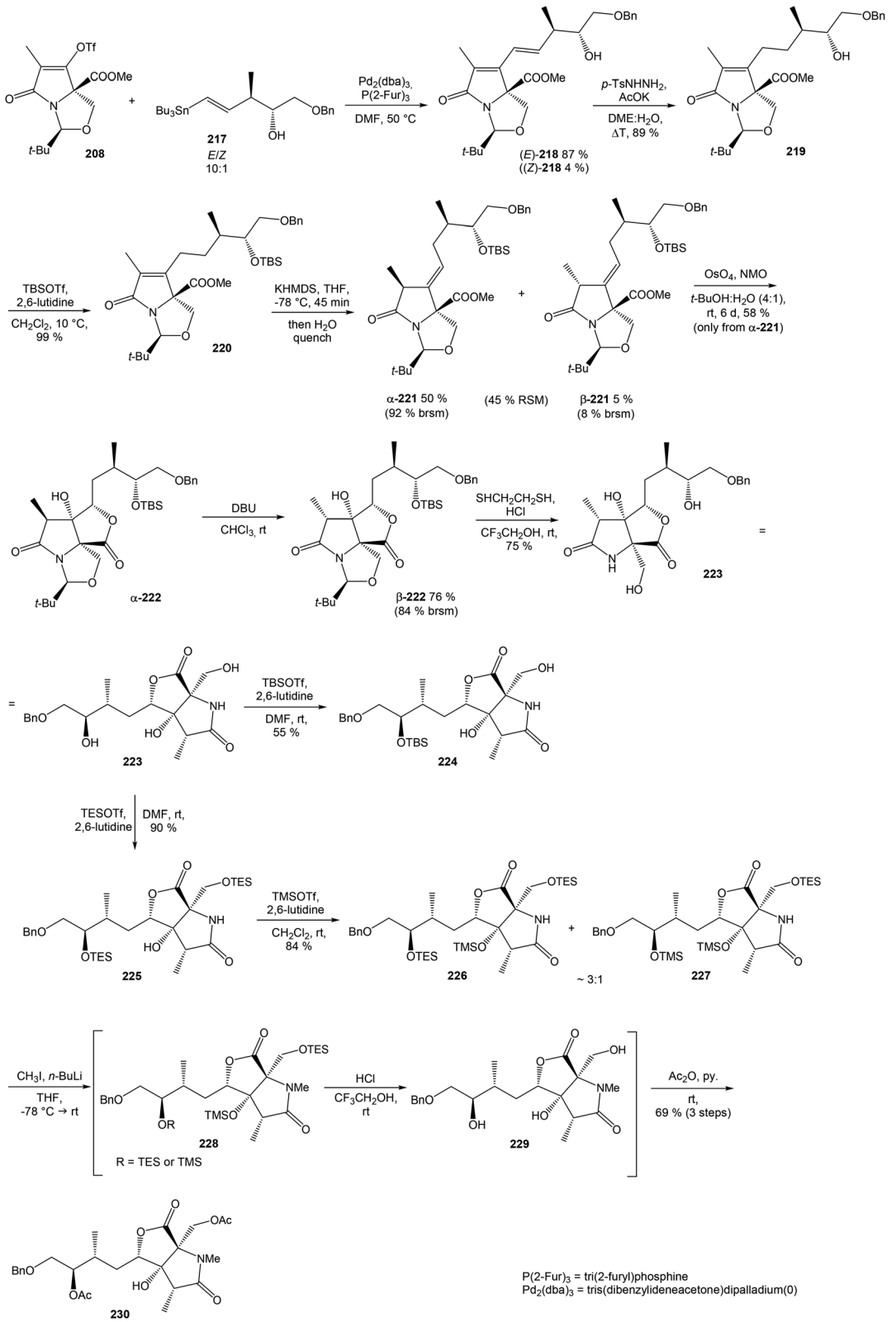

Scheme 24 Synthesis of the right-hand fragment derivative **230** of neooxazolomycin by Taylor.

with the alanate reagent derived from lithium trimethylsilylacetylide and $AlMe_3$ [138] allowed regioselective epoxide opening at the C3 position, to produce desired alcohol **215** in 97% yield, as a mixture 9 : 1 of regioisomers (in favor of desired regioisomer). It was observed that the control of temperature in epoxide opening reaction was essential to ensure high regioselectivity.

Standard conditions of desilylation with TBAF in THF provided alkyne **216** in 86% yield. Finally, radical promoted hydrostannylation with AIBN and *n*-Bu_3SnH led to stannane **217** in 67% yield as a 10 : 1 mixture of (*E*/*Z*)-isomers (Scheme 23). Desired (*E*)-configurated stannane **217** represents a second partner for Stille cross coupling.

The combination of the above-mentioned two fragments, **208** and **217**, was performed under Stille cross coupling conditions with $Pd_2(dba)_3$ and P(2-fur)$_3$ in DMF at 50 °C for 6 h. In this Stille reaction, control of the temperature was essential to afford desired geometric isomer. When the reaction was done at higher temperature, higher formation of unwanted isomer was observed. Under mentioned Stille conditions, diene **218** was obtained with the same crude ratio 10 : 1 of (*E*/*Z*)-isomers as was presented for the stannane precursor **217**. After chromatographic separation, 87% yield of desired (*E*)-**218** and 4% yield of undesired (*Z*)-**218** were obtained. Disubstituted alkene **218** was selectively reduced with *in situ* generated diimide from *p*-$TsNHNH_2$ and KOAc. Not surprisingly, the reduction of (*E*)-**218** proved to be much easier than the reduction of more steric hindered (*Z*)-**218** and alkene **219** was prepared in 89% yield (Scheme 24).

Silylation of secondary hydroxyl group with TBSOTf and 2,6-lutidine in CH_2Cl_2 provided protected derivative **220** in 99% yield. For the purpose of necessary dihydroxylation, the deconjugation of α,β-unsaturated lactam **220** was required. Unfortunately, the applied conditions of deconjugation model studies to unsaturated lactam **220** led only to recovery of starting material. After a series of experiments, appropriate reaction conditions were identified with KHMDS in THF followed with rapid quench by pouring into stirred water. These conditions provided 10 : 1 mixture of **α-221** in 50% yield, **β-221** in 5% yield and the rest of mixture was recovered as the starting material (Scheme 24). The stereoconfiguration of the α-centre, as well as the (*E*)-configuration of alkene were assigned by NOE studies.[18] Interestingly, if a longer reaction time or more basic conditions were applied, none deconjugation product was obtained.

Following dihydroxylation of deconjugated double bond was found to be more difficult than expected as the result of the crowded steric environment around the trisubstituted olefin. Epimer **β-221** with correct configuration at the C2 position proved to be inert under any conditions of dihydroxylation and solely starting material was recovered. In contrast, epimer **α-221** displayed reduced reactivity, but it was able to provide product of dihydroxylation with concomitant lactonization as a tricyclic lactone **α-222** in 58% yield. The dihydroxylation was carried out with OsO_4 and NMO in *t*-BuOH/H_2O for 6 days and provided only single oxidation product derived from attack on concave face of alkene **α-221** (Fig. 30).[18] The obtained tricyclic lactone **α-222** necessitated inversion of configuration on the stereocenter adjacent to the carbonyl group of lactam core. For this purpose, Taylor and co-workers found that a catalytic amount of DBU (10 mol%) is suitable for desired epimerisation. The process of isomerisation was studied by Taylor and co-workers by ^{1}H NMR spectroscopy.[18] It was found that equilibrium process led to >95% conversion over 24 h. Synthetically, epimerisation of **α-222** was accomplished with DBU (10 mol%) in $CHCl_3$ and

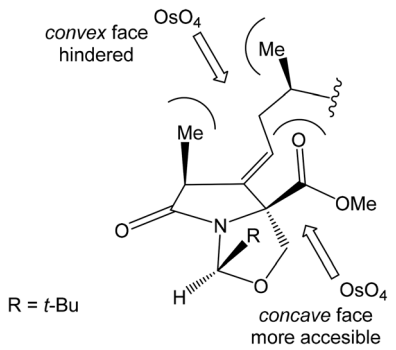

Fig. 30 Model for dihydroxylation reported by Taylor *et al.*

provided **β-222** in 76% yield with 10% of recovered starting material **α-222** (Scheme 24).

Further, acidic deprotection of the oxazolidine moiety under standard Corey conditions[139] with ethane-1,2-dithiol and HCl in CF_3CH_2OH gave a bicyclic triol **223** in 75% yield. Taylor and co-workers focused their attention on the lactam core *N*-methylation without the need for protection of some or all hydroxyl groups. It was found that the most suitable strategy involved the preparation of tris-silyl derivative. Triple silylation in a single step shown to be complicated by poor solubility of triol **223** in common solvents with exception of MeOH and DMF. Protection with TBSOTf and 2,6-lutidine in DMF afforded only monosilyl derivative **224** in 55% yield, presumably due to steric hindrance. Silylation was accomplished with less hindered TESOTf and 2,6-lutidine in DMF and provided double silylated product **225** in 90% yield. TMSOTf and 2,6-lutidine in CH_2Cl_2 for 24 h were used for a tertiary alcohol protection. As the result of this silylation, the mixture 3 : 1 of compounds **226** and **227** in 84% yield was obtained. An inevitable displacement of one of the TES groups with a TMS group led to the mixture of silyl isomers, but chromatographic separation of compounds **226** and **227** was found to be not necessary. The lactam *N*-methylation with CH_3I and *n*-BuLi in THF at −78 °C of both silyl isomers was done. The subsequent total desilylation with HCl in CF_3CH_2OH and finally acetylation under standard conditions with Ac_2O in pyridine was accomplished. The desired diacetate **230** was prepared in 69% yield after 3 steps (Scheme 24).

5.1.3 Combination of prepared fragments and finalization of the formal synthesis by Taylor. On the route to finalize the Taylor's formal synthesis of neooxazolomycin, diacetate **230** underwent reductive debenzylation with H_2 and $Pd(OH)_2$/C in MeOH toward primary alcohol **231** in quantitative yield. Interestingly, when debenzylation was left to proceed for longer time, migration of acetate from the secondary to primary hydroxyl group appeared, but none of this byproduct could be detected after 1 h. Following oxidation of primary alcohol **231** to corresponding aldehyde **232** was achieved with DMP in CH_2Cl_2 in 51% yield. However, no progress was achieved using other oxidation conditions *e.g.* Swern, Ley–Griffith, because of rapid decomposition of reaction product. Thus, aldehyde **232** was subjected directly after chromatography to the Julia–Kocienski olefination[133] with formerly prepared sulfone **201**. Reaction was

carried out in a presence of NaHMDS in THF at −78 °C for 1 h and provided 4.5 : 1 mixture of (4*E*,6*E*) : (4*Z*,6*E*)-isomers. Using chromatographic separation, (4*E*,6*E*)-**91** was isolated in 63% yield along with 14% of its isomer (4*Z*,6*E*)-**91** (Scheme 25). The obtained data were in accordance with those reported by Kende *et al.*[13]

To conclude, Taylor and co-workers completed a formal synthesis of neooxazolomycin in 23 steps with the preparation of Kende's intermediate **91**. In this approach a Moloney's synthetic strategy[136] was used toward key lactam core preparation. The Stille coupling reaction and Julia–Kocienski olefination were used to achieve combination of three key segments. The stereoselective construction of the bicyclic core was achieved with the preparation of Stille adduct *via* strategic deconjugation and dihydroxylation.

6 Discussion

Detailed biosynthesis of oxazolomycin A (**1**) has been investigated in *Streptomyces albus* JA3453 using labeling experiments[20] and gene analysis[25] of the oxazolomycin A gene cluster. These data suggest, that a whole structure of **1** is constructed from six building blocks: *N*-formyl-tetrahydrofolate, glycine, L-methionine, L-serine, malonyl-ACP and methoxymalonyl-ACP (Fig. 7). Zhao *et al.* further proposed disquisitional model for biosynthesis of **1** in *S. albus* (Fig. 6).[25] Despite a precise biosynthetic analysis of **1**, some details remain still unclear to date, *e.g.* domains responsible for cyclizations to afford the oxazole or γ-lactam ring.

As mentioned above, the main biological effects of oxazolomycins are attributed to their right-hand pyroglutamate cores, due the structural similarity with other bioactive pyroglutamates (Fig. 8). The results from biological assays suggest, that the unique spiro-β-lactone-γ-lactam moiety of right-hand fragment in some oxazolomycin members plays a significant role in the bioactivity. For example, oxazolomycin A (**1**) displays a selective antibacterial activity against *Agrobacterium tumefaciens*, while neooxazolomycin (**2**) with bicyclic γ-lactam-γ-lactone core is inactive.[60] Similarly, **1** showed more potent antibacterial activities against: *Bacillus subtilis* ATCC 6633, *Escherichia coli* NIHJ, *Kocuria rhizophila* ATCC 9341, *Staphylococcus aureus* ATCC 6538p and *Xanthomonas campestris* pv. *oryzae* KB 88 at all tested concentrations compared to its hydrolyzed natural member oxazolomycin A2 (**14**). Moreover, the cytotoxicity of **1** against human leukemia HL60 cells growth was considerably higher compared to **14**.[10] These results could suggest higher activity of **1** due the angle strain of the β-lactone moiety. Bagwell *et al.* evaluated the influence of structural subunit **45** localized close to the middle fragment of oxazolomycins.[55] Thorpe–Ingold effect of *gem*-dimethyl amide motif causes a structural U-shaped conformation of oxazolomycins, which is assumed to be beneficial for final biological activity. Additionally, suitable substituted derivatives of subunit **45** exhibit biological activity itself. Further studies revealed the importance of left-hand fragment on the biological activity of oxazolomycins. For example, **1** showed antibacterial activity against *Agrobacterium rhizogenes* IFO 13257, *Agrobacterium tumefaciens* EHA 101 and *Agrobacterium tumefaciens* IFO 13263, while its geometric isomers oxazolomycin B (**3**) and C (**4**) were inactive.[6] Even the phytotoxic activity is likely associated with left-hand fragment geometry. For the inhibition of *Medicago sativa* seeds germination and potato tuber disc necrosis **1** was the most potent geometric isomer, followed by **3** and then by **4**.[6,71] However, left-hand fragment geometric isomers **1**, **3** and **4** inhibited the crown gall formation at the same doses.[6] The biological activity comparison hand in hand with a structural diversity of single fragments could bring a better understanding in oxazolomycin's mechanism of action, thus further bioassays in this field are needed.

The aggregated structures of oxazolomycins as the combination of particular fragments result in unique skeletons with remarkable bioactivity. A widespread antibacterial activity of oxazolomycins against both Gram-positive and Gram-negative bacterial strains was reported. Besides the selective activity of

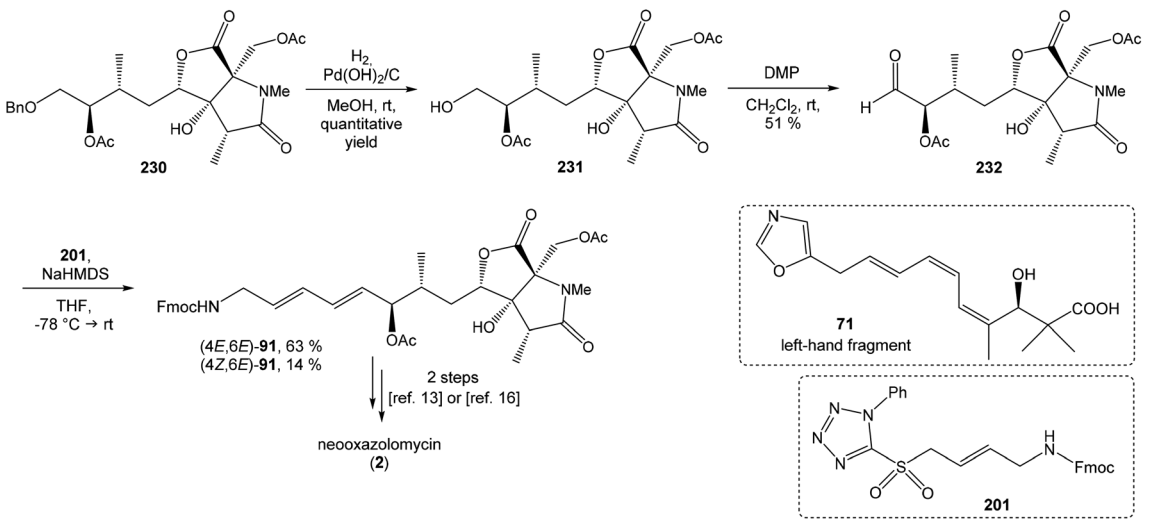

Scheme 25 Finalization of the formal synthesis of neooxazolomycin (**2**) by Taylor.

oxazolomycin A (**1**) against *Agrobacterium tumefaciens*,[60] growth inhibition of several other bacteria including *Agrobacterium rhizogenes*,[6] *Escherichia coli*[10] and *Pseudomonas putida*[60] were found. Curromycin A (**6**) and B (**7**) affect against bacterial strains *Bacillus subtilis*,[61] *Micrococcus luteus*[4] and *Staphylococcus aureus*.[4] Lajollamycin (**10**) showed significant antibacterial properties against *Enterococcus faecalis*, *Staphylococcus aureus*, *Streptococcus pneumoniae* and *Escherichia coli*.[8] Bisoxazolomycin (**15**), oxazolomycin A2 (**14**) and **1** were active against *Staphylococcus aureus* and *Xanthomonas campestris*.[10] These data approved that diverse oxazolomycin members possess a broad antibacterial activity. Moreover, the antiviral activity of some oxazolomycins provided interesting results. The bioactivity of **1** was reported against herpes simplex type 1, influenza A and vaccinia viruses.[63] Further study revealed anti-HIV activity of curromycins **6** and **7**, with indication that curromycins affect in the virus replication cycle in later steps.[64] Similarly, the cytotoxic activity bioassays of oxazolomycins resulted in notable findings. The activity against Ehrlich ascites carcinoma was reported for **1**,[1] as well as for neooxazolomycin (**2**).[2] Significant cytotoxicity against mouse leukemia P388 cells was reported for **1**,[1] 16-methyloxazolomycin (**5**)[5] and for both curromycins **6** and **7**.[3] KSM-2690 B (**8**) and C (**9**) exhibited the inhibition activity against human bladder carcinoma T24 cells.[7] Despite none cytotoxic activity of lajollamycins (**10–13**) was observed against selected cell lines,[9] **10** showed potential against mouse melanoma B16–F10 cells growth.[8] Human leukemia HL60 cell line growth was inhibited by monocyclic oxazolomycin **14**, dimeric structure **15**, but the most potent activity was reported for **1**.[10] As seen, structural diverse oxazolomycins have a strong potential in growth inhibition of different carcinoma cell lines. Further considerable bioactivity of oxazolomycins was observed toward the inhibition of crown gall formation. The highest inhibition activity was reported for **1**, oxazolomycins B (**3**) and C (**4**),[6] although the curromycins **6** and **7** also showed inhibitory potential.[62] The phytotoxic activity was observed for **1**, **3**, **4**, **6** and **7** against *Medicago sativa* seeds germination. Similarly, these five oxazolomycin members induced the necrosis of potato tuber disc.[6,62,71] The broad range of biological activities exhibited by oxazolomycin family members or their fragments indicates their potential research or application in medicine, especially as antibacterial, antiviral, cytotoxic or phytotoxic compounds. Therefore, it is not surprising that different research groups developed many synthetic strategies toward oxazolomycins.

Kende *et al.*[13] achieved first total synthesis of neooxazolomycin (**2**) in 1990, just five years since its discovery by Uemura *et al.*[2] in 1985. Kende's synthesis involved diastereoselective Reformatsky-type condensation, Schöllkopf condensation and Stille coupling. Kende's synthesis started from anhydrogalactoside **73** (Fig. 31), which was also utilized as a chiral source. Longest linear sequence form **73** involves 22 steps with overall yield 1.9%. For the next 17 years it was the only total synthesis of oxazolomycin family member. Second total synthesis of neooxazolomycin was reported by Hatakeyama *et al.* in 2007.[16] Hatakeyama's synthesis of **2** involves Stille coupling, Tamao hydrosilylation, Pd-catalyzed enolate alkenylation, dihydroxylation accompanied by lactonization and a Nozaki–Hiyama–Kishi reaction. Hatakeyama's total synthesis of neooxazolomycin starting from commercially available methyl (*S*)-3-hydroxy-2-methylpropionate (**100**; Fig. 31), which can be convert to neooxazolomycin in 27 steps with 2.2% overall yield (based on the same preparation methodology of **103**, as reported in Hatakeyama's total synthesis of oxazolomycin A[12]). Third total synthesis of neooxazolomycin (**2**) was reported by Kim *et al.* in 2019.[17] Kim's synthesis of **2** using a minimum number of chiral sources. Several chirality propagation processes were employed, including memory of chirality, dynamic kinetic resolution and substrate-controlled asymmetric inductions. Kim's synthesis used as the starting material as well as a source of chirality **D-serine** (Fig. 31), which was in 24 steps of longest linear sequence transformed to neooxazolomycin in 1.7% overall yield. Additionally, Taylor *et al.* reported in 2011 formal synthesis of neooxazolomycin.[18] Taylor's synthesis utilized Stille cross coupling, a base-promoted enone deconjugation and Julia–Kocienski methodology for the preparation of Kende's key intermediate **91**. The longest linear sequence of Taylor's formal synthesis starting from alkene **209** (Fig. 31) and led to neooxazolomycin in 23 steps, in formal overall yield 0.6% (based on the yields of conversion Kende's key intermediate **91** to neooxazolomycin in Kende's total synthesis[13]).

The first total synthesis of oxazolomycin A (**1**) was reported by Hatakeyama *et al.* in 2011.[12] Hatakeyama's synthesis of **1** included stereo controlled construction of the right-hand fragment by taking advantage of an In(III)-catalyzed Conia-ene type cyclization and the asymmetric synthesis of the left-hand fragment with *Cinchona* alkaloid-catalyzed cyclocondensation. Hatakeyama's synthesis of oxazolomycin A started from commercially available (*S*)-Roche ester **100**, which after 34 steps

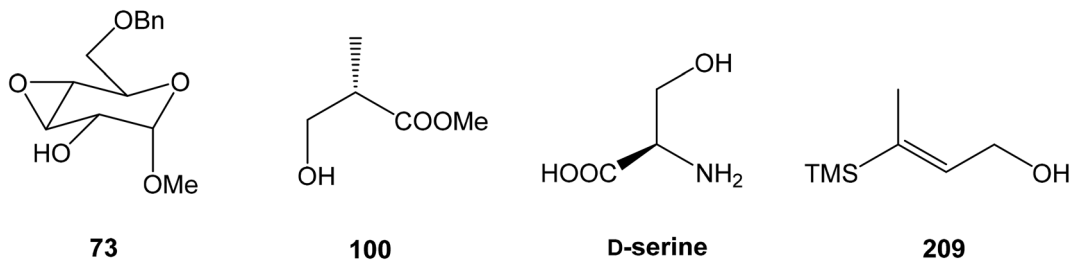

Fig. 31 Used starting materials for total and formal syntheses of oxazolomycin family members.

Table 10 Summary of total and formal syntheses of oxazolomycin family members

Synthesis of	Longest linear sequence	Overall yield	Published in year	Reported by	Used starting material
Neooxazolomycin (**2**)	22 steps	1.9%	1990	Kende *et al.*[88]	**73**
Neooxazolomycin (**2**)	27 steps	2.2%[a]	2007	Hatakeyama *et al.*[16]	**100**
Neooxazolomycin (**2**)[b]	23 steps	0.6%[c]	2011	Taylor *et al.*[18]	**209**
Neooxazolomycin (**2**)	24 steps	1.7%	2019	Kim *et al.*[17]	D-**Serine**
Oxazolomycin A (**1**)	34 steps	1.4%	2011	Hatakeyama *et al.*[12]	**100**
Oxazolomycin A2 (**14**)[d]	33 steps	1.4–3.5%[e]	2011	Hatakeyama *et al.*[12]	**100**
Lajollamycin B (**11**)	35 steps	0.3%[f]	2019	Hatakeyama *et al.*[15]	**100**

[a] Based on the same preparation methodology of **103**, as reported in Hatakeyama's synthesis of **1**.[12] [b] ormal synthesis. [c] Based on the yields of conversion Kende's key intermediate **91** to **2** in Kende's total synthesis of **2**.[13] [d] Product was not isolated, used as a crude mixture to a following reaction.[12] [e] Expected range of overall yield, according to reported procedure.[12] [f] Based on the same preparation methodology of **181**, as reported in Hatakeyama's synthesis of **1**.[12]

of longest linear sequence provided oxazolomycin A in 1.4% overall yield. Notably, Hatakeyama's synthesis of oxazolomycin A involved synthesis of later discovered oxazolomycin A2 (**14**),[10] which represented the penultimate compound in the synthesis. Based on Hatakeyama's synthesis, oxazolomycin A2 could be prepared according to reported procedure[12] from **100** in 33 steps, in 1.4-3.5% range of yield. Thus, Hatakeyama's synthesis of oxazolomycin A is to date the only total synthesis, which involves preparation of two different natural members of oxazolomycin family.

Total synthesis of lajollamycin B (**11**) was reported by Hatakeyama *et al.* in 2019.[15] Hatakeyama's synthesis of **11** involved the construction of nitrodienylstannane and its coupling under Stille conditions with compound prepared form ω-iodoheptadienoic acid and the right-hand fragment **181**, previously utilized for synthesis of oxazolomycin A. The longest linear sequence of Hatakeyama's synthesis of lajollamycin B begun from (*S*)-Roche ester **100** and involved 35 steps, which give to lajollamycin B in 0.3% overall yield (based on the same preparation methodology of **181**, as reported in Hatakeyama's total synthesis of oxazolomycin A[12]). Moreover, Hatakeyama *et al.* revised the structure of lajollamycin B from initially assigned (10′*E*)-configuration to (10′*Z*)-geometry. Hatakeyama's synthesis of lajollamycin B involved synthesis of its (10′*E*)-isomer, too. The results of above-mentioned syntheses are summarized in following table (Table 10).

Further in 2018, Hatakeyama *et al.* reported application of γ-lactone-γ-lactam core **113**,[43] which was formerly utilized in Hatakeyama's synthesis of neooxazolomycin[16] and oxazolomycin A[12] as a common intermediate for the construction of the right-hand fragment of oxazolomycins bearing methyl group at C16 position, with (16*R*)- or (16*S*)-configurated center. Thus, Hatakeyama *et al.* developed methodology toward total syntheses of 16-methylated members of oxazolomycin family: KSM-2690 B (**8**), KSM-2690 C (**9**), lajollamycin (**10**), lajollamycin C (**12**) and lajollamycin D (**13**).[43]

7 Summary and outlook

This review summarizes previously reported structures and biological properties of oxazolomycin family members. Oxazolomycin's family includes 15 different extraordinary structures usually divided into three fragments (left-hand, middle and right-hand fragment). Left-hand fragment represents either oxazole-triene-amide or tetraene-nitro-hydroxy-amide. Middle fragment is identical for all oxazolomycins and it can be described as pentadienylamine. Right-hand fragment of oxazolomycins represents in general pyroglutamate core, which forms different structural scaffolds including spiro-β-lactone-γ-lactam, bicyclic γ-lactone-γ-lactam or monocyclic γ-lactam. Unique pyroglutamate core is presented in the dimeric structure of bisoxazolomycin (**15**). The pyroglutamate core of oxazolomycins shows structural similarities with pyroglutamate core of known proteasome inhibitors such as omuralide (**27**) and salinosporamide A (**28**). These findings support hypothesis of the similar bioactivity for oxazolomycins with β-lactone-γ-lactam core. In addition, all members of oxazolomycin's family were already tested toward some biological targets. The bioassays revealed widespread biological activity including antibacterial, antiviral, cytotoxic activity and ability of enzyme inhibition. These remarkable biological activities shown, that oxazolomycin members have promising medicinal properties, although a better understanding of the mechanism of action as well as further bioassays are needed. Combination of attractive biological properties with a unique structural arrangement of oxazolomycins represents synthetic challenge for organic chemists. Therefore, different research groups developed the synthetic strategies toward oxazolomycins. In summary, total syntheses of four different oxazolomycin members were achieved. Specifically, four syntheses of neooxazolomycin (**2**), one synthesis of oxazolomycin A (**1**) including oxazolomycin A2 (**14**) and one synthesis of lajollamycin B (**11**) were reported to date.

In future years we assume, that novel oxazolomycin members will be discovered and encompassed to the family. We expect further studies of biological activity, which will prove exact oxazolomycin's mechanism of action for particular targets. The beneficial data could be obtained from comparison studies between bioactivity of oxazolomycin's fragments and bioactivity of the whole structures. Analogously, bioactivity comparison of known pyroglutamate core proteasome inhibitors with oxazolomycins would give better insight to biological effect of oxazolomycins. We suppose there would be increasing

number of total syntheses toward oxazolomycins, which have not yet been synthetized. These syntheses will allow faster access to oxazolomycin's preparation in higher yields. It seems likely, that oxazolomycins will attract more attention on fields of organic chemistry and biochemistry.

Conflicts of interest

The authors declare that they have no conflict of interest.

Acknowledgements

The present work was supported by Slovak Grant Agency VEGA (no. 1/0375/19), Slovak Research and Development Agency (no. APVV-14-0883) and University of Hradec Kralove (Faculty of Science, no. VT2019-2021).

References

1 T. Mori, K. Takahashi, M. Kashiwabara, D. Uemura, C. Katayama, S. Iwadare, Y. Shizuri, R. Mitomo, F. Nakano and A. Matsuzaki, *Tetrahedron Lett.*, 1985, **26**, 1073–1076.
2 K. Takahashi, M. Kawabata, D. Uemura, S. Iwadare, R. Mitomo, F. Nakano and A. Matsuzaki, *Tetrahedron Lett.*, 1985, **26**, 1077–1078.
3 M. Ogura, H. Nakayama, K. Furihata, A. Shimazu, H. Seto and N. Otake, *J. Antibiot.*, 1985, **38**, 669–673.
4 Y. Ikeda, S. Kondo, H. Naganawa, S. Hattori, M. Hamada and T. Takeuchi, *J. Antibiot.*, 1991, **44**, 453–455.
5 G. Ryu, S. Hwang and S.-K. Kim, *J. Antibiot.*, 1997, **50**, 1064–1066.
6 H. Kanzaki, K. Wada, T. Nitoda and K. Kawazu, *Biosci., Biotechnol., Biochem.*, 1998, **62**, 438–442.
7 T. Otani, K.-I. Yoshida, H. Kubota, S. Kawai, S. Ito, H. Hori, T. Ishiyama and T. Oki, *J. Antibiot.*, 2000, **53**, 1397–1400.
8 R. R. Manam, S. Teisan, D. J. White, B. Nicholson, J. Grodberg, S. T. C. Neuteboom, K. S. Lam, D. A. Mosca, G. K. Lloyd and B. C. M. Potts, *J. Nat. Prod.*, 2005, **68**, 240–243.
9 K. Ko, S.-H. Lee, S.-H. Kim, E.-H. Kim, K.-B. Oh, J. Shin and D.-C. Oh, *J. Nat. Prod.*, 2014, **77**, 2099–2104.
10 W. Koomsiri, Y. Inahashi, T. Kimura, K. Shiomi, Y. Takahashi, S. Ōmura, A. Thamchaipenet and T. Nakashima, *J. Antibiot.*, 2017, **70**, 1142–1145.
11 H. M. Jacobs, B. A. Burke and A. Brossi, *The Alkaloids: Chemistry and Pharmacology*, 1989, ch. 6, vol. 35.
12 K. Eto, M. Yoshino, K. Takahashi, J. Ishihara and S. Hatakeyama, *Org. Lett.*, 2011, **13**, 5398–5401.
13 A. S. Kende, K. Kawamura and R. J. DeVita, *J. Am. Chem. Soc.*, 1990, **112**, 4070–4072.
14 G. Ryu and S.-K. Kim, *J. Antibiot.*, 1999, **52**, 193–197.
15 T. Nishimaru, K. Eto, K. Komine, J. Ishihara and S. Hatakeyama, *Chem. - Eur. J.*, 2019, **25**, 7927–7934.
16 E. O. Onyango, J. Tsurumoto, N. Imai, K. Takahashi, J. Ishihara and S. Hatakeyama, *Angew. Chem., Int. Ed.*, 2007, **46**, 6703–6705.
17 J. H. Kim, I. Kim, Y. Song, M. J. Kim and S. Kim, *Angew. Chem., Int. Ed.*, 2019, **58**, 11018–11022.
18 R. Bastin, J. W. Dale, M. G. Edwards, J. P. N. Papillon, M. R. Webb and R. J. K. Taylor, *Tetrahedron*, 2011, **67**, 10026–10044.
19 M. Yoshino, K. Eto, K. Takahashi, J. Ishihara and S. Hatakeyama, *Org. Biomol. Chem.*, 2012, **10**, 8164–8174.
20 U. Gräfe, H. Kluge and R. Thiericke, *Liebigs Ann. Chem.*, 1992, **1992**, 429–432.
21 S. C. Wenzel, R. M. Williamson, C. Grünanger, J. Xu, K. Gerth, R. A. Martinez, S. J. Moss, B. J. Carroll, S. Grond, C. J. Unkefer, R. Müller and H. G. Floss, *J. Am. Chem. Soc.*, 2006, **128**, 14325–14336.
22 P. C. Dorrestein, S. G. Van Lanen, W. Li, C. Zhao, Z. Deng, B. Shen and N. L. Kelleher, *J. Am. Chem. Soc.*, 2006, **128**, 10386–10387.
23 Y. A. Chan, M. T. Boyne, A. M. Podevels, A. K. Klimowicz, J. Handelsman, N. L. Kelleher and M. G. Thomas, *Proc. Natl. Acad. Sci. U. S. A.*, 2006, **103**, 14349–14354.
24 B. J. Carroll, S. J. Moss, L. Bai, Y. Kato, S. Toelzer, T.-W. Yu and H. G. Floss, *J. Am. Chem. Soc.*, 2002, **124**, 4176–4177.
25 C. Zhao, J. M. Coughlin, J. Ju, D. Zhu, E. Wendt-Pienkowski, X. Zhou, Z. Wang, B. Shen and Z. Deng, *J. Biol. Chem.*, 2010, **285**, 20097–20108.
26 C. Zhao, J. Ju, S. D. Christenson, W. C. Smith, D. Song, X. Zhou, B. Shen and Z. Deng, *J. Bacteriol.*, 2006, **188**, 4142–4147.
27 D. A. Hopwood, T. Kieser, M. Bibb, M. Buttner and K. Chater, *Practical Streptomyces Genetics*, John Innes Foundation, 2000.
28 T. Stachelhaus, H. D. Mootz and M. A. Marahiel, *Chem. Biol.*, 1999, **6**, 493–505.
29 G. Schoenafinger, N. Schracke, U. Linne and M. A. Marahiel, *J. Am. Chem. Soc.*, 2006, **128**, 7406–7407.
30 L. Rouhiainen, L. Paulin, S. Suomalainen, H. Hyytiäinen, W. Buikema, R. Haselkorn and K. Sivonen, *Mol. Microbiol.*, 2000, **37**, 156–167.
31 T. Stachelhaus, H. D. Mootz, V. Bergendahl and M. A. Marahiel, *J. Biol. Chem.*, 1998, **273**, 22773–22781.
32 A. Tanovic, S. A. Samel, L.-O. Essen and M. A. Marahiel, *Science*, 2008, **321**, 659–663.
33 M. He, M. Varoglu and D. H. Sherman, *J. Bacteriol.*, 2000, **182**, 2619–2623.
34 J. G. Olsen, A. Kadziola, P. von Wettstein-Knowles, M. Siggaard-Andersen, Y. Lindquist and S. Larsen, *FEBS Lett.*, 1999, **460**, 46–52.
35 D. Song, J. Coughlin, J. Ju, X. Zhou, B. Shen, C. Zhao and Z. Deng, *Acta Biochim. Biophys. Sin.*, 2008, **40**, 319–326.
36 R. M. Kagan and S. Clarke, *Arch. Biochem. Biophys.*, 1994, **310**, 417–427.
37 M. Vrljic, H. Sahm and L. Eggeling, *Mol. Microbiol.*, 1996, **22**, 815–826.
38 H. Savage, G. Montoya, C. Svensson, J. D. Schwenn and I. Sinning, *Structure*, 1997, **5**, 895–906.
39 S. Lin, S. G. V. Lanen and B. Shen, *Proc. Natl. Acad. Sci. U. S. A.*, 2009, **106**, 4183–4188.

40 K. Zaleta-Rivera, C. Xu, F. Yu, R. A. E. Butchko, R. H. Proctor, M. E. Hidalgo-Lara, A. Raza, P. H. Dussault and L. Du, *Biochemistry*, 2006, **45**, 2561–2569.
41 J. Staunton and K. J. Weissman, *Nat. Prod. Rep.*, 2001, **18**, 380–416.
42 R. Finking and M. A. Marahiel, *Annu. Rev. Microbiol.*, 2004, **58**, 453–488.
43 K. Eto, J. Ishihara and S. Hatakeyama, *Tetrahedron*, 2018, **74**, 711–719.
44 B. C. Potts and K. S. Lam, *Mar. Drugs*, 2010, **8**, 835–880.
45 M. Groll, R. Huber and B. C. M. Potts, *J. Am. Chem. Soc.*, 2006, **128**, 5136–5141.
46 L. R. Dick, A. A. Cruikshank, L. Grenier, F. D. Melandri, S. L. Nunes and R. L. Stein, *J. Biol. Chem.*, 1996, **271**, 7273–7276.
47 M. Groll, L. Ditzel, J. Löwe, D. Stock, M. Bochtler, H. D. Bartunik and R. Huber, *Nature*, 1997, **386**, 463–471.
48 N. Chandan and M. G. Moloney, *Org. Biomol. Chem.*, 2008, **6**, 3664–3666.
49 T. J. Hill, P. Kocis and M. G. Moloney, *Tetrahedron Lett.*, 2006, **47**, 1461–1463.
50 Y.-C. Jeong and M. Moloney, *Synlett*, 2009, **2009**, 2487.
51 C. L. Bagwell, M. G. Moloney and M. Yaqoob, *Bioorg. Med. Chem. Lett.*, 2010, **20**, 2090–2094.
52 C. A. Holloway, C. J. Matthews, Y.-C. Jeong, M. G. Moloney, C. F. Roberts and M. Yaqoob, *Chem. Biol. Drug Des.*, 2011, **78**, 229–235.
53 M. Anwar and M. G. Moloney, *Tetrahedron Lett.*, 2007, **48**, 7259–7262.
54 P. Angelov, Y. K. S. Chau, P. J. Fryer, M. G. Moloney, A. L. Thompson and P. C. Trippier, *Org. Biomol. Chem.*, 2012, **10**, 3472–3485.
55 C. L. Bagwell, M. G. Moloney and A. L. Thompson, *Bioorg. Med. Chem. Lett.*, 2008, **18**, 4081–4086.
56 R. M. Beesley, C. K. Ingold and J. F. Thorpe, *J. Chem. Soc., Trans.*, 1915, **107**, 1080–1106.
57 S. Omura, Y. Tanaka, I. Kanaya, M. Shinose and Y. Takahashi, *J. Antibiot.*, 1990, **43**, 1034–1036.
58 Y. Tanaka, I. Kanaya, Y. Takahashi, M. Shinose, H. Tanaka and S. Omura, *J. Antibiot.*, 1993, **46**, 1208–1213.
59 M. Kawada, H. Inoue, I. Usami and D. Ikeda, *Cancer Sci.*, 2009, **100**, 150–157.
60 S. Kawai, G. Kawabata, A. Kobayashi and K. Kawazu, *Agric. Biol. Chem.*, 1989, **53**, 1127–1133.
61 M. Ogura, H. Nakayama, K. Furihata, A. Shimazu, H. Seto and N. Otake, *Agric. Biol. Chem.*, 1985, **49**, 1909–1910.
62 H. Kanzaki, T. Ichioka, A. Kobayashi and K. Kawazu, *Biosci., Biotechnol., Biochem.*, 1996, **60**, 1535–1537.
63 E. Tonew, M. Tonew, U. Gräfe and P. Zöpel, *Acta Virol.*, 1992, **36**, 166–172.
64 M. Nakamura, H. Honma, M. Kamada, T. Ohno, S. Kunimoto, Y. Ikeda, S. Kondo and T. Takeuchi, *J. Antibiot.*, 1994, **47**, 616–618.
65 R. L. Willey, D. H. Smith, L. A. Lasky, T. S. Theodore, P. L. Earl, B. Moss, D. J. Capon and M. A. Martin, *J. Virol.*, 1988, **62**, 139–147.
66 J. Carmichael, W. G. DeGraff, A. F. Gazdar, J. D. Minna and J. B. Mitchell, *Cancer Res.*, 1987, **47**, 936–942.
67 A. J. Petit, F. G. Terpstra and F. Miedema, *J. Clin. Invest.*, 1987, **79**, 1883–1889.
68 Y. Hayakawa, M. Akimoto, A. Ishikawa, M. Izawa and K. Shin-ya, *J. Antibiot.*, 2016, **69**, 187–188.
69 M. C. Lorenz and G. R. Fink, *Nature*, 2001, **412**, 83–86.
70 H.-R. Park, A. Tomida, S. Sato, Y. Tsukumo, J. Yun, T. Yamori, Y. Hayakawa, T. Tsuruo and K. Shin-ya, *J. Natl. Cancer Inst.*, 2004, **96**, 1300–1310.
71 K. Kawazu, H. Kanzaki, G. Kawabata, S. Kawai and A. Kobayashi, *Biosci., Biotechnol., Biochem.*, 1992, **56**, 1382–1385.
72 W. Fischetti, K. T. Mak, F. G. Stakem, J. Kim, A. L. Rheingold and R. F. Heck, *J. Org. Chem.*, 1983, **48**, 948–955.
73 R. D. Stephens and C. E. Castro, *J. Org. Chem.*, 1963, **28**, 3313–3315.
74 T. Harada and T. Mukaiyama, *Chem. Lett.*, 1982, **11**, 161–164.
75 A. S. Kende, K. Kawamura and M. J. Orwat, *Tetrahedron Lett.*, 1989, **30**, 5821–5824.
76 D. A. Evans, T. C. Britton and J. A. Ellman, *Tetrahedron Lett.*, 1987, **28**, 6141–6144.
77 M. Ohno and M. Okamoto, *Org. Synth.*, 1973, 281.
78 U. Schöllkopf and R. Schröder, *Angew. Chem., Int. Ed. Engl.*, 1971, **10**, 333.
79 W. J. Scott, G. T. Crisp and J. K. Stille, *J. Am. Chem. Soc.*, 1984, **106**, 4630–4632.
80 J. K. Stille and B. L. Groh, *J. Am. Chem. Soc.*, 1987, **109**, 813–817.
81 J. G. Buchanan and R. Fletcher, *J. Chem. Soc.*, 1965, 6316–6323.
82 K. A. Parker and R. E. Babine, *Tetrahedron Lett.*, 1982, **23**, 1763–1766.
83 J. R. Rasmussen, C. J. Slinger, R. J. Kordish and D. D. Newman-Evans, *J. Org. Chem.*, 1981, **46**, 4843–4846.
84 F. Dasgupta, P. P. Singh and H. C. Srivastava, *Indian J. Chem.*, 1980, **19**, 1056–1059.
85 A. S. Kende and R. J. DeVita, *Tetrahedron Lett.*, 1988, **29**, 2521–2524.
86 T. Fujisawa, T. Mori and T. Sato, *Chem. Lett.*, 1983, **12**, 835–838.
87 K. Takai, K. Nitta and K. Utimoto, *J. Am. Chem. Soc.*, 1986, **108**, 7408–7410.
88 A. S. Kende and R. J. DeVita, *Tetrahedron Lett.*, 1990, **31**, 307–310.
89 J. Cabré and A. L. Palomo, *Synthesis*, 1984, **1984**, 413–417.
90 Y. Watanabe, WO2003006442A1, 2003.
91 C. M. Shafer and T. F. Molinski, *J. Org. Chem.*, 1998, **63**, 551–555.
92 J. P. Marino and H. N. Nguyen, *Tetrahedron Lett.*, 2003, **44**, 7395–7398.
93 B. M. Trost and J. P. N. Papillon, *J. Am. Chem. Soc.*, 2004, **126**, 13618–13619.
94 A. Abiko, O. Moriya, S. A. Filla and S. Masamune, *Angew. Chem.*, 1995, **107**, 869–871.

95 A. Abiko, O. Moriya, S. A. Filla and S. Masamune, *Angew. Chem., Int. Ed. Engl.*, 1995, **34**, 793–795.
96 S. E. Denmark and W. Pan, *Org. Lett.*, 2001, **3**, 61–64.
97 R. Heckendorn, *Helv. Chim. Acta*, 1990, **73**, 1700–1718.
98 X. Liu, J. R. Deschamp and J. M. Cook, *Org. Lett.*, 2002, **4**, 3339–3342.
99 J. S. Panek and P. Liu, *J. Am. Chem. Soc.*, 2000, **122**, 11090–11097.
100 K. J. Hale, Z. Xiong, L. Wang, S. Manaviazar and R. Mackle, *Org. Lett.*, 2015, **17**, 198–201.
101 T. N. T. Huynh, P. Retailleau, C. Denhez, K. P. P. Nguyen and D. Guillaume, *Org. Biomol. Chem.*, 2014, **12**, 5098–5101.
102 H. C. Brown, J. Chandrasekharan and P. V. Ramachandran, *J. Am. Chem. Soc.*, 1988, **110**, 1539–1546.
103 J. Uenishi, R. Kawahama, O. Yonemitsu and J. Tsuji, *J. Org. Chem.*, 1998, **63**, 8965–8975.
104 K. J. Hale, M. Grabski, S. Manaviazar and M. Maczka, *Org. Lett.*, 2014, **16**, 1164–1167.
105 M. Falorni, S. Conti, G. Giacomelli, S. Cossu and F. Soccolini, *Tetrahedron: Asymmetry*, 1995, **6**, 287–294.
106 K. Takeda, A. Akiyama, H. Nakamura, S. Takizawa, Y. Mizuno, H. Takayanagi and Y. Harigaya, *Synthesis*, 1994, **1994**, 1063–1066.
107 D. J. Kempf, *J. Org. Chem.*, 1986, **51**, 3921–3926.
108 A. G. M. Barrett, R. A. E. Carr, S. V. Attwood, G. Richardson and N. D. A. Walshe, *J. Org. Chem.*, 1986, **51**, 4840–4856.
109 S. Zhang, T. Govender, T. Norström and P. I. Arvidsson, *J. Org. Chem.*, 2005, **70**, 6918–6920.
110 G. S. Cortez, S. H. Oh and D. Romo, *Synthesis*, 2001, **2001**, 1731–1736.
111 G. S. Cortez, R. L. Tennyson and D. Romo, *J. Am. Chem. Soc.*, 2001, **123**, 7945–7946.
112 C. Zhu, X. Shen and S. G. Nelson, *J. Am. Chem. Soc.*, 2004, **126**, 5352–5353.
113 J. E. Wilson and G. C. Fu, *Angew. Chem., Int. Ed.*, 2004, **43**, 6358–6360.
114 D. Seebach, J. Aebi and D. Wasmuth, *Org. Synth.*, 1985, **63**, 109.
115 M. R. Webb, M. S. Addie, C. M. Crawforth, J. W. Dale, X. Franci, M. Pizzonero, C. Donald and R. J. K. Taylor, *Tetrahedron*, 2008, **64**, 4778–4791.
116 S. P. H. Mee, V. Lee and J. E. Baldwin, *Chem. - Eur. J.*, 2005, **11**, 3294–3308.
117 K. Takahashi, M. Midori, K. Kawano, J. Ishihara and S. Hatakeyama, *Angew. Chem., Int. Ed.*, 2008, **47**, 6244–6246.
118 J. García-Fortanet, J. R. Debergh and J. K. De Brabander, *Org. Lett.*, 2005, **7**, 685–688.
119 G. V. M. Sharma, K. L. Reddy, P. Sree Lakshmi and P. Radha Krishna, *Tetrahedron Lett.*, 2004, **45**, 9229–9232.
120 D. Sawada and Y. Ito, *Tetrahedron Lett.*, 2001, **42**, 2501–2504.
121 K. Nishide, S. Ohsugi, T. Miyamoto, K. Kumar and M. Node, *Monatsh. Chem.*, 2004, **135**, 189–200.
122 J. Cossy, S. BouzBouz and A. H. Hoveyda, *J. Organomet. Chem.*, 2001, **634**, 216–221.
123 H. Jin, J. Uenishi, W. J. Christ and Y. Kishi, *J. Am. Chem. Soc.*, 1986, **108**, 5644–5646.
124 K. Takai, M. Tagashira, T. Kuroda, K. Oshima, K. Utimoto and H. Nozaki, *J. Am. Chem. Soc.*, 1986, **108**, 6048–6050.
125 L. A. Carpino, *J. Am. Chem. Soc.*, 1993, **115**, 4397–4398.
126 H. Oda, T. Kobayashi, M. Kosugi and T. Migita, *Tetrahedron*, 1995, **51**, 695–702.
127 K. C. Nicolaou, G. Bellavance, M. Buchman and K. K. Pulukuri, *J. Am. Chem. Soc.*, 2017, **139**, 15636–15639.
128 S. E. Denmark and L. Gomez, *Org. Lett.*, 2001, **3**, 2907–2910.
129 S. E. Denmark and L. Gomez, *J. Org. Chem.*, 2003, **68**, 8015–8024.
130 S. P. H. Mee, V. Lee and J. E. Baldwin, *Angew. Chem., Int. Ed.*, 2004, **43**, 1132–1136.
131 J. Ishihara and S. Hatakeyama, *Chem. Rec.*, 2014, **14**, 663–677.
132 B. K. Senapati, L. Gao, S. I. Lee, G.-S. Hwang and D. H. Ryu, *Org. Lett.*, 2010, **12**, 5088–5091.
133 R. Bastin, M. Liron and R. Taylor, *Synlett*, 2008, **2008**, 2183–2187.
134 P. Bickart, F. W. Carson, J. Jacobus, E. G. Miller and K. Mislow, *J. Am. Chem. Soc.*, 1968, **90**, 4869–4876.
135 H. S. Schultz, H. B. Freyermuth and S. R. Buc, *J. Org. Chem.*, 1963, **28**, 1140–1142.
136 M. D. Andrews, A. G. Brewster, K. M. Crapnell, A. J. Ibbett, T. Jones, M. G. Moloney, K. Prout and D. Watkin, *J. Chem. Soc., Perkin Trans. 1*, 1998, 223–236.
137 S. E. Denmark, K. L. Habermas and G. A. Hite, *Helv. Chim. Acta*, 1988, **71**, 168–194.
138 T. Skrydstrup, M. Bénéchie and F. Khuong-Huu, *Tetrahedron Lett.*, 1990, **31**, 7145–7148.
139 E. J. Corey and G. A. Reichard, *J. Am. Chem. Soc.*, 1992, **114**, 10677–10678.